1st International Conference on
SEPARATION PROCESSES – ICSP'17
(26 – 27 April 2017)

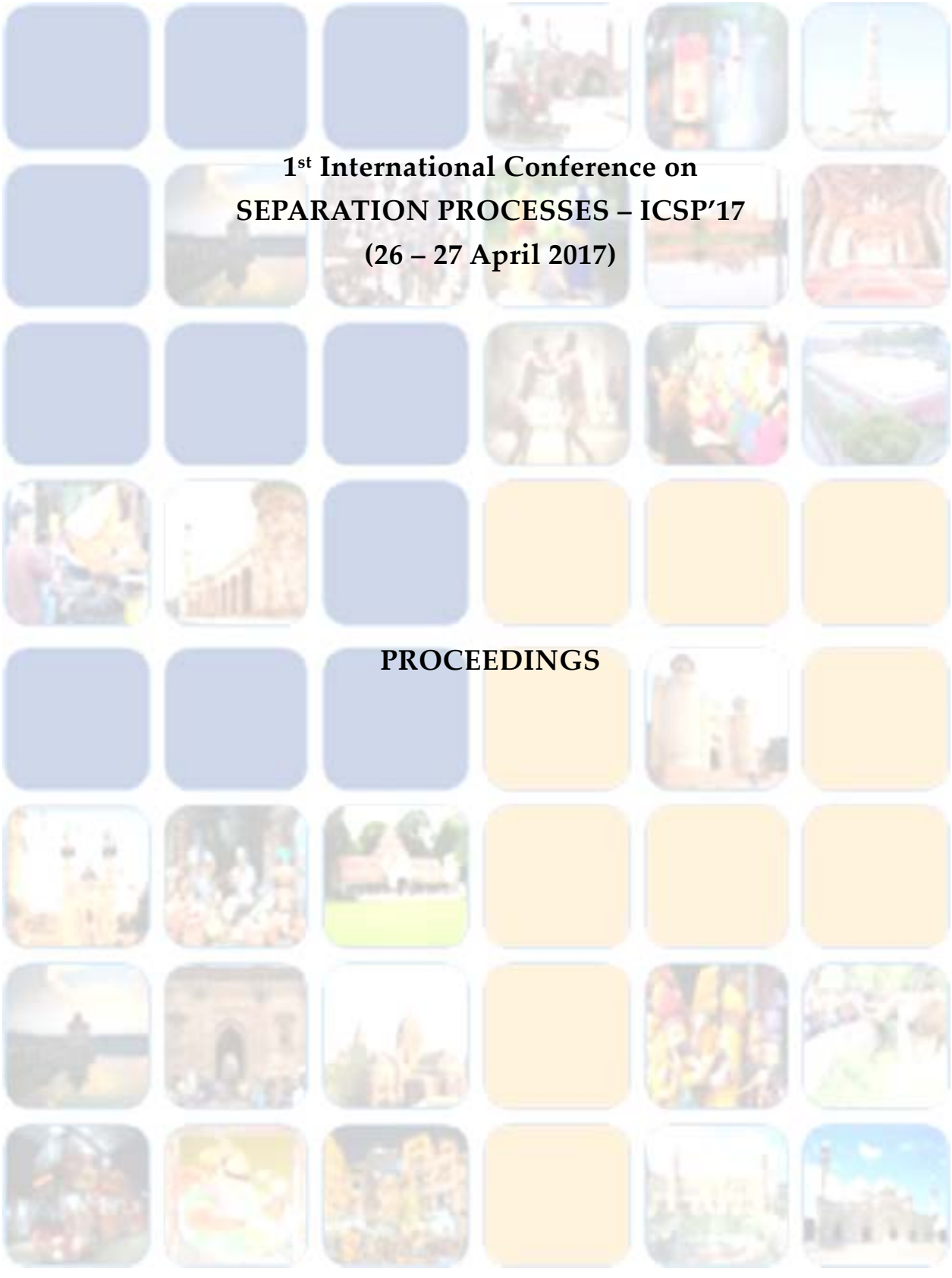

PROCEEDINGS

Organized by

Supported by

Pakistan Membrane Society

SPONSORS

Analytical Measuring Systems (Pvt.) Ltd.
Together We Can Find Solutions

Sentron Asia International

S. R. Traders
Total Testing Solution

POLYDOORS

H.A.Shah & Sons

LINKER ENTERPRISES

1st International Conference on

Separation Processes

April 26 – 27, 2017

COMSATS Institute of Information Technology

Lahore, Pakistan.

First edition 2017

For information on all CIIT publications visit our web site at ciitlahore.edu.pk

GENERAL INFORMATION

Conference Venue

The Grand Ballroom-A
NISHAT Banquet Hall (EMPORIUM MALL)
Trade and Finance Centre Block,
Near Expo Centre
Abdul Haq Road, Johar Town, Lahore
Tel: +92(042)-111-001-007
Email: ICSP@ciitlahore.edu.pk

Language

The official conference language is English.
No translation service will be provided.

Registration Hours

Tuesday, April 25	5:00 PM – 7:00 PM
Wednesday, April 26	8:30 AM – 9:30 AM

Internet Access

Free Internet Service is available inside conference rooms.

FOREWORD

Dear Distinguished Delegates and Guests,

The Organizing Committee warmly welcomes our distinguished delegates and guests to the 1st International Conference on Separation Processes (ICSP-2017) held in Lahore, Pakistan. The objective of ICSP 2017 is to provide a platform for researchers, engineers, academicians as well as industrial professionals from all over the world to present their research results and development activities. The conference provide opportunities for the delegates to exchange new ideas and experiences face to face, to establish business or research relations and to find global partners for future collaboration. We are pleased to have delegates from Belgium, China, Malaysia and UK. This conference is multi-disciplinary we will be covering sessions on Membrane Processes, Adsorption Based Separation Processes, Absorption and Distillation, Novel Separation Techniques, Waste Water and Water Purification Techniques, and Separation Processes in Chemical Engineering.

We would like to thank the plenary and keynote speaker(s), program chairs, and organization staff for their contribution to the success of ICSP 2017. We hope that all participants and other interested readers benefit scientifically from the proceedings and find it stimulating in the process. Finally, we would like to wish you success in your scientific and technical presentations and social networking.

We hope you had a unique, rewarding and enjoyable week at ICSP 2017 in Lahore, Pakistan.

With our warmest regards,

The Organizing Committee
ICSP-2017
May 26-27, 2017
Lahore, Pakistan.

CONFERENCE SECRETARIAT

Prof. Dr. Asad U. Khan	Chair
Dr. Asim Laeeq Khan	Co-Chair
Dr. Muhammad Yasin	Co-Chair
Mr. Amjad Riaz	Member
Dr. Abrar Faisal	Member
Dr. Sikander Rafiq	Member
Mr. Mohsin Ali	Organizing Secretary
Ms. Ayesha Ilyas	Secretary
Mr. Zaman Tahir	Member
Mr. Zufishan Shumair Atari	Member
Mr. Muhammad Raees	Member
Ms. Sadia Bano	Member
AIChE COMSATS Student Chapter	Member

CONTENTS

PLENARY SPEAKERS PROFILE

PL – 01 **Prof. Dr. Ivo F. J. Vankelecom**

KU Leuven, Belgium

He is associated with Centre for Surface Chemistry and Catalysis at KU Leuven. His research involves Development of equipment and strategies to allow fast, automated screening and optimisation of new membranes for separations and catalysis (polymeric, ceramic and organomineral) and process parameters

TOPIC:

"HIGH-THROUGHPUT MEMBRANE TECHNOLOGY AT KU LEUVEN"

PL – 02 **Prof. Dr. Paul Luckham**

Dept. Chemical Engineering, Imperial College London, UK

He has been a part of Imperial College London, UK, having more than 33 years of research experience. His research is focused on the field of colloid and polymer science.

TOPIC:

"UTILIZING THE LAYER BY LAYER TECHNIQUE FOR THE LARGE SCALE MANUFACTURE OF NANOCAPSULES FOR CONTROLLED RELEASE AND CADMIUM EXTRACTION"

PL – 03 **Prof. Dr. Xianfeng Li**

Dalian Institute of Chemical Physics, Chinese Academy of Sciences, China

He is currently working in Dalian Institute of Chemical Physics and Chinese Academy of Science. He has worked on the area of solvent resistant nanofiltration, fuel cell batteries and gas separation with extensive research background.

TOPIC:
"POROUS MEMBRANE IN SECONDARY BATTERY APPLICATION"

PL – 04 **Prof. Dr. Roil Bilad**

University Technology Petronas, Malaysia

He is affiliated with University technology Petronas, Malaysia. He is a renowned scientist and has done breakthrough work in the area of Membrane Bioreactors, Forward Osmosis and Membrane Distillation.

TOPIC:
"FOULING FACTOR IN MEMBRANE MODULE DESIGN"

INVITED SPEAKERS' BRIEF

Prof. Dr. Rahma TAMIME

(Lahore School of Economics, Lahore, Pakistan)

A review of the characterization of the synthetic polymeric membranes and fouled membrane: from the microscopic to macroscopic scale

Prof. Dr. Asif Ali Qaiser

(University of Engineering & Technology, Lahore, Pakistan)

Advanced membranes based on intrinsically conducting polymers: Pervaporation and Ion-exchange applications

Prof. Dr. Arshad Hussain

(School of Chemical and Materials Engineering, National University of Sciences and Technology (NUST), Islamabad, Pakistan)

Techno-economic analysis of membrane based post-combustion CO_2 capture process

Prof. Dr. Nasir M. Ahmad

(Polymer Research Lab, School of Chemical and Materials Engineering (SCME), National University of Sciences and Technology (NUST), Islamabad, Pakistan)

Functional Polymer Membranes for Water Purification: Design, Development, and Applications

Prof. Dr. M. Suleman Tahir

(Department of Chemical engineering, University of Gujrat, Gujrat, Pakistan)

Combustion of Low Rank Coal with Municipal Solid Waste (MSW) and Impact on NOx

Prof. Dr. Tahir Jamil

(Department of Polymer Engineering, University of the Punjab, Lahore, Pakistan)

Membranes for Science & Engineering Applications

Prof. Dr. Mahmood Saleem

(Department of Chemical Engineering, University of the Punjab, Lahore, Pakistan)

Advances in particle separation from flue gases

Prof. Dr. Haq Nawaz Bhatti

(Environmental Chemistry Laboratory, Department of Chemistry, University of Agriculture, Faisalabad, Pakistan)

Adsorption-A low cost separation process for the removal of environmental pollutants

Dr. Shazia Ilyas

(Rural Water Support Program, The Urban Unit Lahore, Pakistan)

Multifunctional weak polyelectrolyte multilayers for membrane applications

Prof. Dr. Sher Jamal

(National University of Science & Technology, Islamabad, Pakistan)

Performance Evaluation of a Full-Scale Membrane Bioreactor (MBR) Plant from Unsteady to Steady State Condition

Dr. Asif Mahmood

(Department of Chemical Engineering, PIEAS, Islamabad, Pakistan)

Solid Electrolyte Membrane Reactors for Efficient Synthetic Fuel Production

Dr. Mohammad Younas

(Department of Chemical Engineering, University of Engineering & Technology Peshawar, Pakistan)

Cu-oxide Coatings as Promising Electrode Materials for Microbial Fuel Cell

RESEARCH ARTICLES

Desalination of Water: Design, Fabrication and Performance Evaluation of Active Solar Still Coupled with Solar Collector

Syed Fawad Ali Shah[1], Muhammad Ayaz[2], *Qazi Sohaib[2], Salm Abdulbari S.M [1], Amir Muhammad[2]

***Abstract* -- The aim of this paper is to design and fabricate a solar still desalination unit to improve its performance by increasing production rate of distillate. Design modifications were, step-wise basin instead of flat basin to increase the surface area and decrease the water film thickness, use of sprinkler for uniform distribution of water in the basin. Heat storage materials, the pebbles were spread in the basin for enhancement of solar still which absorb more heat and sustain evaporation for longer time, also preventing water channeling by distributing it uniformly. Furthermore, solar flat plate collector was used to increase inlet temperature of water entering the solar still. Angle of inclination was chosen according to altitude as 34º at which it gives higher yield. During experiments, temperature of glass cover and water was recorded after each half an hour. The maximum temperature reached at mid-day was 73ºC while glass temperature reached up to 65.8ºC. Average daily output obtained from experiment was 2.24 L/m^2 while theoretical daily output was 3.78 L/m^2; hence efficiency of the solar still observed was 60%. The study also revealed that in absence of solar radiations at night, the distillate output increased due to decrease in glass temperature. Economic analysis was also conducted and the payback period obtained was seven months which could be useful for remote areas where people cannot afford high budget desalination plant.**

***Keywords:* Desalination, Solar still, Water purification, Solar energy**

I. INTRODUCTION

Availability of fresh water is extremely important for the continuity of life and its shortage is serious challenge to mankind. It is considered one of the fundamental key for the socio-economic development of any nation and specifically for regions facing water scarcity [1], [2].The global increase in population and large scale industrial and agriculture development has led to high demand of potable water [3]. Although 70% of world is covered by water but 97% is salty water, 2% is in frozen state and only 1% is potable water [4], [5]. Hence in most regions, the potable water supply is major problem therefore water desalination is possible solution to mitigate this problem. Recently researches are focused on sea water and brackish water desalination using solar energy because of its pollution free nature and availability in abundance without any cost [6]. Solar stills which convert salty water into potable water using solar energy have been used over 100 years for desalination[4]. They are easily operable, low cost and environment friendly. Solar still are less efficient due to loss of heat during evaporation and condensation process within same solar still. Several factors such as ambient temperature, wind velocity, insulation, glass temperature, water depth, salt concentration and inlet water temperature have remarkably affected productivity of solar still [7]–[9]. Performance of the solar still can be improved by different modifications. Many researchers have conducted experimental and theoretical research on solar stills to test different parameters for enhancement of the solar still performance. Stepped or inclined solar still with thinner water film, have high production yield instead of flat basin[5], [10], [11]. Inclination angle of the glass cover has also effect on productivity and maximum production is achieved at inclination angle equal to latitude of the region[12]. Installation of external and internal reflectors have also positive effect on production efficiency[13]. Effectiveness of different absorbing materials was studied to increase performance of the solar still. Use of different materials such as sponge type or wick in the basin also increased productivity of the distillate[9], [14], [15]. Research also showed that modified solar still works efficiently than basic solar still in the absence of sunlight[16].

Main objective of this work was to enhance the performance of the solar still by constructing a modified solar still. Specific aims were to design a stepped basin still to increase the surface area of the still and decrease water film thickness. Second point was to use heat storage materials for increasing evaporation rate. Another aim was designing a sprinkler for uniform distribution of salty water in the basin. Flat plate collector was coupled with the system to increase the production rate. Cost analysis was also conducted to see the feasibility of the system.

II. EXPERIMENTAL

A. *Experimental Setup*

Desalination system consisted of an active solar still coupled with flat plate collector. A stepwise basin solar still was fabricated from 2 mm thick galvanized iron. The back-side wall height was kept 64 cm, side wall height 30 cm while width of each step was 8 cm having a height of 5 cm. Inner surface of the basin was painted black to absorb maximum solar radiations. The metal basin was placed in wooden frame

[1]Department of Civil, Chemical, Environmental and Materials Engineering, University of Bologna, Via Terracini 28, 40131 Bologna, Italy
[2]Department of Chemical Engineering, University of Engineering and Technology, Peshawar, P.O. Box 814, University Campus, Peshawar 25120, Pakistan
* Corresponding author. Tel: +923449192271
Email address: engrsohaib492@uetpeshawar.edu.pk

while the gap was maintained to put Styrofoam. A wooden box was used to prevent solar still from harsh environment and support the still. A 3.8 cm thick Styrofoam sheet was used as an insulator to prevent heat losses from the still to the environment. A 4-mm thick glass sheet of 1 meter length is used to cover the solar still and tilted at 34° angle with horizontal, length of the glass was limited to 1 meter to prevent it from breakage. Heating storage material i.e. pebbles were spread at the bottom of the still to absorb more heat for sustaining long time production and distribute water uniformly by preventing of channelling. Salty water was introduced at the top by using a sprinkler for uniform distribution of water throughout the basin. Collecting trough was arranged near the glass for collection of distilled water. Digital thermometer was used to measure temperature of the basin and glass. Feed tank of 25 L capacity is used, which is made of PVC and kept on metal stand.

Flat plate collector was integrated along with solar still to enhance production efficiency of the solar still by increasing inlet temperature of salty water. Carbon tubes of 18 gauge were used in a wooden box having a length of 100 cm, a width of 50 cm and a height of 10 cm. Total 9 copper tubes were placed at distance of 5 cm from each other. The sheet of galvanized iron was painted black and placed behind tubes to absorb more solar radiations. For insulation Styrofoam was used between the metal sheet and wooden frame. A glass cover is placed on the top to produce greenhouse effect. Finally, exit of the solar collector was connected to solar still while the inlet of solar collector was used to fed water.

B. EXPERIMENTAL PROCEDURE

Experimental setup was placed in north south direction. Saline water was fed from storage tank to the flat plate collector where it was pre-heated to increase its temperature. Pre-heated water after passing through solar collector was introduced to the solar still through sprinkler, which uniformly distributed the water in the basin. Solar radiation passing through the glass entered the still and heated up water resulting in increased water temperature. Due to elevated temperature water evaporated and moved upward. The water vapours condensed on the tilted glass and fell to the collecting trough from where it was sent to the collecting tank. Schematic diagram of stepwise solar still is displayed in fig 2. Experiment started at 7 am and end at 6 pm. During experiment after each half an hour, glass temperature and basin water temperature were recorded. Total distilled water was collected and all the readings were noted down for several days.

Fig. 1. Photograph of flat plate solar collector

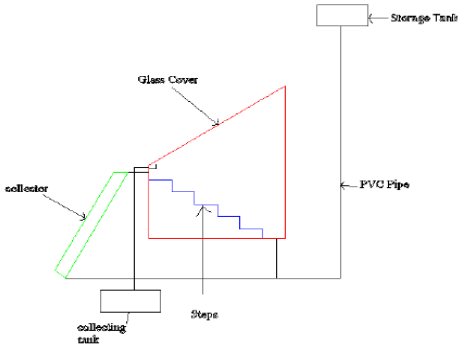

Fig. 2. Schematic diagram of stepwise active single-slope solar still

III. RESULTS AND DISCUSSION

In this study, conventional single basin solar still was modified to stepwise basin solar still. For further enhancement, flat plate collector was integrated along the solar still. The glass and basin water temperature changed with changes in ambient temperature. The temperature gradually increased with increase in solar radiations and reached to maximum at 2 pm. On first day, maximum glass cover temperature and basin water temperature was recorded as 61.2°C and 61.5°C respectively.

TABLE I: Daily maximum and average temperature profile shows maximum and daily average temperature values of glass cover and water in stepwise solar still. Daily average temperature reached up to 60°C in a solar still.

TABLE I: Daily maximum and average temperature profile

Experiments	1	2	3
Basin water temperature (°C)			
Maximum	61.5	73.3	69.1
Daily Average	48.9	60	51.87
Glass temperature (°C)			
Maximum	61.2	65.8	62.2
Daily Average	52	54.96	49.59

Maximum temperatures were noticed on the second day because of high intensity of solar radiations. The amount of distillate was observed to be increased in the evenings due to decrease in ambient temperature. The difference in temperature of glass cover and basin water increased which led to more condensation. Temperature variation of basin water and glass cover is shown in fig.3.which shows that temperature gradually increased and reached to maximum at noon while both in the morning and evening minimum temperature were noticed. From the experiments, it was noticed that until 10:00 am glass cover temperature was higher than basin water temperature due to lower heat capacity of glass as compared to water. As a result, the temperature increases quickly, and also goes down rapidly by releasing heat energy which it had absorbed from solar radiations [17]. Same temperature profiles were also obtained by other researchers [17]–[20]. Maximum basin water temperature achieved was 73.3°C while that of glass was 65.8°C.

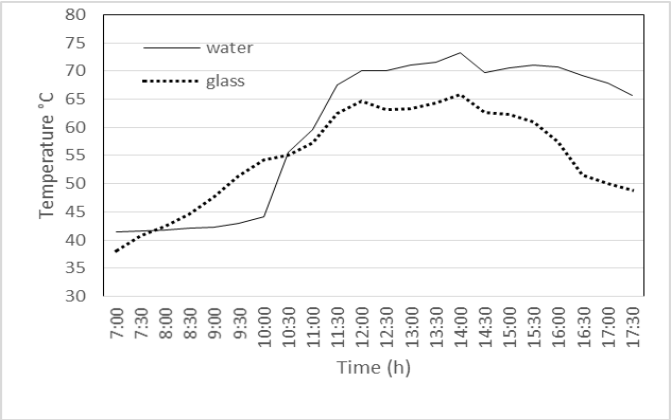

Fig. 3. Temperature variation in glass cover and basin water

The distillate yield of stepwise solar still for different experiments is shown in fig. 4. On first day 1700 ml yield was obtained while on second and third day the yield approached 2150 ml and 1750 ml respectively. Highest yield obtained was 2100 ml when temperature was high as compare to other days. Average daily output obtained was 2.24 L/m^2 while theoretical output was 3.78 L/m^2, which shows 60 % efficiency of the still.

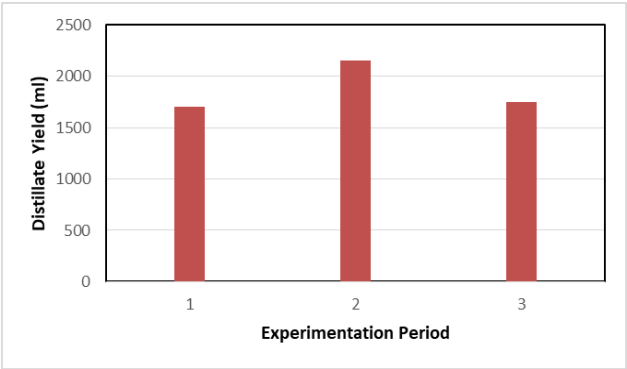

Fig. 4. Distillate yield of step-wise solar still during experimentation

Fresh water production at minimum cost and payback period are very important which assesse feasibility of the solar still. Cost refers to materials cost and labour cost. Fabrication cost of the stepwise solar still is Rs. 11910, assume that system work for 10 years and adding Rs. 1000 variable cost per year so the total cost for 10 years is RS. 21910. Moreover, the total distilled water produced during 10 years for 300 days per year at daily average output is 2 × 300 × 10= 6000 L. The cost of 1 L fresh water is 21910/6000=Rs 3.65. In market the price of 1 L water bottle is Rs. 50 and 2 L average output is obtained in one month 2*50*30= Rs. 3000 is obtained so the payback period is 7 months.

IV. CONCLUSION

In the present study performance of the solar still was investigated by carrying out experiments on stepwise solar still coupled with flat plate solar collector. Average daily output of fresh water was 2.24 L/m^2 which gave 60% efficiency of the desalination unit. Solar radiation had direct impact on distillate yield and high production rate was obtained with maximum solar intensity. Depth of water in the basin had also prominent impact on production yield, higher distillate output was observed with lower water depth. Introduction of pebbles in the basin increased the product yield and solved channelling problem by distributing water uniformly. Cost analysis and payback period shows that desalination unit is feasible and operable.

REFERENCES

[1] H. Sharon, K. S. Reddy, D. Krithika, and L. Philip, “Experimental performance investigation of tilted solar still with basin and wick for distillate quality and enviro-economic aspects,” *Desalination*, vol. 410, pp. 30–54, 2017.

[2] H. Pak, “Building Integrated Solar Desalination (BIDSAL) : Preliminary works with multiple effect solar still,” *Energy Procedia*, vol. 62, pp. 639–646, 2014.

[3] G. Xiao, X. Wang, M. Ni, F. Wang, W. Zhu, Z. Luo, and K. Cen, “A review on solar stills for brine desalination,” *Appl. Energy*, vol. 103, pp. 642–652, 2013.

[4] S. Joe Patrick Gnanaraj, S. Ramachandran, and David Santosh Christopher, “Enhancing the design to optimize the performance of double basin solar still,” *Desalination*, vol. 411, pp. 112–123, 2017.

[5] S. A. El-Agouz, Y. A. F. El-Samadony, and A. E. Kabeel, “Performance evaluation of a continuous flow inclined solar still desalination system,” *Energy Convers. Manag.*, vol. 101, pp. 606–615, 2015.

[6] O. Bait and M. Si-Ameur, “Numerical investigation of a multi-stage solar still under Batna climatic conditions: Effect of radiation term on mass and heat energy balances,” *Energy*, vol. 98, pp. 308–323, 2016.

[7] M. S. S. Abujazar, S. Fatihah, A. R. Rakmi, and M. Z. Shahrom, “The effects of design parameters on productivity performance of a solar still for seawater desalination: A review,” *Desalination*, vol. 385, pp. 178–193, 2016.

[8] S. W. Sharshir, A. H. Elsheikh, G. Peng, N. Yang, M. O. A. El-Samadony, and A. E. Kabeel, “Thermal performance and exergy analysis of solar stills – A review,” *Renew. Sustain. Energy Rev.*, vol. 73, no. December 2016, pp. 521–544, 2017.

[9] V. Velmurugan and K. Srithar, “Performance analysis of solar stills based on various factors affecting the productivity — A review,” *Renew. Sustain. Energy Rev.*, vol. 15, no. 2, pp. 1294–1304, 2011.

[10] H. Aybar, F. Egeliofglu, and U. Atikol, “An experimental study on an inclined solar water distillation system,” vol. 180, pp. 285–289, 2005.

[11] H. Ş. Aybar, “Mathematical modeling of an inclined solar water distillation system,” vol. 190, pp. 63–70, 2006.

[12] A. K. Singw, G. N. Tiwarit, P. B. Sharma, and E. Khan, “OPTIMIZATION OF ORIENTATION FOR HIGHER YIELD OF SOLAR STILL FOR A GIVEN LOCATION,” vol. 36, no. 3, pp. 175–181, 1995.

[13] Z. M. Omara, A. E. Kabeel, and A. S. Abdullah, “A review of solar still performance with reflectors,” *Renew. Sustain. Energy Rev.*, vol. 68, no. September 2016, pp. 638–649, 2017.

[14] Z. M. Omara, M. A. Eltawil, and E. A. ElNashar, “A new hybrid desalination system using wicks/solar still and evacuated solar water heater,” *Desalination*, vol. 325, pp. 56–64, 2013.

[15] A. N. Minasian, “A. N. MINASIAN and A. A. AL-KARAGHOULI,” vol. 36, no. 3, pp. 213–217, 1995.

[16] S. Abdallah, O. Badran, and M. M. Abu-khader, “Performance evaluation of a modified design of a single slope solar still,” vol. 219, pp. 222–230, 2008.

[17] B. I. Ismail, “Design and performance of a transportable hemispherical solar still,” *Renew. Energy*, vol. 34, no. 1, pp. 145–150, 2009.

[18] E. Rubio-Cerda, M. A. Porta-Gándara, and J. L. Fernández-Zayas, “Thermal performance of the condensing covers in a triangular solar still,” *Renew. Energy*, vol. 27, no. 2, pp. 301–308, 2002.

[19] O. O. Badran, “Experimental study of the enhancement parameters on a single slope solar still productivity,” vol. 209, pp. 136–143, 2007.

[20] M. Sakthivel, S. Shanmugasundaram, and T. Alwarsamy, “An experimental study on a regenerative solar still with energy storage medium - Jute cloth,” *Desalination*, vol. 264, no. 1–2, pp. 24–31, 2010.

Synthesis of Geopolymeric Membrane Using Locally Available Rice Husk Ash as a Source Material

Fazli Saeed[a], Amir Naveed[b], Saeed Gul[c]

Abstract **-- Rice husk (RH) is mainly produced in the rice processing industry which is then used for burning, resulting in high percentage of ash as waste. These ashes contain up to 95 % SiO2 which are highly porous with low density and amorphous in nature. In the present study, the rice husk ash (RHA), which is a waste, has been utilized for the synthesis of Geopolymer inorganic membrane. The RHA was characterized through XRF for mineralogical composition and XRD for phase identification. The characterization results showed that the RHA is suitable for synthesizing geopolymeric membrane.**

Key words**— Geopolymerization, Rice husk ash, Microporous membrane, Chemical activation.**

I. INTRODUCTION

Geopolymerization is a geo-synthesis and innovative technology that involves a heterogeneous chemical reaction between solid aluminosilicate oxides and alkali metal silicate solutions in a highly alkaline conditions at a low temperatures [1]. Joseph Davidovits discovered a new class of inorganic materials in 1978 as geopolymer resins/ binders as a substitute of cements at the Cordi-Géopolymère private research laboratory, Saint-Quentin, France. Generally the inorganic geopolymer are synthesize by the alkali activation of aluminum-silicate minerals which are rich in SiO2 and Al2O3 [2] and [3]. These depends on the linkage Structure of alumino-silicate as sialate bond (Si-O-Al) and siloxo bond (Si-O-Si). The ratio between Si and Al has a great contribution in the formation of geopolymer structure such as Si/Al = 1 refers to poly (sialate), Si/Al = 2 refers to poly (sialate-siloxo), Si/Al = 3 refers to poly (sialate-disiloxo) and the cross link bridge structure.

So, the mechanism of geopolymerization can be done by three steps:

i. Dissolution of the aluminosilicate in highly alkaline solution
ii. Polycondensation reaction into an amorphous, cross-linked, 3D structure
iii. Transportation via a water-assisted mechanism

Geopolymers are mainly composed of two main parts such as source material and chemical activator (alkali solution). Source material should be high percentage in silicon and Aluminium. These aluminium silicate materials could be available either naturally (kaolinite clay, mica) or as a by-product/ waste materials (fly ash,silica fumes, slag, rice husk ash and red mud)

RH is one of the abundantly available biomass fuels in many rice producing countries. Approximately 600 million tons of rice paddy is produced every year. Rice paddy produces about 20 % husk, resulting an annual total production of 120 million tons of rice husk [4].

Si:Al=1 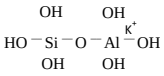 Ortho- Sialate

Si:Al=2 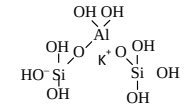 Ortho (Sialate-siloxo)

Si:Al=3 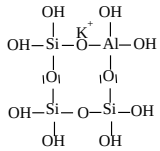 Ortho (Sialate-disiloxo)

Figure 1: Different linkage structures of geopolymer

Burning of rice husk in ambient atmosphere leaves a residue about 25 % which is termed as rice husk ash (RHA) [5]. As the RHA contains large percentage of silica content, therefore, the extraction of silica from RHA is comparatively more economical. The ash from the Rice husk contain about 85-98% silica which is highly porous (87 %) and light in weight, with a very high specific surface area of 450 m2/gm [6-7]. RHA can be used as an economical, cheap and substitute source of amorphous silica for creating silicon based materials with different industrial and technological interests. The avg. particle size of RHA is 150.46 µm, bulk density is 105 kg/cm3, BET surface area is 36.44 m2/gm, average pore diameter by BET is 42.6 0A and BJH (method for evaluation of mesopore size distribution) pore area showed 80% of the pore area due to the mesoporous [8].

Inorganic membrane synthesis is comparatively costly due lengthy steps involved during preparation. Most of the membrane have different problems at synthesizing steps such as operational problem, life of membrane, amorphous in nature etc.

The benefits of ceramic and composite membranes have high resistance against high temperature and harsh chemicals while the permeability to liquid and gases are relatively low in ceramic membrane as compared to organic membranes. The manufacturing of ceramic membranes involve a sintering

Fazli.saeed@yahoo.com
[c] University of Engineering & Technology, Peshawar, Pakistan

process having high temperature upto 1000 °C which make the manufacturing process highly temperature intensive.

In the present study, RHA has been used as a silica source material for the synthesis of porous geopolymeric membrane. Geopolymerization bonding avoid flaws such as disorder of pore arrangement, pore shrinkage and pore collapse hence resulting in comparatively regular pores.

II. MATERIAL AND METHODS

The basic raw materials used in the synthesis of inorganic geopolymer membranes are:

- Silicon
- Aluminium
- Alkali activator

The present study focused on the selection of economical source of silicon from waste material. Rice husk ash is one of the waste source for silicon as SiO_2. Different samples of rice husk (RH) and rice husk ash (RHA) were collected from different spots of the swat region of kpk Pakistan. All variety of RH and RHA were collected separately in polythene bags and combine together as RH and RHA sample respectively. The burning of RH in air depends on various factors such as the variety of RH, burning conditions and type of furnace used. It was treated and tested for the synthesis of geopolymer inorganic membrane for micro filtration. It was found that the RHA possess high quality and high percentage of amorphous silicon dioxide (SiO_2).

Figure 2: (a) Rice Husk (RH) (b) Rice husk Ash (c) Thermally treated (RHA)

The RH was processed carefully to achieve a high quality amorphous silica (SiO_2) as a source material that use in the fabrication of geopolymer membrane. The RH was washed with a 0.1 M solution of HCL for half an hour, for the removal of physical and chemical contaminations. After acid washing, rinsed with distilled water thoroughly and dried it at a temperature of 100 °C. The washed dry rice husk was then burned in an open ambient environment.

The processed RHA was activated by three different activation techniques such as

Thermal activation,
Mechanical activation and
Chemical activation.

Aluminium Sulphate ($Al_2 (SO_3)_4$) was used as a second source material to create the ratio between Silicon and Aluminium (Si/Al) for geopolymerization. The mass percentage of Aluminium in $Al_2 (SO_4)_3$ was calculated as 15.8 %. The density of anhydrous Aluminium sulphate [$Al_2 (SO_3)4.6H_2O$] is 2.672 gm/cm^3 is used.

The Aluminosilicate materials from RHA as a SiO_2 and Aluminium from $AL_2 (SO_4)_3$ were typically activated by various alkali hydroxides and silicates under a high pH values. Sodium hydroxide and sodium silicate were used for the activation of source materials. The 99.5 % concentrated sodium hydroxide flake from Haq chemicals Pakistan Pvt Ltd. were used. A 15M solution of NaOH was prepared for the dissolution of source material to develop a micro-structure in the synthesis of geopolymeric membrane. For 15M solution, the mass of 600 gm was dissolved in water to prepared one litre alkali solution.

The sodium silicate (liquid glass) are usually available in hydrated form. In the present study, sodium silicate ($Na_2SiO_3.24\ H_2O$) was used from Haq Chemicals Pakistan Pvt Ltd. The composition of used sodium silicate was Na_2O=16.29 %, SiO_2= 34.51 % and H_2O=49.22 %.

III. METHODOLOGY

Geopolymer paste was prepared by mixing a source material and alkali activators using different ratios. Four samples of source material having different ratios of Si/Al in source material were 2.5, 3.0, 3.5, and 4.0 were represented by M_1, M_2, M_3, and M_4. Each of the sample was alkali activated with a various ratios of 1, 1.5, 2.0 and 2.5 as represented by (M_{11}, M_{12}, M_{13}, and M_{14}), (M_{21}, M_{22}, M_{23}, and M_{24}), (M_{31}, M_{32}, M_{33}, and M_{34}) and (M_{41}, M_{42}, M_{43}, and M_{44}). Separate mixing were adopted. In a 1st step, source materials were thoroughly mixed with 15M NaOH solution for 15 -20 minutes to make the mixture homogeneous for each sample. Then added the sodium silicate solution in the required mixture and was blended carefully.

In the present study, the resultant geopolymeric paste was achieved by sol-gel technique and covered with aluminium foil. The high density plastic moulds of 50 mm were used with a thickness of 5 mm. Before casting the geopolymeric paste, an oily layer was used to prevent adhesion between the paste and mold. The casted moulds were then treated hydrothermally at a temperature of 60 ˚C for 24 hr. as shown in figure 3a and 3b.

Figure 3a: Hydrothermal treated geopolymer membranes

The hydrothermal process is responsible for developing nucleation in minerals under the condition of circulating the pressurized hot water in closed vessel.

Figure 3b: High compressive strength Polished geopolymer inorganic membrane

IV. RESULTS AND DISCUSSION

The elemental composition of as-received and processed RHA was analyzed through x-ray florescence (XRF) whereas the loss on ignition (LOI) was performed at 1050 °C for half an hour in muffle furnace. The results are shown in table 2.

Table 2: XRF of As-received and Processed RHA

Comp-%	As-received	Processed RHA
SiO_2	70.17	87.34
Al_2O_3	0.49	0.74
Fe_2O_3	0.27	0.39
CaO	2.67	3.00
MgO	0.48	0.26
Na_2O	0.50	0.43
K_2O	0.71	0.78
LOI	14.3	1.17

The processed RHA was then grinded and analyzed by coulter Counter particle analyzer. The particle size distribution is shown in figure 4. The average particle size obtained was 8.12 µm which is in the range for the synthesis of inorganic microfiltration membrane. The lower particle size creates large surface area, which is very useful in the first step of geopolymerization (dissolution) and consequently increases the reactivity of amorphous RHA.

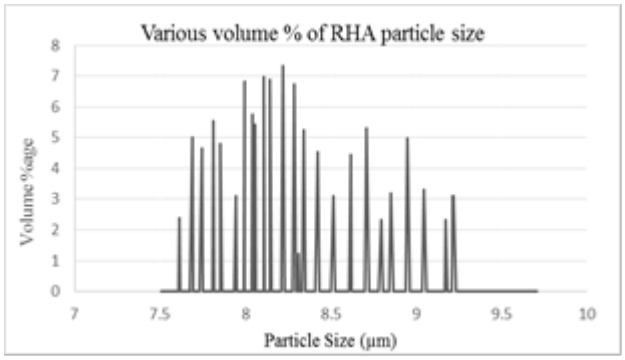

Fig. 4: RHA volume-% and Particle Size (µm).

The powered diffraction XRD apparatus, Model: JDX-3532-JEOL, Japan was used in this research having the copper tube of voltage 40.0 kV with a tube current of 30.0 mA and count time is 2 second thermally activated RHA was analyzed using XRD technique as shown in figure 5 . It was found from the broad and hump type graph that the silica obtained from RHA was amorphous in nature. The amorphous nature of RHA may expect a tangled solid mass having long chain molecules or a 3-dimentional network atoms with small order chain molecule. The structure form from the amorphous SiO2 of RHA could be of short range order in-between the silicon and oxygen atoms as sialate, poly sialate-siloxo or poly sialate disiloxo.

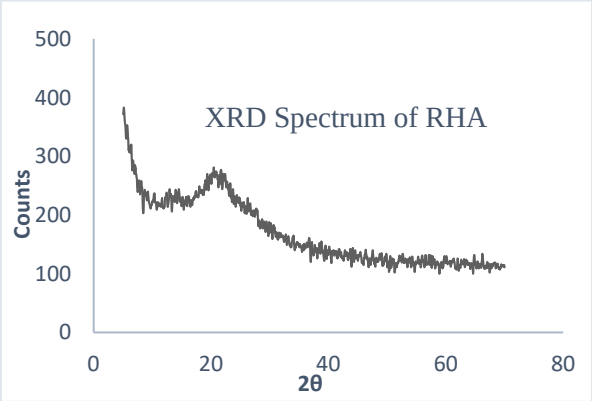

Fig. 5: XRD spectrum of RHA

V. CONCLUSIONS

It has been concluded that the rice husk biomass produced large amount of ash as compared to other bio-mass fuels. The ash from rice hush, produced about 87 % SiO2, The phase identification of RHA through XRD found that the SiO2 is amorphous in nature which is suitable for the process of geopolymerization.

Both the thermal and mechanical activation of RHA exhibit a high compressive strength in the synthesis of geopolymeric membranes.

REFERENCES

[1] D. Dimas, I. Giannopoulou and D. Panias, Polymerization in sodium silicate solutions: a fundamental process in geopolymerization technology, J. Mater Sci., 44, 3719-3730, 2009.

[2] Davidovits J., Geopolymer Chemistry and Applications 4th edition, Published by: Institut Géopolymère 16 rue Galilée F-02100 Saint-Quentin France, November 2015, polymer and geopolymer, Ch. 1, pp 3-5.

[3] Davidovits J., Geopolymer cement to minimize carbon-dioxide greenhouse-warming. Ceramic Transaction, 37, 165–182, 1993.

[4] Giddel M.R and. Jivan A.P, Waste to Wealth, Potential of Rice Husk in India, a Literature Review, International Conference on Cleaner Technologies and Environmental Management PEC, and Pondicherry, India, Jan 4-6, 2007.

[5] Koteswara Rao. D and Pranav. P.R.T, Stabilization of expansive soil with rice husk ash, lime and gypsum–an experimental study, International Journal of Engineering Science and Technology (IJEST), Vol. 3 (11), 8076-8085 November 2011.

[6] Della, V.P., Kuhn, I. and Hotza, D. Rice husk ash as an alternate source for active silica production. Material Letters, 57(4), 818– 821, 2002.

[7] TakanoriI Watari , Akihiro Nakata, Yoshimi Kiba, Toshio Torikai, Mitsunori Yada, Fabrication of porous SiO2/C composite from rice husks Journal of the European Ceramic Society 26, 797–801, 2006.

[8] Vimal Chandra shrivastava, indra deo mall, indra mani Mishra, , characterization of mesoporous rice husk ash (RHA) and adsorption kinetics of metal ions from aqueous solution onto RHA, journal of hazardous materials, B134, 257-267, 2006

Development of PEBAX 2533/ZIF-7 MMMs for Gas Separation

Muhammad Wajahat ur Rehman and Jamil Ahmad

Abstract— **Apart from the fact that there are number of technologies under evaluation for separation for carbon dioxide from flue gases, but membrane based separation technology has captured the attention of many researchers because of its advantages over other conventional methods which include environmental stability, simplicity and small footprints. The trade-off between permeability and selectivity introduced by Robeson in 2008 restricts the application of membrane technology on industrial scale. This research work lead to fabrication of self-supported mixed matrix membrane MMM which used Pebax-2533 as polymer matrix in combined effect of zeolitic imidazole framework ZIF-7. ZIF-7 used as inorganic filler in Pebax membrane is expected to improve the permeation performance of MMM. The developed self supported MMM was characterized to investigate the morphological, structural and chemical properties. This research also includes the synthesis of ZIF-7 at room temperature instead of conventional methods which use high temperature and pressure. The selectivity and permeability of pristine Pebax membrane is 33.8 and 351 respectively which are expected to rise because of introduction of ZIF-7.**

Index Terms- Pebax, ZIF-7, Mixed Matrix Membranes, Gas Separation

I. Introduction

The increasing concentration of CO_2 in earth's atmosphere leading to global warming is accepted worldwide. According to a study, the concentration of CO_2 can double in 2050 if this issue is not addressed properly. However the recent research is focused on taking solid actions to combat this problem which include CO_2 capture and storage, renewable energy and energy efficiency [1]. Fossil fuels have been used on large scale for various purposes which result in production of huge amount of CO_2, fueling the global warming. Studies show that CO_2 concentration in atmosphere has increased from 276-387ppm in the last century. If usage of fossil fuel for energy production keep at same rate then it can lead to 32Gton/year of CO_2 emission till 2050 [2].

There are different technologies used for CO2 capture which include adsorption, cryogenic distillation, absorption and membrane processes. Amine absorption is the commonly used for post combustion CO_2 capture which can separate almost 90% of CO_2 in the flue gas but in amine absorption processes solvent is lost because of evaporation along with formation of stable complexes which add to the cost of separation process. Recently membrane processes are receiving more attention as they have advantages like energy efficiency, environmental sustainability and small footprints [2]. Besides many studies and experimental evaluations the permeability selectivity trade-off restricts the application of polymeric membranes on large scale [3].

On lab scale, high selectivity and permeability is given by inorganic materials but their fragile structure and expense make them a poor choice to be applied on large scale [4]. However the mixed matrix membranes (MMM), comprising polymers as base and inorganic particles as filler media have been evaluated and investigated for separation of gases and to transcend their results on Robeson's upper bound [5].

Different combinations of polymeric materials and inorganic fillers have been evaluated for gas separation in last decade [6-10]. New MMM have been developed by incorporating many inorganic fillers like carbon molecular sieves, TiO_2, silica and zeolites have been incorporated in to polymeric materials. Similarly inorganic fillers have also been modified to improve the permeation performance of MMMs [11-13]. Ethylene oxide (EO) has shown reasonable potential to separate CO_2 from light gases since it has polar ether group [14] but its application has been restricted because of lack of mechanical stability and partial crystalline structure [15]. Different research works conducted recently have considered poly ethylene oxide (PEO) since it is feasible for fabrication of membranes designed for CO_2 separation [16,17].

Pebax is an elastomer which comprise elastic segment polyether and a rigid segment called polyamide. Pebax copolymers are made up of dicarboxilic acid and polyoxyalkene glycol and has shown huge potential for separation of CO_2 from light gases after series of investigations [18]. The polyamide segment provides mechanical strength to membrane where as soft and amorphous polyether facilitates the gas permeation [19]. Pebax has the following structure.

Muhammad Wajahat ur Rehman is research scholar at University of Engineering and Technology, Peshawar, Kyber Pakhtunkhwa, Pakistan (email: engrwaji@yahoo.com)
Jamil Ahmad is serving as Associate Professor at Department of Chemical Engineering, University of Engineering and Technology, Peshawar, Khyber Pakhtunkhwa , Pakistan (engrjamilahmad@gmail.com)

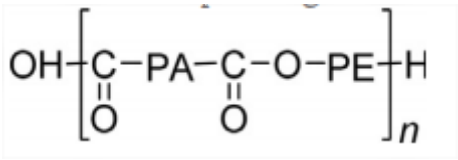

Where PA= polyamide
And PE= polyether

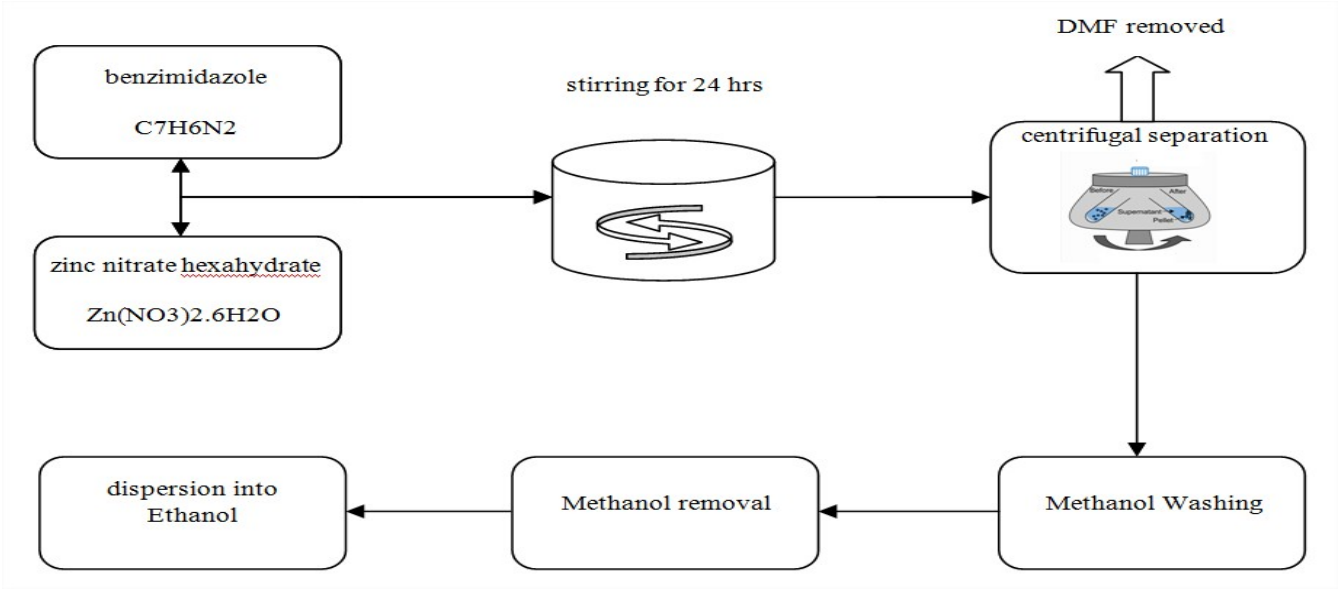

Fig. 1. Synthesis of ZIF-7 nano particles at room temperature

Pebax has several grades in which polyamide and polyether phases are in different ratios. Pebax series has been investigated by Rezac. et al. This series comprise Nylon-12 which serves as hard phase and polytetramethylene oxide is soft phase. The results from research work carried out Rezac et al. clearly indicates that Pebax-2533 shows excellent permeation performance as compared to other grades which included 6333, 3533 and 5533[20]. This research work is based on synthesis of MMM comprising Pebax-2533 and ZIF-7 nano particles which were also characterized for chemical and morphological properties.

Metal organic framework (MOF) have been incorporated in many MMMs with promising permeation performances [21,22]. Good compatibility have been shown by ZIF-7 nano-fillers with Pebax [23] which makes it reasonable choice for incorporation in MMMs.

II. Theory and Background

Solution diffusion mechanism explains the gas transportation in polymer based dense membranes, according to which the penetrant molecules from upstream are adsorbed in to membranes and then diffused across the membrane to downstream. The driving force in this permeation is chemical potential gradient. Permeability of a membrane is the product of solubility and diffusivity coefficient which has been shown by the equation below:

$P_i = D_i.S_i$

Where P= permeability of component *i*
D= diffusivity coefficient and
S= sorption coefficient

Permeability is commonly measured in Barrers.

1 barrer= 10^{-10} $cm^3.cm/(cm^2.sec.cm\ Hg)$

Permeability is also expressed as

$P_i = \frac{LN_i}{\Delta P_i}$

Where L= membrane thickness (cm)
N_i= flux through membrane (cm^3/s)
ΔP_i= trans membrane pressure

III. Experimental

A. Materials

Benzimidazole was purchased from Sigma-Aldrich and Pebax 2533 was provided by Arkema. All other chemicals were provided by department of Chemical Engineering, UET Peshawar, Pakistan.

B. ZIF-7 synthesis

A mixture of $Zn(NO_3)_2$ and benzimidazole was dissolved in Dimethylformamide by stirring the solution for 24 hours at room temperature. The resulting product was separated by centrifugal separation. Later the product was washed three times with methanol. Finally the solid portion of the solution was dispersed in 30/70 wt% H_2O/Ethanol solution. This step

is performed to avoid the agglomeration that happen in drying step. Fig.1 illustrates the different steps involved in ZIF-7 synthesis [24].

C. *MMM and ZIF-7 characterization*

JDX-3532 X-ray diffractometer was used to measure X-ray diffraction (XRD) patterns of ZIF-7. Scanning Electron Microscope (JSM-5910) was used examine the morphology of ZIF-7 and MMMs. MMMs are broken under liquid nitrogen to investigate the cross- section of MMMs.

D. *Membrane Synthesis*

Solvent evaporation technique is used to synthesize flat sheet Pebax-2533 membrane. A homogeneous 3wt% solution of Pebax 2533 was prepared by adding polymer into ethanol and stirring for 4 hours at 70°C. The homogeneous polymer solution was slowly brought to room temperature and then poured in to Teflon Petri Dish to prepare pristine Pebax-2533 membrane. Suitable quantities of ZIF-7 were added to polymer solution to prepare MMM solutions. Ultrasonic mixing was used to for dispersion of ZIF-7 nanofillers into polymer solution. The MMM solution was then casted on Teflon Petri Dishes and funnels were used to cover them to avoid any dust particles. These solutions were kept at room temperature for one day for solvent evaporation and then placed in vacuum oven for almost 12 hours. Then the temperature was gradually increased up to 70°C. The membranes were kept at this temperature for almost 15 hours and then cooled gradually to room temperature. Fig. 2 shows different steps involved in membrane synthesis.

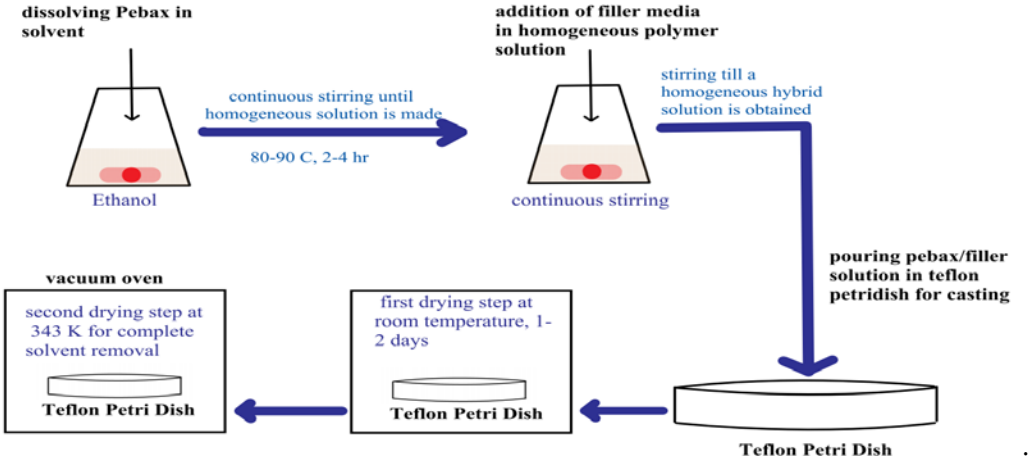

Fig. 2. synthesis of Pebax based mixed matrix membrane by solution casting method

IV. Results and Discussion

A. *Characterization*

The XRD pattern of synthesized nano-particles in fig. 3, when compared with previous works clearly indicate that resultant product is ZIF-7. SEM images show that ZIF-7 particles as shown in fig. 4 have size range of 60-90nm which is also in accordance with several studies [25]. The gold coating of almost 10nm was applied to the particles.

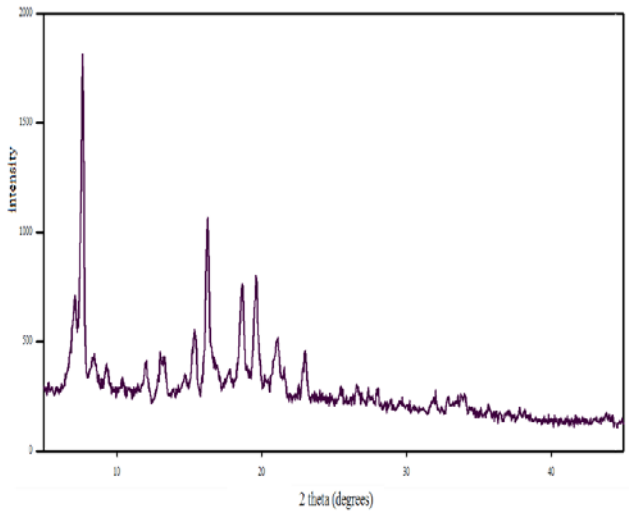

Fig. 3. Xrd pattern of synthesized ZIF-7 particles.

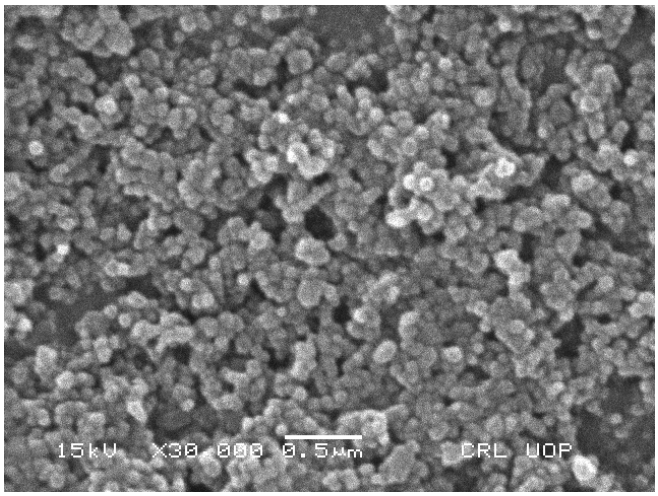

Fig. 4. SEM image of synthesized ZIF-7 particles

The aperture size of synthesized particles is almost 0.32 nm [23]. Carbon dioxide has relatively wider kinetic diameter (0.34nm) as compared to aperture size of ZIF-7 but the gate opening ability of ZIF-7 particles allows the passages of larger molecules to pass through it. ZIF-7 nanofillers do not show any gate opening effect for N_2 molecules.

The SEM images of MMM composed of ZIF-7/2533 in Fig.5 show that ZIF-7 particles are dispersed in polymer phase and does not show any agglomeration with no wetting property between filler phase and Pebax phase. Similarly no

voids were observed with incorporation of ZIF-7. It should be noted that filler particles were not given pretreatment before incorporation. It can be concluded that Pebax chain mobility and ZIF-7 hydrophobic nature contributed to such excellent contact between the two media. Most of the recent work on glassy polymer based MMMs show particles agglomeration which was not spotted in this research work. Dispersion of filler media is crucial for good separation performance of MMMs, especially when a thin layer of membrane is fabricated.

B. *Permeation*

Recent works [23] have shown that the addition of ZIF-7 in Pebax grades can increase the permeability and selectivity of MMM by high percentages which has been shown in Table I . ZIF- 7 has shown impressive morphological and structural results on addition with Pebax-2533 which are also expected to transcend in the form of gas permeation performance of resultant MMM. The permeability and selectivity of pristine Pebax 2533 membrane is 351 barrer and 33.8 [27] respectively which are expected to increase considerably upon addition of ZIF-7.

TABLE I. PERMEATION PERMFORMANCE OF PEBAX BASED PRISTINE AND MMMS.

Pebax Grade	Material incorporated	Permeability (barrer)	Selectivity CO_2/N_2
1657	non	72 [23]	34 [23]
2533	non	351 [27]	33.8 [27]
1657	ZIF-7	111 (54% increase) [23]	97 (185% increase)[23]
2533	ZIF-7	400+ (expected)	50+ (expected)

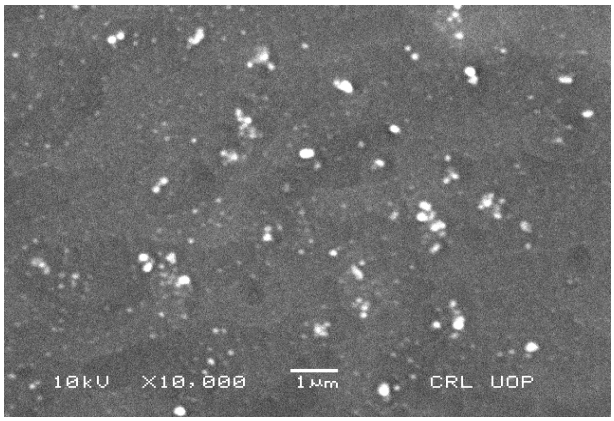

Fig. 5. SEM suface image of ZIF-7/Pebax2533 MMM.

V. CONCLUSIONS

In present study an inorganic filler called ZIF-7 has been incorporated in to Pebax 2533 phase to prepare a self supported mixed matrix membrane for gas separation, aiming more specifically at separation of CO_2 from flue gases. ZIF-7 particles were synthesized at room temperature. SEM images of ZIF-7 particles indicate that ZIF-7 particles were discrete with size range of 60-90nm. The XRD pattern of synthesized ZIF-7 particles were also in accordance previous studies. The mixed matrix membrane prepared also exhibited excellent morphology with impressive adhesion between the ZIF-7 and polymer phase. Apart from that no agglomeration of ZIF-7 particles was observed in synthesized MMM. These results are expected to lead good permeation results.

REFERENCES

[1] H. Yang, Z. Xu, M. Fan, R. Gupta, R.B. Slimane, A.E. Bland, I. Wright. (2008). Progress inmcarbon dioxide separation and capture: a review, J. Environ. Sci. 20. pp. 14–27.

[2] R.W. Baker, Membrane Technology and Applications, Wiley, Chicester, 2012

[3] L.M. Robeson. (2008) . The upper bound revisited, J. Membr. Sci. 320. pp. 390–400.

[4] H. Cong, M. Radosz, B.F. Towler, Y. Shen. (2007). Polymer–inorganic nanocomposite membranes for gas separation, Sep. Purif. Technol. 55. pp. 281–291.

[5] F. Peng, L. Lu, H. Sun, Y. Wang, J. Liu, Z. Jiang. (2005). Hybrid organic–inorganic membrane: solving the tradeoff between permeability and selectivity, Chem. Mater. 17. pp. 6790–6796.

[6] S. Kulprathipanja. (2003). Mixed matrix membrane development, Ann. NY Acad. Sci. 984. pp. 361–369.

[7] D.Q. Vu, W.J. Koros, S.J. Miller. (2003). Mixed matrix membranes using carbon molecular sieves: I. Preparation and experimental results, J. Membr. Sci. 211. pp. 311–334.

[8] Y. Dai, J.R. Johnson, O. Karvan, D.S. Sholl, W.J. Koros. (2012). Ultems/ZIF-8 mixed matrix hollow fiber membranes for CO_2/N_2 separations, J. Membr. Sci. 401– 402. pp. 76–82.

[9] J. Ahmad, M.-B. Hägg. (2013). Preparation and characterization of polyvinyl acetate/ zeolite 4A mixed matrix membrane for gas separation, J. Membr. Sci. 427. pp. 73–84.

[10] K. Díaz, M. López-González, L.F. del Castillo, E. Riande, Effect of zeolitic imidazolate frameworks on the gas transport performance of ZIF8-poly(1,4- phenylene ether-ether-sulfone) hybrid membranes, J. Membr. Sci. 383. pp. 206–213.

[11] N.P. Patel, J.M. Zielinski, J. Samseth, R.J. Spontak. (2011). Effects of pressure and nanoparticle functionality on CO_2-selective nanocomposites derived from crosslinked poly(ethylene glycol), Macromol. Chem. Phys. 205 (2004) 2409–2419.

[12] D. Shekhawat1, D.R.L., a.H.W.P., A Review of Carbon Dioxide Selective Membranes, U.S. Department of Energy, 2003

[13] C.H. Lau, D.R. Paul, T.S. Chung. (2012). Molecular design of nanohybrid gas separation membranes for optimal CO_2 separation, Polymer 53. pp. 454–465.

[14] W. Yave, A. Car, K.V. Peinemann. (2010). Nanostructured membrane material designed for carbon dioxide separation, J. Membr. Sci. 350. pp . 124–129.

[15] H. Lin, B.D. Freeman. (2005). Materials selection guidelines for membranes that remove CO_2 from gas mixtures, J. Mol. Struct. 739. pp. 57–74

[16] W. Yave, A. Car, S.S. Funari, S.P. Nunes, K.V. Peinemann. (2009). CO_2-philic polymer membrane with extremely high separation performance, Macromolecules 43. pp. 326–333.

[17] S.R. Reijerkerk, M.H. Knoef, K. Nijmeijer, M. Wessling. (2010). Poly(ethylene glycol) and poly(dimethyl siloxane): combining their advantages into efficient CO_2 gas separation membranes, J. Membr. Sci. 352. pp. 126–135.

[18] [18] V.I. Bondar, B.D. Freeman, I. Pinnau. (2000). Gas transport properties of poly(ether-bamide) segmented block copolymers, J. Polym. Sci. Part B: Polym. Phys. 38. pp. 2051–2062.

[19] V. Barbi, S.S. Funari, R. Gehrke, N. Scharnagl, N. Stribeck. (2003). SAXS and the gas transport in polyether-block-polyamide copolymer membranes, Macromolecules 36. pp. 749–758.

[20] M.E. Rezac, T. John, P.H. Pfromm. (1997). Effect of copolymer composition on the solubility and diffusivity of water and methanol in a series of polyether amides, J. Appl. Poly. Sci. 65. 1983–1993.

[21] T.X. Yang, Y.C. Xiao, T.S. Chung. (2011). Poly-/metal-benzimidazole nano-composite membranes for hydrogen purification, Energ. Environ. Sci. 4. pp. 4171–4180.

[22] C. Zhang, Y. Dai, J.R. Johnson, O. Karvan, W.J. Koros. (2012). High performance ZIF-8/6FDA-DAM mixed matrix membrane for propylene/propane separations, J. Membr. Sci. 389. pp. 34–42.

[23] T Li, Y.C Pan, K.V Peinemann, Z Lai. (2013). Carbon dioxide selective mixed matrix composite membrane containing ZIF-7 nano-fillers, Journal of Membrane Science 425-426. pp. 235–242.
[24] Y.S. Li, F.Y. Liang, H. Bux, A. Feldhoff, W.S. Yang, J. Caro. (2010). Molecular Sieve Membrane: supported metal–organic framework with high hydrogen selectivity, Angew. Chem. Int. Edit. 49. pp. 548–551.
[25] T.X. Yang, Y.C. Xiao, T.S. Chung. (2011). Poly-/metal-benzimidazole nano-composite membranes for hydrogen purification, Energ. Environ. Sci. 4. pp. 4171–4180
[26] K.S. Park, Z. Ni, A.P. Cote, J.Y. Choi, R.D. Huang, F.J. Uribe-Romo, H.K. Chae, M. O'Keeffe, O.M. Yaghi. (2006). Exceptional chemical and thermal stability of zeolitic imidazolate frameworks, P. Natl. Acad. Sci. USA 103. 10186–10191.
[27] V Nafisi, M-B Hägg. (2014). Development of dual layer of ZIF-8/PEBAX-2533 mixed matrix membrane for CO2 capture, J. Membr. Sci. 459. pp. 244–255.

Risk Management and Analysis of Silica Dust Hazards in Local Stone Crushing Industry

Wajid Ali[1], Sarfaraz Khan[1] and Nehar Ullah[1]

Abstract **-- Silica dust hazards associated with local stone crushing industry causes Silicosis; Inhaling a prolonged crystalline silicon dioxide or silica causes this terrible disease. The current study was carried out among stone crusher workers to assess the hazards of silica dust and associated effects on the workers health due to their exposure to silica dust. Stone crusher impact zones are covered with Granite, Silica sand and Morrum. The various crushing operations involved in stone crushing, e.g. blasting, manual cutting, crushing and transportation, emit fleeting stone dust. These fine particles of stone dust cause health problems like silicosis, asthma etc. among the stone crusher workers. Spirometery (pulmonary function test) and radiology was carried out to assess lungs function of the worker and to find the occurrence of silicosis and other associated diseases in the workers. The study was carried on 157 male workers of age group 25-35, 35-40 and >45 with exposure time 8-12 hours and >12 hours in stone crushers and cement factories in Peshawar, Charsadda, Kohat, Karak, Bannu and Lakki Marwat areas. To find suspended particles and respirable particulate matter in the stone crusher atmosphere high volume sampler was used. Occupational exposure to silica dust leads to development of various pulmonary disorders, silicosis is most important of them. On comparing pulmonary function test of the workers and results derived from high volume sampler, it is concluded that due to exposure of silica containing dust it leads to deterioration of pulmonary functions in workers. Wet working, suitable ventilation where applicable, usage of PPE's and information about preventive measures is recommended for better protection to the worker's health.**

Key words: PPE, Silicosis, Spirometry

I. INTRODUCTION

World Health Organization (WHO) Fact sheet, number 238, of the month of May 2000, recorded for the period 1991-1995, in China only, greater than 500,000 cases of silicosis were recorded, recorded statistics reveals that reported new cases were 6,000, and death tool per year was 24,000. Amongst the dead's statistics shows that most workers were in old ages. Whereas data recorded in Vietnam shows that silicosis effected workers were almost 9,000. However statistics recorded in India shows that silicosis exist in a particular group of workers who were in tender ages, working in the extracting of sandy rock and following work in tiny and unhygienic improper ventilated sheds.[1]

air contained dust is always of greater concern because the airborne dusts containing crystalline silica are of particular worry because they are well known to be associated with different pulmonic diseases e.g chronic obstructive pulmonary disease pneumoconiosis, occupational asthma. Workers associated with dust producing processes are always vulnerable particularly in developing countries, wherever there is more poverty and low job availability [2].

Norbert Wagner Mannarswami Nithiyananthan Laura Farina [3], studied to provide guidance and information regarding improvement of working condition and to provide how working condition can be made better in stone crushing units to guide govt, workers, employers and implementers for proper application of OSH at working sites because stone crushing and grinding is important for development because without these processes we can't build roads, buildings etc and other modern facilities of life.

Polluted ambient air around stone crusher industries impacts human and vegetation. Study of The concentration of particulate matter was found above the permissible limit in most of the sites while the concentration of gaseous pollutants was found within the permissible limit as per the standards given by Central Pollution Control Board (CPCB, 2009) G. S. GUPTA1, ANJANI GUPTA2, M. K. GUPTA [4]. Those workers who come across with particulate matter during work at dusty process, analysis indicated serious threat to their health because of high amount of fine particles and silica content. A health survey conducted on stone crusherl workers and local people with the help of annual hospital medical reports. This study indicates that most of the people were suffering from ARI (Acute respiratory infection), bronchitis, asthma, skin disease, eye irritations, and heart diseases. Particulate matter and gaseous pollutants exposure, also affected vegetation growth due to adsorption of above pollutants on leaf, which prevented the process of respiration and photosynthesis. [5,6]

II. 2. METHODOLOGY

A. Selection of Filter Medium

Usually in most of the cases while using HVS concentration is focused on finding the amount of PM10 and TSP (total suspended particulate) concentration. For this particular purpose Glass Micro fiber filters are used because they have little resistance to flow of air, smaller moisture attraction and gathering competence of 99% for smaller particle of size 0.3

[1]Department of Chemical Engineering, University of Engineering & Technology Peshawar, Khyber Pakhtunkhwa, Pakistan

(microns) or particle in bigger size are proper for this purpose. But where there is a need of additional investigation of the particulates is to be tried, to determine precise elements/radicals. For this very purpose those filter should be selected which have a low background concentration of particular substances.[7,8,9]

B. *Preparing the filter prior to use:*

Preparation of filter is the key point of the process because the data afterward gathered will depend upon this step. For this reason all the filter used were kept bare to light and looked for small holes and dirt on surface as filters with deficiencies are unable to be used. To remove small particle of dirt from the filter surface a soft brush was used.
For better results and avoiding imperfections filter paper must not be holed from middle but rather to be hold from. Care should be taken that creasing and folding of filter paper prior to use can affect results. Prior to use Filter papers were desiccated to remove humidity. All the filter papers to be used were numbered and marked and weighed. All the process was recorded with numbers time dated etc [11].

C. *Health Assessment*

To conduct Health assessment of stone crusher workers two steps were taken i) clinical examination ii) pulmonary function examination. Pulmonary function test were conducted through handy data logging spirometer (MIR SPIROBANK Model, A23 made in Italy) according to procedures of the American Thoracic Society (ATS 1991). Pulmonary function assessment was based on values of forced vital capacity (FVC), forced expiratory volume at the end of 1s (FEV1) and peak expiratory flow rate PEF). All workers underwent an anthropometric assessment i-e height and weight. After fixing a nose clip the test was executed in a seating position. A complete flow volume circle was gained from the spirometer. [14] The best values of PEF, FVC & FEV1 from three tries were obtained and used for analysis.

D. *Pulmonary Function Test*

(a) Spirometry of Stone Crusher Workers

Spirometric measurement (Pulmonary function test) was carried out for measuring lung function volume of 177 stone crusher workers through Spirometer and to analyze the factors affecting them. FVC and FEV1 were measured to find out the ratio FEV1/FVC. In the normal person the ratio is about eighty (80%).However in airway blockade this value has decreased to 47 %.In serious airway impediment this reduces to 20 %.The lung function parameters were measured with respect to age, sex and exposure duration which are presented in following tables. Values obtained during the spirometery and lungs function tests were matched with standards obtained for the control group.

(b) Radiology
The chest X-ray of some workers working from more than ten years and was done to find out the effect of silica dust on lungs.

III. RESULTS AND DISCUSSIONS

A. *Health Effect of dust & medical investigations of workers*

Stone crushing industry in Khyber Pakhtunkhwa is an important labour intensive industry engaged in crushing hard rock stone into gravels of dissimilar sizes used as construction of roads, buildings, dames etc. Stone crushing in those areas where this study was conducted is one of the main economic activities that engaged many people. During the process of stone crushing fine powdery fugitive dust is emitted. These substantial fugitive dust emissions pollute the ambient air quality and surrounding environment. Silica dust is not only harmful to human health and local agricultural farm but it adversely affect the environment in local areas and reduce visibility. Air bore Silica from stone crushing units causes serious lungs diseases like silicosis, cancer, Tuberculosis (TB). [13, 14]

B. *Spirometric measurements (Pulmonary Function Test)*

Spirometric measurement (Pulmonary function test) was carried out for measuring lung function volume of stone crusher workers through Spirometer and to analyze the factors affecting them. Values of FVC and FEV1 were measured to find out the ratio FEV1/FVC. For this purpose workers were divided in grouped with respect to ages and were group inyears in categories <25, 25-35, 35-45 and >45. However workers of above category of ages were examined cluster wise i- e (P1-P3), (P4-P6) and (P7-P9).
In the normal humans the ratio of FEV1/FVC is 80 %.However for those individuals having airway obstruction this value decreases to 47 %.In serious airway obstruction this reduces to 20 %.The lung function parameters were measured in relation to age, sex and duration of exposure which are presented in following tables:

TABLE 1: LUNG FUNCTION PARAMETERS OF STONE CRUSHER WORKERS ACCORDING TO AGE GROUP

Study area	Age group	No. of workers	FEV1 (lit.)	FVC (lit)	FEV1/FVC %
Peshawar	<25	10	2.28±0.52	3.30±0.20	69-78
	25-35	16	2.30±0.20	3.40±0.18	67-69
Charsadda (P1-P3)	35-40	13	2.10±0.87	3.31±0.98	63-72
	>45	12	1.97±0.99	3.50±0.11	56-63
	<25	23	2.50±0.73	3.35±0.45	74-79
Kohat	25-35	15	2.30±0.40	3.40±0.30	67-72
	35-40	16	2.07±0.37	3.03±0.35	68-70
Karak (P4-P6)	>45	13	1.93±0.97	3.29±0.20	58-61
	<25	14	2.20±0.73	3.35±0.70	65-73
Bannu	25-35	16	2.00±0.30	3.30±0.40	60-67
Lakki Marwat (P7-P9)	35-45	16	1.70±0.97	3.25±0.50	52-56
	>45	13	1.50±0.83	3.20±0.30	46-55

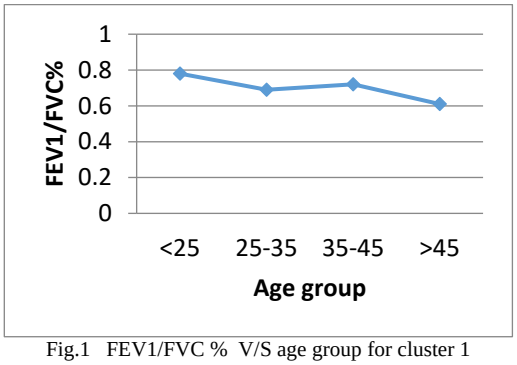

Fig.1 FEV1/FVC % V/S age group for cluster 1

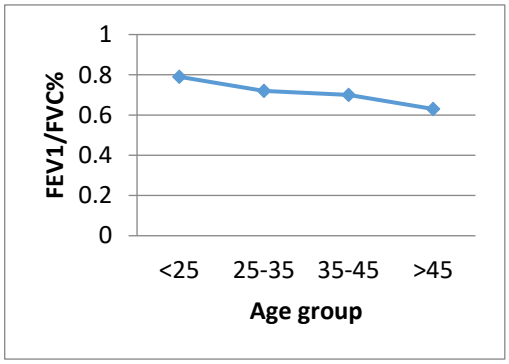

Fig.2 FEV1/FVC % V/S age group for cluster 2

IV. CONCLUSION

A Stone Crushing industry is one of the informal sectors which can create more employment opportunities. It can improve infrastructure facilities at lower cost of production. In the study it was observed that in stone crushing industry health challenges are more due to unhealthy process and non-provision of proper PPE's. Workers need more facilities. Infrastructure facilities are in poor condition in the study areas. On regulation side it was also observed that most of the stone crushers are not cover under any health and safety law. Government should make favorable changes law and should formulate laws for strict implementation in stone crushers.

V. RECOMMENDATIONS

1. Govt of KP must formulate an exclusive law on OSH covering stone crushers to provide Legal coverage to stone crusher workers
2. Provision of PPE'S To Workers must be made mandatory for crusher owners
3. Dust Control techniques must be adopted to reduce effect respirable dust in stone crusher.
4. workers working stone crusher must be educated regarding dust and other hazard and Provide with proper training
5. Workers must be periodically examined for their health condition to monitor their for their respiratory and lungs functions.

VI. ACKNOWLEDGMENT

The authors would like to acknowledge the Department of Chemical Engineering, University of Engineering and Technology, Peshawar, Pakistan for providing the support for this research and the Department of Industries Khyber Pakhtunkhwa and Especially EPA Khyber Pakhtunkhwa for allowing me using their equipment and lab facility and their human resource. In the last I would appreciate the efforts and help provided by the staff of labour Department inspection staff for arrangement of field visits to different stone crushers and cement plants. I can rightly say that without their efforts this research work would have never made possible.

REFERENCES

[1] Weihong Chen, Yuewei Liu, Xiji Huang and Yi Rong Respiratory Diseases Among Dust Exposed Workers 2012; page 134-142.
[2] G. S. GUPTA1, ANJANI GUPTA2, M. K. GUPTA Assessment of Ambient Air Quality of Stone Crusher Industries and its Impacts on Human and Vegetation in and around Bharatkoop Region, Chitrakoot (U.P.) 2014 page 4-6.
[3] Norbert Wagner Mannarswami Nithiyananthan Laura Farina, SAFETY & HEALTH IN THE STONE CRUSHING INDUSTRY, 2009.
[4] Krishnendu MUKHOPADHYAY, Ayyappan RAMALINGAM, Raghunathan RAMANI, Venkatesan DASU1, Arulselvan SADASIVAM, Pramod KUMAR2, Shyam Narayan PRASAD2, Sankar SAMBANDAM1 and Kalpana BALAKRISHNAN, Exposure to Respirable Particulates and Silica in and around the Stone Crushing Units in Central India, 2012, page 223- 235.
[5] James A . Merchant, M.D., Dr. P.H., Silicate pneumoconisis. Occupational respiratory diseases, September 1986: p. 243.
[6] Pannett B, K.T., Toikkanen J et al, Occupational exposure to carcinogens in Great Britain in 1990–93: preliminary results. Carex: International Information System on Occupational Exposure to Carcinogens. Helsinki, Finland: Finnish Institute of Occupational Health. , 1998.
[7] NIOSH Hazard Review. Health Effects of Occupational Exposure to Respirable Crystalline Silica. DHHS 2002-129: p. 5.
[8] Berman, D.W.C., Kenny S, Final draft: technical support document for a protocol to assess asbestos-related risk. . Washington DC: U.S. Environmental Protection Agency., 2003: p. 474.
[9] R. Guild, R.I.E., Airbone pollutants: asbestos. Occupational health practice in the South African mining industry. , 2001: p. 88.
[10] Organization, W.H., Elimination of Silicosis. The global Occupational Health Network Issue No.12-2007.
[11] Coal Dust at the Work Site. CH063 — Chemical Hazards. Government of Alberta, April 2010.
[12] NIOSH., Health Effects of Occupational Exposure to Respirable Crystalline Silica. DHHS (NIOSH) Publication No. 2002–129. Cincinnati, OH, USA, 2002.
[13] M., L., Interspecies comparisons of particle deposition and mucociliary clearance in the tracheobronchial airways. J Toxicol.Environ.Health., 1984. 13441-69.
[14] MM., F., Silica, silicosis, and lung cancer: a risk assessment. Am.J Ind.Med, 2000. 38(1):8-18.
[15] James A. Merchant, M.D., Dr. P.H., Pneumoconiosis: Slicosis. Occupational respiratory diseases, 1986: p. 230.
[16] preventing silicosis. Centers for Disease Control and Prevention. U.S. Department of Health and Human Services., October. 2004.

Textile Industry Wastewater Treatment using DAP, Urea, and Polymer AQUATREAT @AR 06

Qazi M. Omar[1], Ahmad Mukhtar[2], Umar Shafiq[2], Masooma Qizilbash[3], Fatma Safdar[2]

***Abstract*--- Textile Industry is one of the most important and largest industrial sectors in Pakistan. It has a high importance in terms of its environment impact, since it consumes large quantity of textile industrial processed water and produces highly polluted discharge water. The textile industry uses high volume of water throughout its operation, from the washing of fibers to bleaching, mercerizing, dyeing, printing and washing of finished products. A process data collection was performed and integrated with a characterization of the process effluents in terms of treatability and reusability. In this research we use 98% Concentrated Sulfuric Acid for the Neutralization i.e. to maintain pH, Di Ammonium Phosphate (DAP) and Urea for the bacterial growth i.e. to decrease Biological Oxygen Demand (BOD), and we use AQUATREAT @AR 06 for as an efficient coagulation and flocculation agent. The water treated and purified by using this method can be used for the agricultural purposes or can be drain to sewer without any hesitation.**

***Keywords*---Wastewater, Neutralization, Coagulation, Flocculation**

I. INTRODUCTION

The world's water consumption rate is doubling every 20 years, outpacing by two times the rate of population growth. The availability of good quality water is on the decline and water demand is on the rise. Worldwide availability of fresh water for industrial needs and human consumption is limited. Various industrial and developmental activities in recent times have resulted in increasing the pollution level and deteriorating the water quality. Water shortages and unreliable water quality are considered major obstacles to achieve sustainable development and improvement in the quality of life. The water demand in the country is increasing fast due to progressive increase in the demand of water for irrigation, rapid industrialization, and population growth and improving life standards. The existing water resources are diminishing (i) due to unequal distribution of rain water and occasional drought, (ii) excessive exploitation of ground water sources and its insufficient recharge, (iii) deterioration of water quality due to the discharge of domestic and industrial effluents without adequate treatment. This is resulting into water stress/ scarcity. Country is currently passing through social and economic transition. The proportion of the population which is urban has doubled over the last thirty years (and is now about 30%), agriculture now accounts for about 25% of GDP and the economy has been growing at around 7-9% a year. Country has a highly seasonal pattern of rainfall, with 50% of precipitation falling in just 15 days and over 90% of river flows in just four months [1-3].

Textile Industry is one of the most important and largest industrial sectors in Pakistan. It has a high importance in terms of its environment impact, since it consumes large quantity of textile industrial processed water and produces highly polluted discharge water. The textile industry uses high volume of water throughout its operation, from the washing of fibers to bleaching, mercerizing, dyeing, printing and washing of finished products [4].

other public sewer. Major pollutants load from the

Textile industry causes considerable higher impacts to water pollution by discharging their effluents into various receiving bodies includes ponds, rivers and textile industries are from the several of their wet - processing operations like scouring, bleaching, mercerizing and dyeing [5]. Among these various processes, dyeing process normally uses large amount of water for dyeing, fixing and washing processes [6]. Thus, textile wastewater possess a high COD concentration, large amount of suspended solids, broadly fluctuating pH, strong color, high temperature

[1]Institute of Chemical Engineering and Technology, University of the Punjab, Lahore, Pakistan
[2]Department of Chemical Engineering, NFC IE&FR Faisalabad, Pakistan
[3]Department of Chemical Engineering, Universitat Politecnica de Catalunya-UPC, Spain

and low biodegradability caused by varying contaminates within water environment [7].

The textile industry is one of the most polluting industries in term of discharge volume and effluent composition. The dye effluent is characterized by strong color, high chemical oxygen demand (COD) with pH varying from 2 to 12. The removals of color and COD reduction pose greatest problems in textile industry [8,9]. Conventionally effluents containing organics are treated with adsorption, biological oxidation, coagulation, etc. Thought the conventional methods have individual advantages, they are lacking in effectiveness, if applied individually. For example, biological treatment is the most efficient and economical way of reducing the environmental impact of the industrial effluents containing organic pollutants, but this technique is time consuming and cannot be employed for textile effluent, as textile effluent is recalcitrant to biodegradation. On the other hand, the physical adsorption is expensive for adsorbent regeneration difficult. Furthermore, biological and chemical methods generate considerable quantity of sludge, which itself requires treatment. Due to the large variability of the composition of textile wastewater, most of the traditional methods are becoming inadequate [10-13]. A Table I: given below containing specific pollutants from textile wet processing. A Table II: given below shows the possible treatments of textile wastewater along with their advantages and disadvantages.

Textile dying processes are one of the most environmentally unfriendly industrial processes because they produced colored wastewater that is heavily polluted with dyes, textile axillaries, and chemicals. Colloid particles are removed from the water via coagulation and flocculation process. Effect of coagulant dose, polyelectrolyte dose, pH of the solution, and addition of polyelectrolyte as coagulant aid was investigated and found to be important parameters for the effective treatment of beverages industrial wastewater. Aluminum Sulfate (Alum), Ferrous Sulfate, and Ferric Chloride were commonly used as coagulants. During the high COD removal capacities it has been observed that combined use of Alum and Lime link with Alzheimer's disease [30-34].

Apparently no major studies have been done to clarify the textile waste water by using Urea, DAP, and Polymer AQUATREAT @AR 06. Therefore the aim of this research is to investigate the effect of Urea, DAP, and Polymer AQUATREAT @AR 06 in the treatment of textile wastewater.

TABLE I: POLLUTANTS FROM TEXTILE WET PROCESSING

Process	Various Physico Chemicals
Desizing	Enzymes, Starch, Waxes, CMC
Bleaching	H_2O_2, Sodium Silicate, Organic Stabilizer, Surfactant
Mercerizing	NaOH, Cotton Wax
Dyeing	Dyes, Salts, Surfactants, Urea, Soda Ash
Printing	Urea, Dyes, Pigments, Binder, Soda Ash, Thickener
Finishing	Resins, Formaldehyde, PVA, Waxes, Hydrocarbon

TABLE II: TREATMENT METHODS OF TEXTILE WASTEWATER

Processes	Advantages	Disadvantages
Biodegradation [14,15]	Rates of Elimination by Oxidizable Substances about 90%	Low Biodegradability of Dyes
Coagulation-Flocculation [16]	Elimination of Insoluble Dyes	Production of Sludge, Blocking Filter
Adsorption on Activated Carbon [17]	Suspended Solids and Organic Substances well Reduced	Cost of Activated Carbon
Ozone Treatment [18,19]	Good Decolorization	No Reduction of the COD
Electrochemical Processes [20,21]	Capacity of Adaption to Different Volumes of Pollution Loads	Iron Hydroxide Sludge
Reverse Osmosis [22]	Removal of all Mineral Salts, Hydrolyzes Reactive Dyes and Chemical Auxiliaries	High Pressure
Nanofiltration [23-26]	Separation of Organic Compounds of Low Molecular Weight and Divalent Ions from Monovalent Salts, Treatment of High Concentrations	----------
Ultrafiltration-Microfiltration [27-29,22]	Low Pressure	Insufficient Quality of the Treated Water

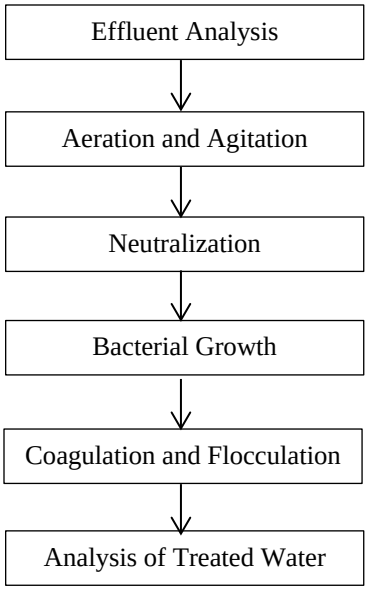

FIG 1: METHODOLOGY OF WATER TREATMENT

II. EXPERIMENTATION

The analysis of the wastewater samples of a well-known textile industry in Faisalabad, PAKISTAN has been taken and it is given below in Table III: as follows

TABLE III: ANALYSIS OF EFFLUENT SAMPLES

Parameters	Values		
	Sample 1	Sample 2	Sample 3
pH	11.8	12.0	10.9
Conductivity (µs/cm)	7.96×10^3	5.24×10^3	5.49×10^3
TDS (mg/L)	3050	3605	3810
TSS (mg/L)	2800	1800	2237
BOD (mg/L)	421.4	312.8	410.2
COD	920	880	840

The sample is taken into a beaker and continuously agitated for the purpose of Aeration that is necessary for the bacterial growth in the wastewater.

In this step we add sulfuric acid by dosing. We add sulfuric acid in the ratio of 2.057 mL/1L of wastewater. This will reduce the pH of the sample and neutralize the sample. The resulting pH of the samples after the dosing of sulfuric acid is to be found in the range of (7-8.5). The results are tabulated in Table IV: given below as follows.

Add fertilizer like Di Ammonium Phosphate (DAP) and Urea in order to increase the bacterial growth i.e. Biological Oxygen Demand (BOD) and maintain to a specific level. This will be beneficial for the next step of treatment that is coagulation and flocculation. Add an equal mixture of Di Ammonium Phosphate (DAP) and Urea that is about 26.78 gram per liter of wastewater. The results are tabulated in Table V: given below as follows.

In this step add some polymers like AQUATREAT @AR 06 this will cause a sudden agglomeration and it will appear on the surface of wastewater. The AQUATREAT @AR 06 is actually a light weight Poly Acrylic Acid used as an anti-scalant agent for wastewater treatment purposes. Add 7.14 mg of AQUATREAT @AR 06 in powder form in the beaker and agitate continuously. This will result the formation of coagulation of insoluble dyes, colors, and pigments etc.

III. RESULTS AND DISCUSSION

TABELE IV: pH RESULTS OF SAMPLES

	pH of Samples		
	Inlet	Outlet	Percentage Neutralization
Sample 1	11.8	8.3	70.33%
Sample 2	12.0	7.9	65.83%
Sample 3	10.9	7.4	67.88%

TABLE V: BOD RESULTS OF SAMPLES

	Biological Oxygen Demand (BOD) of Samples		
	Inlet	Outlet	Percentage BOD Change
Sample 1	421.4	526.75	+80%
Sample 2	312.8	376.86	+83%
Sample 3	410.2	519.24	+79%

IV. CONCLUSIONS

This scientific research shows that the 98% Concentrated Sulfuric Acid efficiently neutralize the sample of textile industry waste water. This research also shows that Di Ammonium Phosphate (DAP) and Urea are found to be effective in order to increase the bacterial growth i.e. Biological Oxygen Demand (BOD) and maintained at a specific level. The AQUATREAT @AR 06 is found to be efficient coagulation and flocculation agent for the removal of insoluble dyes, colors, and pigments etc. the water treated and purified by using this method can be used

for the agricultural purposes or can be drain to sewer without any hesitation.

REFERENCES

1. Soteris A. Kalogirou, *Seawater Desalination using Renewable Energy Sources*, Progress in Energy and Combustion Sciences, 31, 242-281, March 2005.
2. Gleick, *Water Resources in Encyclopedia of Climate and Weather*, In: Schneider, S. H. (ed.) Vol. 02, 817-823, University Press New York, 1996.
3. Technical Information Document, *Desalination and Water Purification Technologies*, Department of Atomic Energy, Bhabha Atomic Research Centre, Government of India, 2010.
4. S. M. Imtiazuddin, Majid Mumtaz, and Khalil A. Mallick, "Pollutants of Wastewater Characteristics in Textile Industry," Journal of Basic and Applied Sciences, 08, 554-556, 2012.
5. K.V. Radha, V. Sridevi, and K. Kalaivani, Bioresource, Electrochemical Oxidation for the Treatment of Textile Industry Waste Water, Technol., 100, 987-990, 2008.
6. D. Rajkumar, B. J. Song, and J. G. Kim, "Electrochemical Degradation of Reactive Blue 19 in Chloride Medium for the Treatment of Textile Dyeing Wastewater with Identification of Intermediate Compounds," Dyes and Pigments, 72(1), 1–7, 2007.
7. J. Chen, M. Liu, J. Zhang, Y. Xian and L. Jin, "Electrochemical Degradation of Bromopyrogallol Red in Presence of Cobalt Ions," Chemosphere, 53, 1131-1136, 2003.
8. J. Naumczyk, L. Szpyrkowicz and F. Zilio Grandi, "Electrochemical Treatment of Textile Waste Water," Water Science and Technology, 11, 17–24, 1996.
9. V.J.P. Poots, G. Mckay and J.J. Healy, "The Removal of Acid Dye from Effulent using Natural Adsorbents," Water Research, 10, 1061-1066, 1976.
10. O.J. Hao, H. Kim and P.C. Chiang, Decolorization of Wastewater, Critical Reviews in Environmental Science and Technology," 30(4), 449–505, 2000.
11. Fernandes, Morˇ ao, M. Magrinho, A. Lopes, I. Goncalves, Electrochemical Degradation of C.I. Acid Orange 7, Dyes Pigments, 61, 287–297, 2004.
12. A. Sakalis, Mpoulmpasakos K.,Nickel U., Fytianos K., Voulgaropoulos A, "Evaluation of a novel electrochemical pilot plant process for azodyes removal of textile wastewater," Chemical Engineering, 111, 63-70, 2005.
13. M.C. Gutierrez and M. Crespi, "A Review of Electrochemical Treatments for Color Elimination, Coloration Technology, 115(11), 342-345, 1999.
14. Pala A, Tokat E, "Color Removal from Cotton Textile Industry Wastewater in an Activated Sludge System with various Additives," Water Research, 36, 2920-2925, 2002.
15. Ledakowicz S, Solecka M, Zylla R, "Biodegradation, Decolorization and Detoxification of Textile Wastewater Enhanced by Advanced Oxidation Processes," Journal of Biotechnology, 89, 175-184, 2001.
16. Gaehr F, Hermanutz F, Oppermann W, "Ozonation, An important Technique to Comply with new German Laws for Textile Wastewater Treatment," Water Science and Technology, 30, 255-263, 1994.
17. Arslan I, Balcioglu IA, Bahnemann DW, "Advanced Chemical Oxidation of Reactive Dyes in Simulated Dye House Effluents by Ferrioxalate-Fenton/UV-A and TiO2/UV-A Processes," Dyes Pigments, 47, 207-218, 2000.
18. Adams CD, Fusco W, Kanzelmeyer T, "Ozone, Hydrogen Peroxide/Ozone and UV/Ozone Treatment of Chromium and Copper Complex Dyes: Decolorization and Metal release," Ozone Science and Engineering, 17, 149-161, 1995.
19. Scott JP, Ollis D, "Integrated Chemical and Biological Oxidation Processes for Water Treatment, Review and Recommendations, Environmental Progress, 14, 88-103, 1995.
20. Lin SH, Peng FC, "Treatment of Textile Wastewater by Electrochemical Method," Water Research, 28, 277-282, 1994.
21. Lin SH, Chen ML, "Treatment of Textile Wastewater by Chemical Methods for Reuse," Water Research, 31, 868-876, 1997.
22. Ghayeni SB, Beatson PJ, Schneider RP, Fane AG, "Water Reclamation from Municipal Wastewater using Combined Microfiltration-Reverse Osmosis (MERO): Preliminary Performance Data and Microbiological Aspects of System Operation," Desalination 116, 65-80, 1998.
23. Erswell A, Brouchaert CJ, Buckley CA, "The Reuse of Reactive Dye Liquors using Charged Ultrafiltration Membrane Technology," Desalination, 70, 157-167, 1998.
24. Xu Y, Lebrun R, Gallo PJ, Blond P, "Treatment of Textile Dye Plant Effluent by Nanofiltration Membrane," Separation Science and Technology, 34, 2501-2519, 1999.
25. Akbari A, Remigy JC, Aptel P, "Treatment of Textile Dye Effluent using a Polyamide-Based Nanofiltration Membrane," Chemical Engineering Processing, 41, 601-609, 2002.
26. Tang C, Chen V, "Nanofiltration of Textile Wastewater for Water Reuse," Desalination, 143, 11-20, 2002.
27. Watters JC, Biagtan E, Sener O, "Ultrafiltration of Textile Plant Effluent," Separation Science and Technology, 26, 1295-1313, 1991.
28. Rott U, Minke R, "Overview of Wastewater Treatment and Recycling in the Textile Processing Industry," Water Science and Technology, 40, 37-144, 1999.
29. Ciardelli G, Ranieri N, "The Treatment and Reuse of Wastewater in the Textile Industry by means of Ozonation and Electro-flocculation," Water Research, 35, 567-572, 2001.
30. Rouss, J. Vooren, M. V. Demprcy. B. A. and Guibal, F. "Influence of Chitosan Characteristics on the Coagulation and the Flocculation of Bentonite Suspension" Water Research, 39, 3247-3258, 2005.
31. Amudaa, O. S. and Amoob, I. A. "Coagulation/Flocculation Process and Sludge Conditioning in Beverage Industrial Wastewater Treatment" Journal of Hazardous Materials, 141, 778-783, 2007.

32. Pan J. R. Huang C. P. Chen S. C. and Chung Y. C. “Evaluation of Modified Chitosan Biopolymer for Coagulation of Colloidal Particles” Colloids and Surfaces A, 147, 359-364, 1999.
33. Amokrane, A. Comel, C. and Ueron J., “Landfill Leachates Pre-Treatment by Coagulation Flocculation” Water Research, 31, 2775-2782, 1997.
34. Mohammad Sayem Mozumder, A. S., “Amphiphilic Polyelectrolytes Characterization and Applications in Coagulation/Flocculation” King Fahad University of Petroleum and Minerals, Thesis Master, 2004.

Tannery Industry Wastewater using Potash Alum and Drewfloc

Qazi M. Omar[1], Umar Shafiq[2], Ahmad Mukhtar[2], Fatma Safdar[2], Masooma Qizilbash[3]

***Abstract*--- The tannery industry is considered to be a vital industry from economic point of view. But its wastewater is an important source of water pollution as it contains high concentration of both organic and inorganic pollutants. Disposal of such untreated wastewater is a serious environmental threat. It is therefore necessary to treat this wastewater before the final disposal. In this research work, coagulation and flocculation followed by biological treatment is used to treat the wastewater of tannery. Potash alum was used for coagulation and Drewfloc 270 was used for flocculation. Different dose rates of coagulant and flocculent were adjusted and their effects on different parameters were observed. It was concluded that this treatment method was found successful in reducing the pollutant concentration of the tannery effluent to achieve National Environmental Quality Standards (NEQS).**

***Keywords*---Wastewater, Flocculation, Sludge, Coagulation, NEQs, TSS, TDS, pH, BOD, COD.**

I. INTRODUCTION

Tanning is the process in which collagen fibers present in the animal skin react with tannins or other chemical agents to form a stable product called leather [1-8]. Approximately 30 – 35 liters water is used in the processing of a kg of hide/skin [9]. Tannery wastewater can be categorized as follow:

1. Effluents discharged from pre-tanning process. The operations include liming, deliming/bating, water from fleshing and splitting machines. Such effluents contain sulphides and have high pH, but they are chrome-free.
2. Effluents discharged from tanning process. The operations include tanning and re-tanning, sammying. Such effluents contain high Cr content and are acidic.
3. Effluents discharged from post-tanning process. The operations include fat-liquoring, dyeing. Such effluents contain low Cr content.

[1]Institute of Chemical Engineering and Technology, University of the Punjab, Lahore, Pakistan
[2]Department of Chemical Engineering, NFC IE&FR Faisalabad, Pakistan
[3]Department of Chemical Engineering, Universitat Politecnica de Catalunya-UPC, Spain

Wastewater treatment is a process comprised of different stages, aiming to purify wastewater before it is discharged to natural waters, applied on land or reused. In wastewater treatment, pollutants do not disappear; rather they are just converted into the form which is acceptable to the environment and easy to dispose of. Removal or reduction of organic matter, solids, nutrients, Cr and other pollutants is the main aim of wastewater treatment. Every effluent treatment plant has to meet the standards set by the relevant environmental authority for the allowable levels of pollutants expressed as BOD5, COD, suspended solids (SS), Cr, total dissolved solids (TDS) and others.

Different phases of tannery wastewater treatment are as follows:

1. Preliminary treatment
2. Primary treatment (Physical-chemical treatment)
3. Secondary treatment (Biological treatment)
4. Tertiary treatment (advanced treatment)
5. Sludge treatment and handling
6. Utilization and disposal

Preliminary treatment is done to remove coarse particles, sand/grit and grease from the effluent. It also reduces chrome and sulphide contents before discharging of the effluent into the collection network. Different types of screens are used to remove large particles. After that the effluent is sent to the next section for primary treatment.

Primary treatment aims to remove settle able organic and inorganic solids by sedimentation and floating materials by skimming. At this process stage bio-chemical oxygen demand (BOD5) is reduced by 25-50%, total suspended solids (SS) by 50-70%, and oil and grease by 65% approximately. The effluent and

sludge obtained after primary treatment are known as primary effluent and sludge respectively.

Primary treatment is a two-step process;

1. Equalization
2. Primary sedimentation

The objectives of equalization are to homogenize the effluent and to eliminate sulphides. For this purpose the settling of solids should be avoided i.e. all the particulate matter should be kept in suspension. For this purpose equalization tank is used. Mixing-cum-aeration devices are used to avoid settling. In primary treatment, chemicals are added which improve and accelerate the settling of suspended solids. This enhances the separation of colloidal in downstream processes such as sedimentation and filtration. Following processes are employed to separate suspended solids from water.

1. Coagulation
2. Flocculation

In coagulation, colloids are destabilized by neutralizing the forces that keep them apart. Finely dispersed solids (colloids) which are suspended in wastewater contain negative electric charges on their surfaces. The negative charge of the colloids is reduced by the cationic coagulants which provide positive electric charges. Consequently, larger particles (flocs) are formed due to the collision of the particles. Flocculation is the polymeric action in which bridges are formed between the flocs, and destabilized particles are bind into large agglomerates or clumps. Flocculent should be added slowly and mixed gently to ensure proper contact between the small flocs and their agglomeration into larger particles. Flocs can be removed from the liquid by different operations like sedimentation, filtration, floatation etc. Primary sedimentation aims to remove suspended solids mainly along with fats, waxes, mineral oils, floating non-fatty materials, etc. which could not be removed in the grit-and- oil chamber. It is done in Primary settling tanks. As the wastewater enters a sedimentation tank, it slows down. Thus the suspended solids gradually sink to the bottom under the effect of gravity. Primary settling tanks are commonly circular with a mechanism to remove grease (scum) from the top and sludge from the bottom. After primary treatment, BOD, COD and SS content of the effluent are reduced to a large extent.

In secondary treatments, aerobic biological treatment processes are employed to remove biodegradable dissolved and colloidal organic matter left after primary treatment. Up to 90% of the organic matter in wastewater can be removed by using biological treatment processes. Aerobic micro-organisms consume organic matter present in the wastewater to produce more micro-organisms and inorganic end products (principally CO_2, NH_3, and H_2O). This process is carried out in the presence of oxygen. Secondary treatment is a two-step process;

1. Aeration
2. Secondary sedimentation

Aeration is the process of bringing contact between air and the wastewater. In the aeration tank, the wastewater containing microorganisms is mixed vigorously with air. Proper supply of oxygen is necessary to maintain aerobic conditions and to the keep the active biomass suspended. Activated sludge treatment with extended aeration is commonly used for tannery wastewater treatment. In activated sludge process, metabolism of micro-organisms is used to remove substances causing oxygen demand. In short micro-organisms consumes (eat and digest) harmful and oxygen-demanding organic compounds and convert them into environmentally more acceptable form i.e. micro-organisms and stable and low-energy compounds like carbon dioxide and water. In Secondary sedimentation tank, the flocs formed in the aeration basin are allowed to settle down. The effluent obtained after sedimentation is fully treated effluent which is ready for final discharge or further treatment if required. The sludge is removed from the bottom which is bulkier and difficult to dewater. A part of it is then recycled back to the aeration tank while the rest is send to the sludge handling section for further processing.

Tertiary treatments are used when effluent does not meet the allowable discharge limits even after primary and secondary treatments. The reason behind is COD. This situation arises when the micro-organisms present in the floc could not decompose certain compounds. In such cases, more sophisticated and expensive treatments are employed to further reduce

the solids and organic content of the effluent. In short, tertiary treatments are used when specific constituents of the effluent are not removed by previous treatments. Tertiary treatment include absorptive processes like use of activated carbon, more efficient oxidation as with ozone, foam separation of impurities, and demineralization using distillation or reverse osmosis etc. Sludge from different sections of the plant is send to the sludge handling section. Water content of the sludge is reduced for its easy handling and disposal. This can be achieved by different means i.e. using sludge thickeners, mechanical dewatering in filter presses etc. or natural drying in sludge-drying beds. The tannery sludge has greater inorganic matter and heavy metal (i.e. chromium and sulfur compound) content. A variety of methods for utilization and/or safe disposal of tannery sludge have been used. They include landfill, land application, vitrification, composting, anaerobic digestion, thermal treatment, pyrolysis, brick making, etc. [10-18].

II. EXPERIMENTAL SETUP

The experimental set up is a wastewater treatment plant of a tannery industry. The plant treats 600 m^3 of tannery effluent per day. The tannery wastewater treatment plant consists of the following Equipments:

1. Equalization Basin
2. Primary Clarifier
3. Aeration basins
4. Secondary clarifier
5. Sludge drying beds

The wastewater from different sections of the tannery is collected in the equalization basin. Equalization basin is equipped with surface aerator and air diffuser to allow proper mixing. As the poor settling is caused by the stability of the colloidal present in the tannery effluent, a coagulant tank was installed on the equalization basin. The coagulant used was potash alum. This tank was used to introduce coagulant solutions of different concentrations into the equalization basin. Proper mixing minimizes the variations in wastewater flow rates and composition. From the equalization basin, the wastewater is sent to the primary clarifier through a pump. A flocculent was introduced into the primary clarifier in order to improve the settling of the suspended solids. The flocculent used was Drewfloc 270. For this purpose flocculent tank was installed on the primary clarifier. This tank was used to introduce flocculent solutions of different concentrations into the secondary clarifier. Slow mixing of the flocculent was required in order to avoid the breakage of the flocs. The velocity of the water coming to the secondary clarifier was sufficient enough for the required mixing. Here the sludge is allowed to settle at the bottom of the clarifier while the wastewater overflows towards the next section of the plant under the effect of the gravity. Sludge collected from the primary clarifier is sent to the primary sludge drying beds. The next section of the plant comprises of two aeration basins. Here activated sludge method is employed for the treatment of the wastewater. These basins are provided with the surface aerators to ensure proper aeration. Proper aeration is very important to maintain aerobic conditions and to the keep the active biomass suspended. MLSS concentration is maintained at 4,500 to 5,000 mg/L in the aeration basins. From the aeration basins the wastewater moves towards the secondary clarifier under the effect of gravity. Here the sludge is allowed to settle down. Clear water overflows from the secondary clarifier towards the final disposal. A part of the sludge collected from the bottom of the secondary clarifier is sent to the aeration basins to maintain MLSS concentration while the rest of the sludge is sent to the sludge thickener. From sludge thickener, the sludge is sent to the sludge drying beds. After getting dried, sludge is used for land filling.

III. RESULTS AND DISCUSSIONS

The tannery wastewater contains a high concentration of pollutants. In the experimentation, different dose rates of coagulant and flocculent were used to treat the tannery effluent. The effect of varying the dose rates on the tannery effluent was examined. Following parameters were studied i.e. pH, chemical oxygen demand (COD), total dissolved solids (TDS) and total suspended solids (TSS). After the treatment, wastewater comes to the secondary clarifier. The samples were collected from the secondary clarifier to perform analysis. Table I: shows the limits of different parameters prescribed by National Environmental Quality Standards (NEQS). These standards should be met for the safe disposal of the tannery effluent. Table II: shows the concentration of the pollutants in the tannery wastewater before the chemical treatment. It shows that tannery wastewater is highly polluted. This wastewater is extremely harmful if exposed to the

environment. It may affect the soil as well as water bodies. It is, therefore, necessary to treat this wastewater so that its harmful effects could be reduced.

TABLE 1: NATIONAL ENVIRONMENTAL QUALITY STANDARDS (NEQS) FOR WATER

Parameters	NEQS (For Inland waters)
pH	6 – 9
COD (ppm)	150
TSS (ppm)	200
TDS (ppm)	3,500

TABLE 2: INFLUENTS RESULTS BEFORE TREATMENT

Parameters	Influents
pH	10.29
COD (ppm)	2594
TSS (ppm)	1026
TDS (ppm)	5512

In the chemical treatment, coagulant used was potash alum and flocculent was Drewfloc 270. The chemical treatment was followed by biological treatment. Different dose rates for coagulant and flocculent were adjusted to study the effect on different parameters. Table III: shows the results of different parameters against different dose rates.

The variations in pH of the wastewater against different dose rates of coagulant and flocculent are tabulated below in Table III. NEQS for pH of tannery effluent were achieved using chemical & biological treatment methods. There are not many variations in pH with the change in dose rates of coagulant and flocculent. pH values for all the samples lie within the limits prescribed by NEQS. Results for pH of the wastewater against different dose rates are shown in Fig. 01.

The variations in COD values of the wastewater against different dose rates of coagulant and flocculent are tabulated below in Table IV. The data shows that there is a gradual variation in the COD values against different dose rates of coagulant and flocculent. The lowest value of COD was achieved at dose rate of 100 ppm and 2 ppm for coagulant and flocculent respectively as shown in Fig. 02. Results for COD of the wastewater against different dose rates are shown in Fig. 02.

TABLE 3: VARIATIONS IN pH AGAINST DIFFERENT DOSE RATES

Dose Rate (ppm) (Coagulant + Flocculent)	pH
DR – (20+1)	7.91
DR – (40+1)	7.67
DR – (50+1)	7.15
DR – (60+1)	7.53
DR – (60+2)	7.48
DR – (80+2)	7.23
DR – (80+4)	7.78
DR – (100+6)	7.85
DR – (100+4)	7.52
DR – (100+2)	7.72

TABLE 4: VARIATIONS IN COD AGAINST DIFFERENT DOSE RATES

Dose Rate (ppm) (Coagulant + Flocculent)	COD
DR – (20+1)	347
DR – (40+1)	324
DR – (50+1)	295
DR – (60+1)	375
DR – (60+2)	252
DR – (80+2)	183
DR – (80+4)	205.2
DR – (100+6)	263
DR – (100+4)	270
DR – (100+2)	148

The variations in TDS values of the wastewater against different dose rates of coagulant and flocculent are tabulated below in Table IV: The data shows that TDS values are dependent upon coagulant and flocculent dose rates. Results for TDS of the wastewater against different dose rates are shown in Fig. 03.

The variations in TSS values of the wastewater against different dose rates of coagulant and flocculent are tabulated below in Table VI: All the values lie within limits prescribed by NEQS. Higher dose rates may affect settling and floc formation of the suspended solids. Lowest value for TSS was achieved at dose rate of 100 ppm and 2 ppm for coagulant and flocculent respectively as shown in Fig. 04.

TABLE 5: VARIATIONS IN TDS AGAINST DIFFERENT DOSE RATES

Dose Rate (ppm) (Coagulant + Flocculent)	TDS
DR – (20+1)	3902
DR – (40+1)	3853
DR – (50+1)	3803
DR – (60+1)	3907
DR – (60+2)	3952
DR – (80+2)	3988
DR – (80+4)	4307
DR – (100+6)	4998
DR – (100+4)	4896
DR – (100+2)	4705

TABLE 6: VARIATIONS IN TSS AGAINST DIFFERENT DOSE RATES

Dose Rate (ppm) (Coagulant + Flocculent)	TSS
DR – (20+1)	86
DR – (40+1)	79
DR – (50+1)	74
DR – (60+1)	83
DR – (60+2)	62
DR – (80+2)	53
DR – (80+4)	55
DR – (100+6)	64
DR – (100+4)	67
DR – (100+2)	43.5

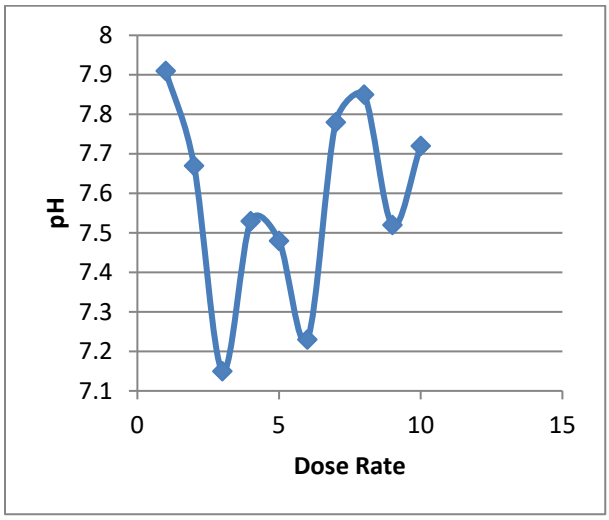

Fig. 01: Variations in pH against Different Dose Rates

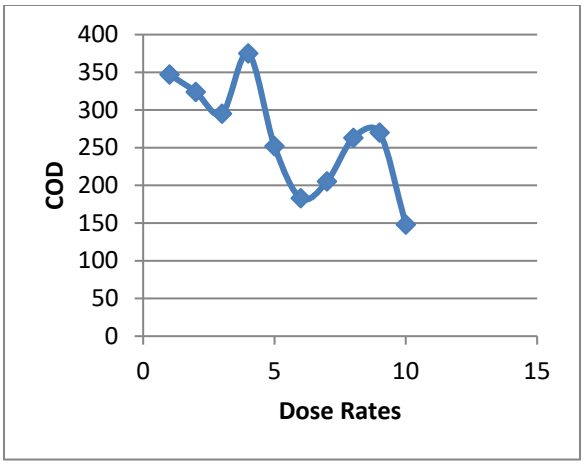

Fig. 02: Variations in COD against Different Dose Rates

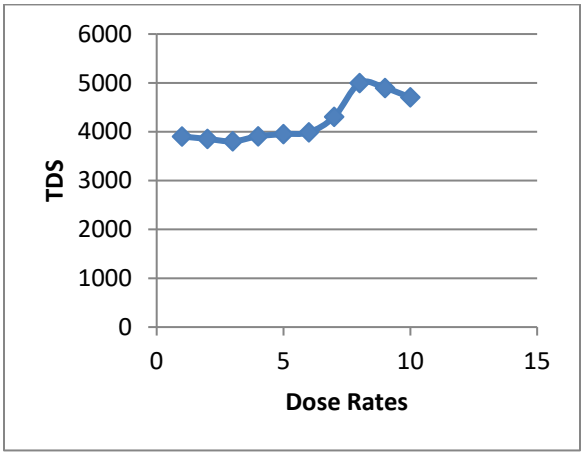

Fig. 03: Variations in TDS against Different Dose Rates

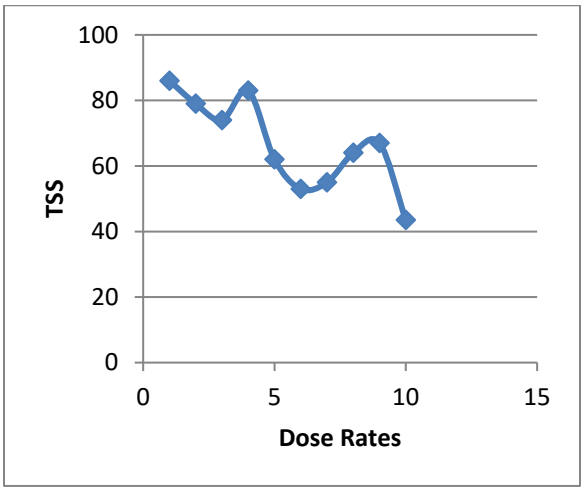

Fig. 04: Variations in TSS against Different Dose Rates

TABLE 7: WASTEWATER TREATMENT ANALYSIS AGAINST DIFFERENT DOSE RATES

Dose Rate	Dose Rate (ppm) **Coagulant (Potash Alum)**	**Flocculent (Drewfloc 270)**	pH	COD (ppm)	TDS (ppm)	TSS (ppm)
DR – 1	20	1	7.91	347	3902	86
DR – 2	40	1	7.67	324	3853	79
DR – 3	50	1	7.15	295	3803	74
DR – 4	60	1	7.53	375	3907	83
DR – 5	60	2	7.48	252	3952	62
DR – 6	80	2	7.23	183	3988	53
DR – 7	80	4	7.78	205.2	4307	55
DR – 8	100	6	7.85	263	4998	64
DR – 9	100	4	7.52	270	4896	67
DR–10	100	2	7.72	148	4705	43.5

IV. CONCLUSIONS

This research work aims to suggest some techniques to reduce pollution concentration in the wastewater of tannery industry. The main findings of this work are: Chemical treatment followed by biological treatment has been found successful for wastewater treatment of tannery industry. pH of the wastewater before the treatment was 10.29. After treatment it was reduced to 7.72 COD before the treatment was 2594 and it was reduced to 148 after the treatment. Initial value of TSS was 1026 before the treatment. After treatment it was 43.5. TDS valued prior to the treatment was 5512. After treatment it was reduced to 4705. But it is still high. The reason behind high TDS is addition of coagulant and flocculent. This value of TDS can be reduced by using some tertiary treatment In the chemical treatment, coagulant used was potash alum and flocculent was Drewfloc 270. The chemical treatment was followed by biological treatment. Different dose rates for coagulant and flocculent were adjusted to study the effect on different parameters. Table 07: shows the results of different parameters against different dose rates. Table VII: shows that chemical treatment followed by biological treatment has been found successful for the treatment of tannery wastewater. Best results have been achieved at the DR-10, i.e. coagulant 100 ppm and flocculent 2 ppm. All the values have been reduced to NEQS except TDS. TDS value is high due to coagulant and flocculent added. All the parameters are discussed below in detail.

methods. Overdosing of the coagulant/ flocculent should be avoided as it may disturb the settling of the flocs.

REFERENCES

1. K. Bienkiewicz, Physical Chemistry Of Leather making, Krieger Publishing Co., Malabar, FL, 1983.
2. Development Document For Effluent Limitations Guidelines And Standards For The Leather Tanning And Finishing Point Source Category, EPA-440/1-82-016, U. S. Environmental Protection Agency, Research Triangle Park, NC, November, 1982.
3. 1992 Census Of Manufactures, U. S. Department of Commerce, Bureau of Census, Washington, DC, April 1995.
4. Telecon, A. Marshall, Midwest Research Institute, with F. Rutland, Environmental Consultant, Leather Industries of America, August 7, 1996.
5. 1996 Membership Directory, Leather Industries of America Inc.
6. M. T. Roberts and D. Etherington, Bookbinding And The Conservation Of Books, A Dictionary Of Descriptive Terminology.
7. T. C. Thorstensen, Practical Leather Technology, 4th Ed., Krieger Publishing Co., Malabar, FL, 1993. 6/97 Food And Agricultural Industry 9.15-5
8. Locating And Estimating Air Emissions From Sources Of Chromium, EPA-450/4-84-007g, U. S. Environmental Protection Agency, Research Triangle Park, NC, July 1984.
9. Wastewater Treatment Technology for Tannery Industry by R. A. Ramanujam, R. Ganesh, J. Kandasamy.
10. J. Buljan and I. Kral, G. Clonfero, M. Bosniç and F. Schmel, “Introduction to treatment of tannery

effluents", United Nations Industrial Development Organization, 2011.
11. M. Giles, G. Brothers, Girard, "Chemical Treatment Solves Tannery Waste Problem", Industrial Wastes, 1980.
12. J. Landgrave, "A Pilot Plant for Removing Chromium from Residual Water of Tanneries", Environ Health Perspect, Vol 103(Suppl 1), 1995.
13. V. F. Kurenkov, H. G. Hartan, and F. I. Lobanov , "Application of Polyacryamide Flocculent for Water Treatment", Review, 2002.
14. J. Naumczyk, M. Rusiniak, "Physicochemical and Chemical Purification of Tannery Wastewaters", Polish Journal of Environmental Studies, Vol. 14, No 6, 789-797, 2005.
15. V Midha and A. Dey, "Biological Treatment Of Tannery Wastewater For Sulfide Removal", Int. J. Chem. Sci., 6(2), 472-486, 2008.
16. D. Rameshraja and S. Suresh, "Treatment of Tannery Wastewater by Various Oxidation and Combined Processes", Int. J. Environ. Res, 5(2), 349-360, 2011.
17. Gidhamaari, Boominathan and E. Mamidala, "Studies of Efficiency of Immobilized Bacteria in Tannery Effluent Treatment", J.Bio.Innov 2(2) , pp:33-42, 2012.
18. S. Banuraman, T. P. Meikandaan, "Treatability Study of Tannery Effluent by Enhanced Primary Treatment", International Journal of Modern Engineering Research, Vol.3, Issue.1, pp-119-122, 2013.

Geopolymerization: A Green & Sustainable Approach for Inorganic Membrane Synthesis

Amir Naveed[a], Fazli Saeed [a], Saima Hassan [a]

Abstract: **Inorganic membranes have got attraction due to their high thermal stability, relatively high chemical stability and good corrosion resistant. However, inorganic membrane synthesis is inherently more expansive and complicated. Therefore, the research has been focused to synthesize inorganic membrane with relatively low cost. The conventional inorganic membrane is typically sintered at high temperature above 1000 °C while the geo-polymer membrane can harden at ambient temperature; therefore, geopolymer membrane synthesis is low cost compared to conventional ceramic membranes. In the present study self-supported inorganic membrane has been synthesized through geopolymerization using locally available kaolinite material. The average pore diameter of 1.0 – 1.2 µm is obtained before Curing and Hydrothermal treatment by using metakaolin with average particle size 9.13 µm. Curing and Hydrothermal treatment resulted in average pore diameter of about 0.6 – 0.8 µm.**

Keywords: Kaolinite, metakaolinite, Geopolymerization, Ceramic Inorganic microfiltration membrane.

I. INTRODUCTION

Membrane technology is replacing conventional processes and finding a wide spread application in chemical and process industries due to its environmental friendly nature, low energy consumption, high selectivity, small foot print and easy scale up [1]. Polymeric membranes share the major portion because they are very competitive in performance and economics. However, polymeric membranes have limitations to be used in very harsh operating conditions. Inorganic membranes have got attraction due to their high thermal stability, relatively high chemical stability and good corrosion resistant. However, inorganic membrane synthesis is inherently more expansive [2]. Therefore, the research has been focused to synthesize inorganic membrane with relatively low cost.

Geo-polymers are non-crystalline or quasi-crystalline gels with three-dimensional network structures that were first introduced by Joseph Davidovits in 1978 [3]. In general, geo- polymers are prepared from natural minerals or solid wastes through the polymerization of silicon–oxygen tetrahedral and aluminum–oxygen tetrahedral. Geo-polymers are well-known for their excellent mechanical properties, fire and acid resistance and durability [4].

The conventional inorganic membrane is typically sintered at high temperature above 1000°C while the geo-polymer membrane can be hardening at ambient temperature; therefore, geo-polymer membrane synthesis needed less energy compared to conventional ceramic membranes.

In the present study, self-supported inorganic membrane has been synthesized through geo-polymerization using locally available kaolinite material.

II. MATERIALS AND METHODOLOGY

The schematic of synthesis process for geo-polymeric membrane has been shown in Figure 1.

The introductory source mineral material was obtained from a local reservoir in KPK region of Pakistan and is placed in the dryer for 1 hour. To overcome the partial crystal nature of the geo-polymer membrane, the samples were subjected to a curing process at 50°C for 6 hours followed by hydrothermal treatment at 80°C for 14hours [4,5]. The structural and surface characterization of the developed membrane was examined by Scanning Electron Microscope (SEM) and Universal Testing Machine (UTM) respectively [6].

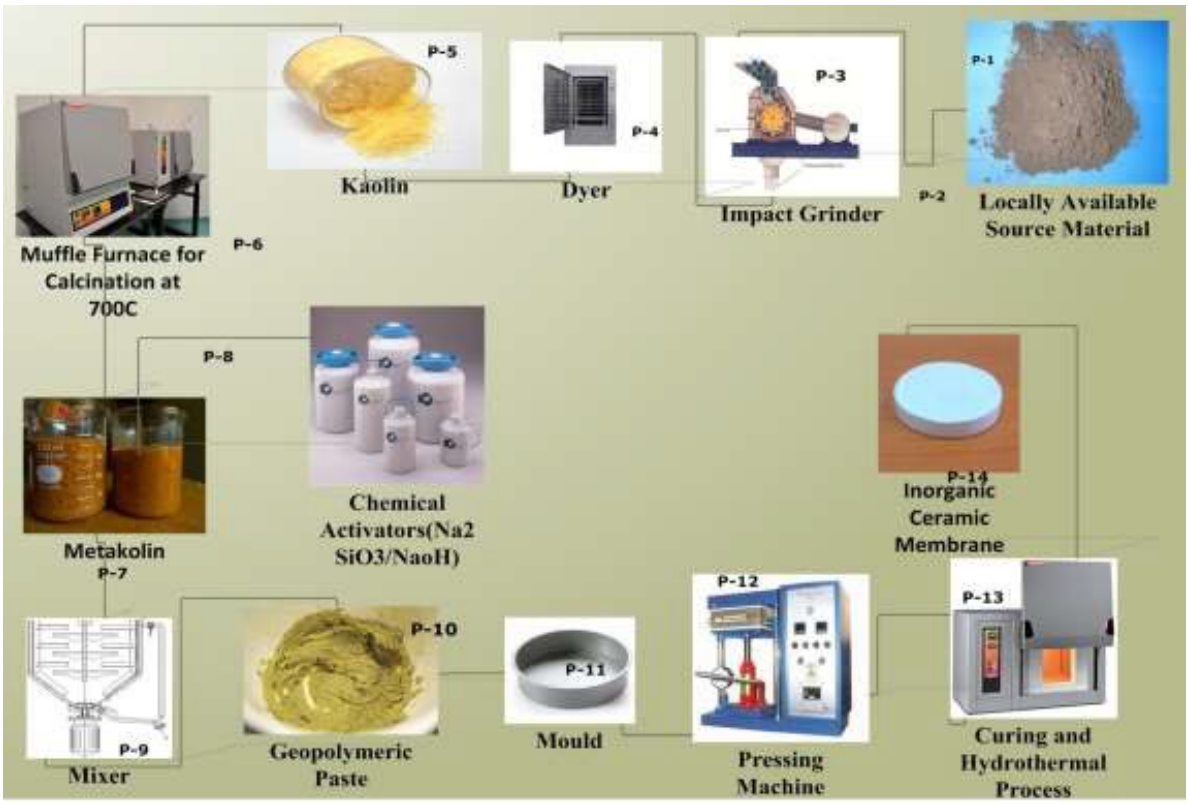

Fig 1: Schematic of Geo-polymeric membrane synthesis.

Fig. 2: Molded paste.

Fig. 3: Pressing machine of paste.

III. RESULTS AND DISCUSSIONS

A. Mineral & Activated Materials Characterization

Table 1, shows the XRF results to analyze the characterization of kaolinite material and thermally activated metakaolin material at 650°C & 700 °C having a mesh size of 200 to 250. It is found that later material at a temperature of 700 °C has the maximum Si to Al ratio of 2.97. Figure 4, presents the XRD

analysis respectively and it was prevailed that Kaolinite material is perfectly converted into metakaolin at 700 °C.

Table 1: XRF Results kaolin and metakaolin at 650°C and 700°C

Chemical Composition	Kaolin	Metakaolin	
	%	650 °C	700 °C
SiO_2	54.98	59.55	60.51
Al_2O_3	17.54	19.56	20.33
Fe_2O_3	5.33	4.68	4.75
CaO	5.40	5.17	5.58
MgO	0.20	0.21	0.15
SO_3	0.00	0.00	0.00
Na_2O	0.95	0.07	0.07
K_2O	0.09	0.86	0.86
L.O.I.	14.50	4.18	4.28

B. Effect of Applied Load on Membrane Thickness and Compressive Strength

In this research work two different diameters such as 10 and 13 mm moulds were used respectively. The membranes of various morphologies were synthesis by changing the applied load shown in Table 2.

Table 2: Load applied on geo-polymeric paste in different diameter of mould, Compressive Strength after 4days

Load Applied(MPa)	**Thickness of Membrane(mm)**	**Resulting Compressive Strength(MPa)**
18.38	6.01	25
27.58	4.08	32
36.76	3.98	37
40.17	3.73	39
46.55	2.73	50

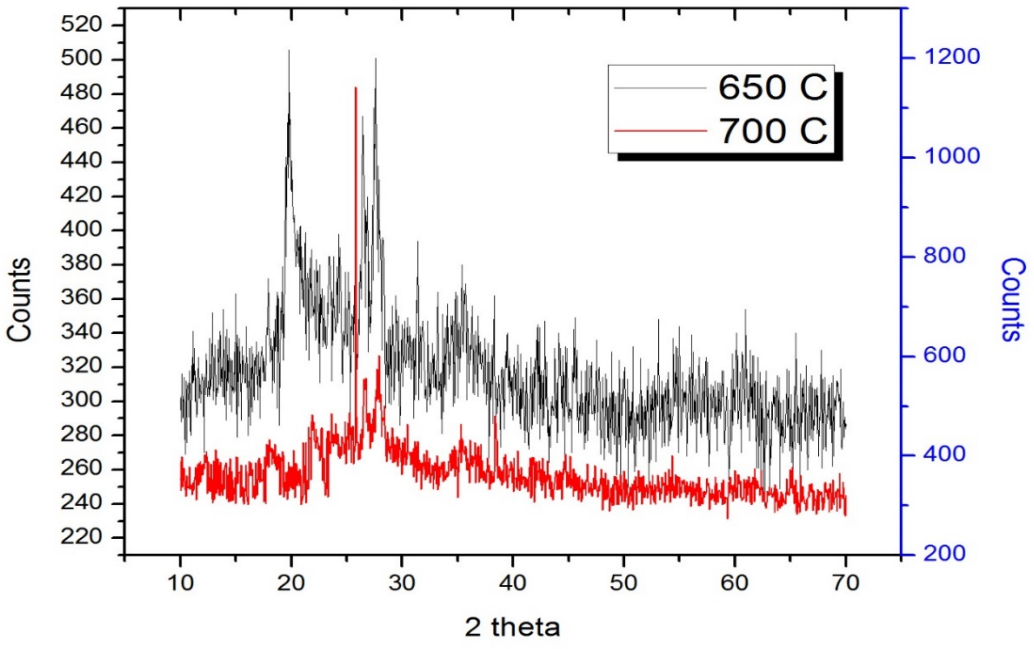

Figure 4: XRD Pattern of Activated Material at 650 °C and 700°C

IV. Conclusion

Morphological study of the fabricated membrane has been done through scanning electron microscopy (SEM). Surface SEM micrograph of geo-polymeric membrane for pore size without and with hydrothermal treatment. The membrane has a compressive strength of 62MPa after curing and hydrothermal process. The average pore diameter of 1.0 – 1.2 µm is obtained before Curing and Hydrothermal treatment by using metakaolin with average particle size 9.13 µm. Curing and Hydrothermal treatment resulted in average pore diameter of about 0.6 – 0.8 µm. This advanced technique is preferable over other membrane production processes because it produces cost effective membranes which can extensively survive in harsh and demanding environments. It is also found that the developed membrane with a higher compressive strength of 62MPa is achieved under the appropriate mixing of Metakaolin to alkalis and Na2SiO3 to NaOH by 4.4 and 2.5 molar ratios respectively with 18M concentrated NaOH solution. The synthesized microfiltration membrane will be used for waste water treatment.

V. References

1. M. X. Xu, Yan H, C. Q. Wang, X. Feng He, X. Qing He, J. Liu, Preparation and characterization of a self-supporting inorganic membrane based on metakaolin-based geopolymers, Applied Clay Science 115 (2015) 254–259.
2. J. Zhang, Y. He, Y. P. Wang, J. Mao, X. M. Cui, Synthesis of a self-supporting faujasite zeolite membrane using geo-polymer gel for separation of alcohol/water mixture, Materials Letters116 (2014) 167–170.
3. M. Sarkar, K. Dana, S. Das, Microstructural and phase evolution in metakaolin geopolymers with different activators and added aluminosilicate fillers, Journal of Molecular Structure 1098 (2015) 110-118.
4. P. Duxson, A. Ferna, J. L. Provis, Lukey A, Palomo S, J.V. Deventer. (2006) Geopolymer technology: the current state of the art. J Mater Sci (2007) 42:2917–2933.
5. Ub allub Rattansak and Prinay chindaprasit. Influence of NaOH Solution on the synthesis of fly ash geopolymer, Minerals Engineering 22(2009)1073-1078.
6. A. Bernal, E. D. R.Guez, R. Mejı, M. G. John L. Provis. Mechanical and thermal characterization of geopolymer based on silicate-activated metakaolin/slag blends. J Mater Sci (2011) 46:5477–5486

Computational Analysis of an Oscillating Membrane

Umar Wahid[1] and Asmat Ullah[2]

Abstract: **In the membrane filtration process the flux drops due to the rapid and severe fouling of the membrane. Fouling of membrane results in high trans-membrane pressure and lower permeate flux rate. High trans-membrane pressure (TMP) results in faster and further fouling of membrane. To keep the filtration process at low values of TMP and with the high flux rate, shear rate is applied to the membrane surface by oscillation. This paper aims to reduce the fouling of membrane in microfiltration process. The shear rate is applied at the membrane surface using membrane oscillation. A mathematical model for the process was simulated computationally to investigate the shear rate at the membrane surface with different frequencies. The result shows that shear rate increases with an increase in vibrational frequency. High induced shear rate makes the separation process economical and reduces the operational cost.**

Keywords: membrane oscillation, fouling, slotted pore membrane, shear rate.

I. INTRODUCTION

Separation through the membrane is preferred compared to conventional processes because it has lower footprint, require no chemical to add, less amount of input energy is needed, no harm effect to environment, and high product that is permeate quality [1]. But a major problem related to filtration through membrane, is the deposition of solute particles on membrane or in the interior of membrane pores. This deposition of solute is nothing but membrane fouling. Membrane fouling is unwanted in membrane separation processes because it reduces the productivity of the process. The fouling layer on the surface of membrane module alters the outer surface properties of membrane [2]. Membrane fouling might be due to pore blocking, concentration polarization, or cake layer formation [3] and are obstacles to permeate flux rate. The fouling also depends upon, membrane slot/pore dimensions, the quantity of solute in feed/bulk stream, size distribution of solute, nature of membrane material, depth filtration or surface filtration, and operating conditions of the filtration process [3]. The flux rate drops considerably for an immersed membrane because of the deposition of foulants i-e cake formation on membrane surface, followed by compactness of the cake [4].

Some kind of demarche is needed to overcome membrane fouling and keep the permeate quantity at constant rate. These might be chemical, mechanical, hydraulic or electric cleaning of the membrane module, or back flushing and backwashing. In aeration bubbles generate vortices that result in dispersion of the concentration polarization layer [5] is also fouling reduction procedure. Another technique to reduce fouling is membrane cleaning by sonication. In Sonication practice a high energy is used in the form of ultrasonic pulses to barrage on the surface [6]. This bombardment of the ultrasonic pulses removes the fouling species from the surface of membrane. It was found after using the sonication technique, that the permeate flux rate increase considerably, but the initial flux rate through membrane was not attained [6]. A recovery of 87.5 %was achieved in first sonication cycle after an interval of 10 minutes [6].

But a major issue with all these processes is high energy consumption. Therefore another technique, in which a relative hgb e motion is created between feed or bulk stream and membrane module, is launched to reduce membrane fouling. This relative motion creates a shear rate which reduces the membrane fouling. Giving a high velocity to feed stream is another technique to create substantial shear rate and reduce fouling [7]. As discussed above, there also the main disadvantage of high velocity cross flow filtration is high energy consumption.

So to decouple high energy consumption from high productivity that is permeate, another novel and robust technique is employed called dynamic shear enhanced technique, where shear is create at the membrane surface through which membrane fouling is reduced progressively. In this system membrane module itself

[1]M.Sc Student, Chemical Engineering Department, University of Engineering and Technology Peshawar

[2]Assistant Professor, Chemical Engineering Department, University of Engineering and Technology Peshawar

is rotated, oscillated, or something near the membrane surface is rotated or vibrated. The created shear rate actually strokes away the suspensions, and hence fouling of membrane is reduced [8]. There are two types of dynamic shear enhanced systems: intermittent shear enhanced systems like vibrating shear enhanced process (VSEP) systems and constant shear producing systems e-g rotating disk system (RD). Normally intermittent systems are using less energy than the other one. These membrane oscillation systems was used for the treatment of produced water [3] and an increase in the permeate flux rate was reported [9]. It was reported for a submerged vibratory hollow fiber membrane that the shear rate produced at membrane surface was a prominent mechanism to reduce membrane fouling [10]. In this research work the concept of intermittent shear rate is used and aims to reduce the fouling of membrane. Using this technique there is no product loss, the system needs no chemical additions and no high energy. The shear is applied at the membrane exterior surface using different frequencies of vibration/oscillation, and its resulting shear rates are computationally investigated. High induced shear rate makes the separation process economical and reduces the operational cost.

II. MATERIALS AND METHODOLOGY:

A mathematical equation was derived for shear rate when a membrane is oscillating in the fluid along z-axis.

Using Navior-Stoke equation as the starting equation, the final derived shear rate equation is given as:

$$\gamma_{(y)} = \Re e\{e^{i\omega t} V \exp(-\lambda y).(-\lambda)\} \quad A$$

Where

$\gamma_{(y)} = Shear\ rate$, ω = Angular Frequency, y = Distance from membrane surface, V = Product of Amplitude & Angular Frequency and $\lambda = \sqrt{\frac{i\omega}{v}}$

$v = kinematic\ viscosity\ of\ feed\ fluid$

Matlab R2011b was used for computational analysis. Matlab statements and loops were used and the model was simulated

III. RESULTS AND DISCUSSION

The shear rate at membrane surface can be calculated from equation A. Putting y=0 for membrane surface shear rate, the equation reduces to:

$$\gamma_{(0)} = \Re e\{e^{i\omega t} V(-\lambda)\}$$

Where, $\gamma_{(0)} = Shear\ rate\ at\ membrane\ surface$

Input frequencies of 20 and 30 Hz are taken for amplitude 0.005 mm and the shear rates at membrane surface are investigated. The value of feed fluid kinematic used as that for water at 298K.The results are shown in below table no 1 and figure no 2. Experimental and predicted data is compared to validate the model. It is found that predicted date is in reasonable agreement with the experimental data. Moreover the shear rate values for high frequency and lower frequency is observed, while keeping all other input parameters constant.

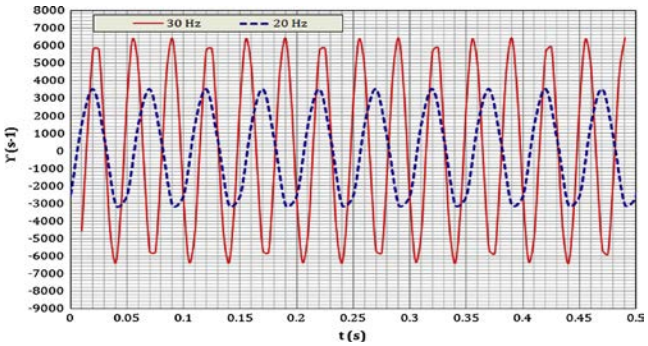

Fig 1: Experimental shear rates values for frequencies, 20Hz and 30Hz.

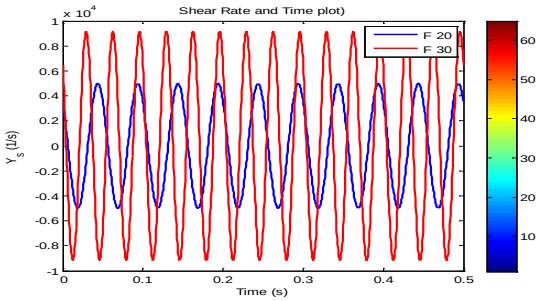

Fig 2: Predicted shear rates values for frequencies, 20Hz and 30Hz.

Table 1: Membrane surface shear rate for different sets of frequencies.

F(Hz)	*w(Hz)*	*A (m)*	*v* *(m^2/s)*	*V (m/s)*	$\gamma_{sp}(1/s)$ Predicted	$\gamma_{se}(1/s)$ Experimental
20	125.6	0.005	0.000002	0.628	4979	4500
30	188.4	0.005	0.000002	0.942	9145	6832

IV. Conclusion:

The model was developed for the immersed oscillating membrane and simulated in Matlab R2011b. It was found that the shear rate at membrane surface was a function of the frequency of oscillation. Moreover shear rate is also a function of vibrational amplitude as well as fluid kinematic viscosity. It means that that the shear rate increases with increase in frequency of oscillation and vibrational amplitude.

References:

1. A. Ullah et al. / Separation and Purification Technology 144 (2015) 16–22
2. Alkhudhiri, A., Darwish, N., & Hilal, N. (2013). Produced water treatment: application of air gap membrane distillation. Desalination, 309, 46-51.
3. Xu, P., Drewes, J. E., Kim, T.-U., Bellona, C., & Amy, G. (2006). Effect of membrane fouling on transport of organic contaminants in NF/RO membrane applications. Journal of Membrane science, 279(1), 165-175.
4. Ullah, A., Holdich, R. G., Naeem, M., Khan, S. W., & Starov, V. M. (2014). Prediction of size distribution of crude oil drops in the permeate using a slotted pore membrane. Chemical Engineering Research and Design, 92(11), 2775-2781.
5. Tansel, B., Dizge, N., & Tansel, I. N. (2017). Analysis of high resolution flux data to characterize fouling profiles of membranes with different MWCO under different filtration modes. Separation and purification technology, 173, 200-208.
6. Cui, Z. F., Chang, S., & Fane, A. G. (2003). The use of gas bubbling to enhance membrane processes. Journal of Membrane science, 221(1), 1-35.
7. Lim, A. L., & Bai, R. (2003). Membrane fouling and cleaning in microfiltration of activated sludge wastewater. Journal of Membrane science, 216(1), 279-290.
8. Sarrade, S., Schrive, L., Gourgouillon, D., & Rios, G. M. (2001). Enhanced filtration of organic viscous liquids by supercritical CO 2 addition and fluidification. Application to used oil regeneration. Separation and purification technology, 25(1), 315-321.
9. Ullah, A., Holdich, R. G., Naeem, M., & Starov, V. M. (2012). Shear enhanced microfiltration and rejection of crude oil drops through a slotted pore membrane including migration velocities. Journal of Membrane science, 421, 69-74.
10. Gomaa, H. G., Rao, S., & Al Taweel, M. (2011). Flux enhancement using oscillatory motion and turbulence promoters. Journal of Membrane science, 381(1), 64-73.
11. Pourbozorg, M., Li, T., & Law, A. W. K. (2016). Effect of turbulence on fouling control of submerged hollow fibre membrane filtration. *Water Research*, *99*, 101-111.

Investigation of the Effect of Microwaves on Minerals Grindibilety and liberation

Usman Ghani[1] and Ishaq Ahmad[2]

Abstract: **Liberation of valuable minerals from gangues in mineral processing is achieved by comminution up to the grains size of the valuable minerals. Comminution is responsible for more than 50% of total energy consumption however only 1% of total energy is actually used to break the minerals up to desired optimum mesh of grind. Microwave processing of minerals is an emerging technique of ore liberation and exploits the heating property of mineral to liberate concerned mineral from the associated gangue minerals. Microwave also increase grindibilety, increase minerals liberation, more efficient downstream processing by reducing fines production and reduce the wear of mill, liner and charge i.e. reduce operating cost. Molecule with dielectric polarity tends to align itself in an electric field inducing a temporary dipole movement and reverting to original position when the field is removed. This movement generates friction inside dielectric material with the energy dissipated as heat. Household microwave unit with frequency 2.45GHz and power 800W was taken. Microwaves were applied for various times ranging from 10 sec to 30 minutes. The samples were then ground for 20 min in laboratory ball mill. Experimental investigation for grinding of North Waziristan Copper ore showed that microwave pretreatment of 10 seconds is optimum exposure time prior to grinding and gave high output of nearly 25% passing at sieve size of 300□m as compare to grinding without prior application of microwave which results in only 5.78% passing at 300□m. It was also observed that microwave treatment has more pronounced effect on course grained particle being good absorbers as compare to fine grained ore.**

Keywords: Mineral liberation, grindibilety, microwave, North Waziristan copper, comminution.

I. INTRODUCTION

There has been a tremendous increase in the metal demand particularly the base metals. Aluminum and Copper outputs have increased by a factor of 900 and 250 respectively [1]. Consequently most metal reserves will be depleted in approximately 50 or 60 years. Therefore low grade ores need to be mine out in order to meet the needs of increasing population. Also in today mineral processing industry large amount of valuable minerals are wasted because of the inability of the industry to treat low grade ores economically and to fully liberate the valuable minerals from the associate gangue particles. Liberation is achieved by comminution processes. However comminution is energy intensive with typically only 1% of the energy input available for breakage. This result in energy requirements for comminution is more than 50% of the total energy used in the extraction process [2], [3]. Alternative methods should be employed to increase the grindibilety and reduce the energy consumption in grinding operation and increase liberation efficiency. Microwave treatment can be employed to increase the grind ability of the ore up to 50% and reduce the energy requirement of the comminution circuit up to 44% of the total energy consumption. Microwave treatment can be used to reduce grinding energy and increase liberation [4]. Microwave heating generates heat internally with in material and cause selective heating [5]. Such differential hearing results in differential stresses at minerals grain boundaries and weaken the ore body. It is to be noted that most valuable minerals are microwave radiation absorber and gangues are transparent to these radiation [6]. Materials which absorb microwave radiation is referred to as dielectric and microwave heating is referred to dielectric heating. Molecule with dielectric polarity tends to align itself in an electric field inducing a temporary dipole movement and reverting to original position when the field is removed. This movement generates friction inside dielectric material [7]. Heats produced with in material depend on electric field strength, frequency and dielectric property of material. Microwave treatment is energy and time reduction and low cost has more pronounced effect on coarse grained particle as compare to fine grain particles [8].

[1]M.Sc Student, Mining Engineering Department, University of Engineering and Technology Peshawar
[2]Assistant Professor Mining Engineering Department, University of Engineering and Technology Peshawar

II. MATERIALS AND METHODOLOGY:

Test were conducted on north Waziristan copper ore of grade ranges from 0.3856 %to 2%. Samples were subjected to standard procedure of crushing and grinding. Effect of microwave treatment on ore liberation and grinding is determined by grinding the ore sample without microwave treatment and other samples are placed in microwave for different times and effect of grindibilety and liberation is determined by grinding the sample in laboratory ball mill for 20mints and than sieve analysis is carried out. After careful sieve analysis the results are plotted in the form of density curve distribution. Twelve representative samples of North Waziristan chalcopyrite ore samples are prepared. Sieve analysis of the first sample is carried out after crushing it in roll crusher. Sieve analysis of sample 2 is carried out after crushing in roll crusher and then ground it in ball mill for 20 mints. Sample 3 was kept in house hold microwave of frequency 2.45GHz, power 800W for time 15 mints after crushing and then grinded it in ball mill for 20 mints and then sieve analysis is carried. Same procedure were applied for sample 4 to 12 but different microwave treatment time ranges from 15mints to 10 sec. 2100um, 2000um, 1000um, 300um, 150um, 106um, 75um, 63um and 45um sieves were used and mass fractions of each sieve were noted for each sample treated for different in microwave for different time.

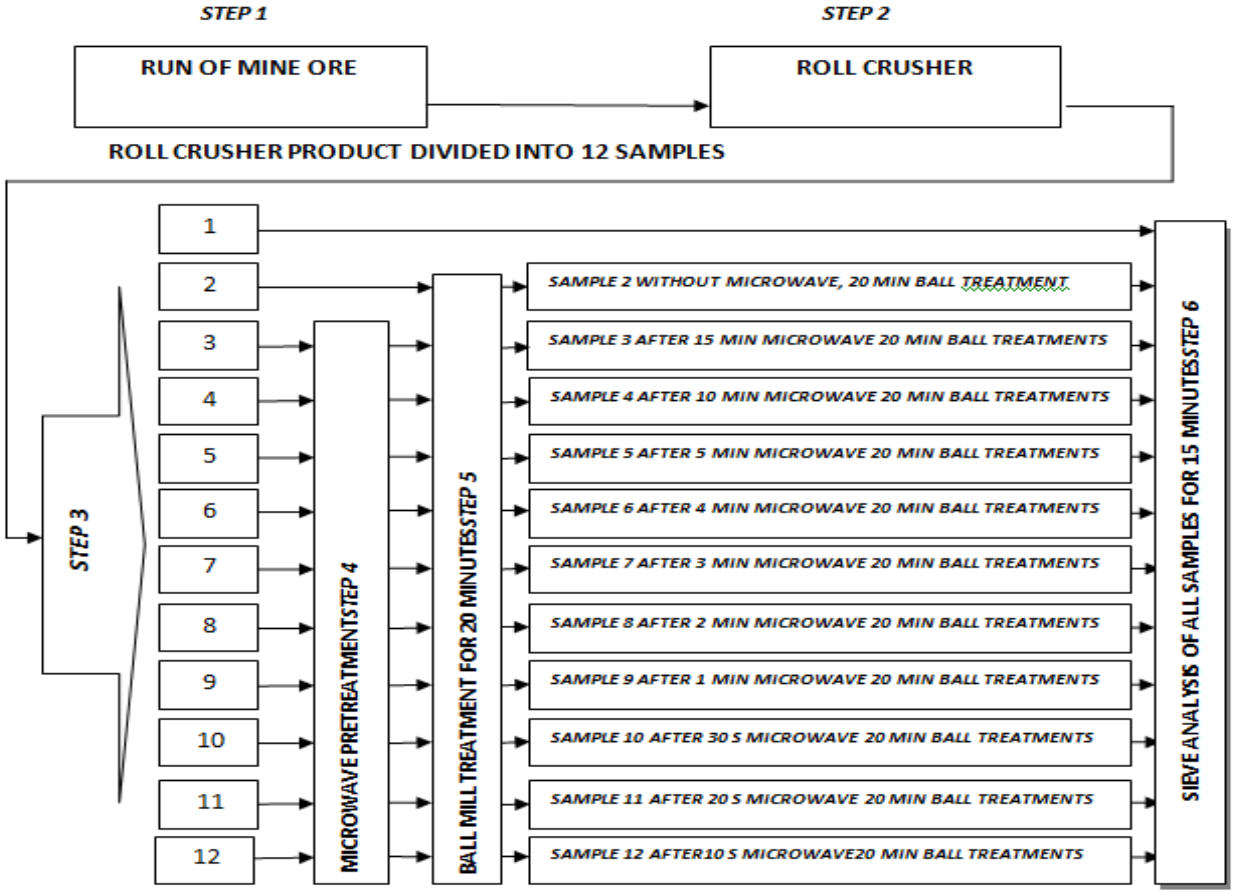

Fig. 1: Line diagram showing the experimental procedure of Microwave assisted grinding.

III. RESULTS AND DISCUSSION:

It was observed that time has significant effect on grindibilety of North Waziristan copper. Grindibilety increase with increase in time for which the samples are placed in microwave but at the same time electrical energy consumption also increases which adversely affect feasibility. Energy consumption for 30 second treatment in microwave is 21.166kWh/t and work index for copper ore is rarely greater then 30kWh/t therefore microwave exposure time greater than 30

second should be discarded. From the results it is clear that 10 second particle size distribution curve(PSD) leads 20 seconds PSD curve by 4.06% to 0.30% at sieve size 45um, 4.7% to 2.57% at sieve size 75um, 10.11% to 4.29% at sieve size 106um, 18.6% to 8.36% at sieve size 150um, and 24.91% to 19.53% at sieve size 300um. At sieve size 1000um 10 second curve lags behind 20 second curve only by 28.92% to 33.83% which is not significant because 10 second treatment gave more recovery and utilizes half of energy as compare to 20 second treatment. The optimum microwave treatment time for North Waziristan chalcopyrite ore is 10 second with in size range of 100um to 300um at power 800W and frequency2.45GHz.

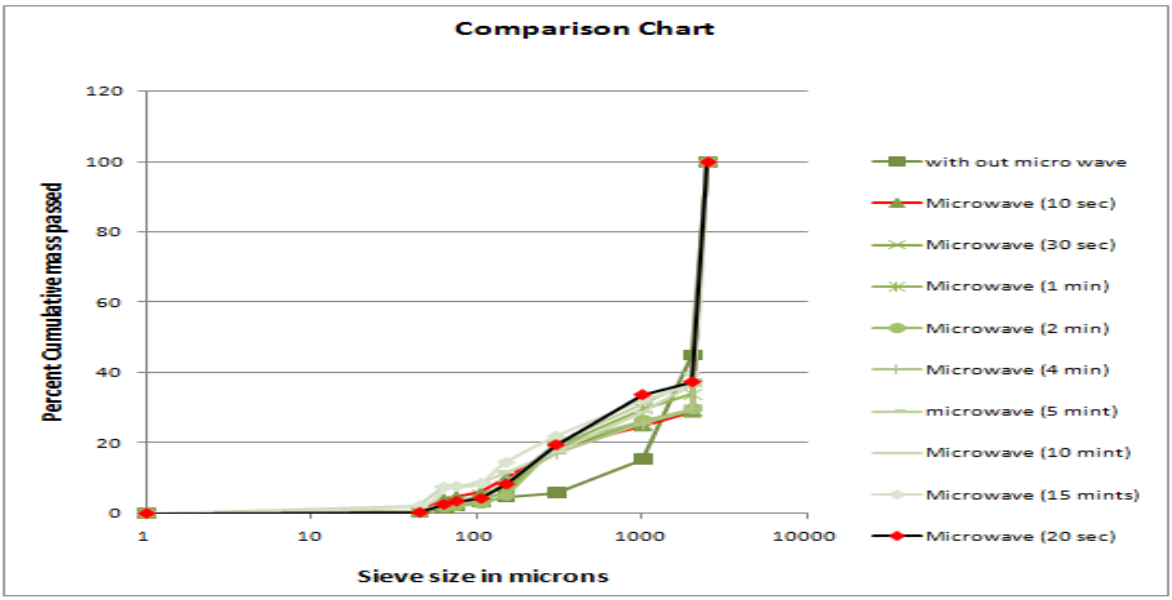

Fig 2: PSD curve for various duration of Microwave treatment time

IV. CONCLUSION:

Effect of Microwave energy on liberation of North Waziristan copper ore from the associated gangue is determined and investigated and it is concluded that Microwave assisted grinding have better results as compare to unassisted grinding. Treatment of sample in Microwave at frequency 2.45GHz, Power 800W for time interval of 10 seconds gave best result i-e 24.91% passing at sieve size of 300□m as compare to unassisted grinding which results only 5.78% passing at 300□m. As compare to conventional heating technique Microwave heating have higher heating rate and no direct contact between heating source and heating materials.

V. RECOMMENDATIONS:

Main focus of the study was to determine the effect of Microwave energy on North Waziristan copper ore liberation which proved to be feasible and viable. Microwave treatment increase liberation i-e release of valuable minerals from the associated gangue particles; reduce fine production in grinding operation. Economic aspects of the operation and interaction of different operational parameters with each others should be studied so that to find whether the Microwave process is viable on pilot scale or not. House hold microwave with frequency of 2450MHz was employed for experimental work which is less efficient in penetration power as compare to 945MHz which have too high penetration power in mineral.

REFERENCES:

1. Wills B.A, 1997. Mineral Processing Technology, 6th Edition, Butterworth Heinemann, Oxford, ISBN 0 7506 2838 3.
2. Wills B.A and Atkinson K, 1993. Some Observations on the fracture and liberation of mineral assembles, Minerals Engineering, vol 6, no 7, p 697 – 706.
3. Esk, C.S; 1986, Energy usage in mineral processing, Mineral processing at Acrossroads, Martinus Nijhoff Publishers, Dordrecht, ISBN 90 247 3410 X, pp 133 – 155.

4. Standish.N, Unusual effects of Microwave irradiation in granular materials, proceeding of the First Australian Symposium on Microwave Power Application, p 227- 234.
5. Haque, K.E; 1999 Microwave energy for Mineral Treatment Process- A brief review, international journal of Mineral processing, vol. 57, pp 1_24.
6. Kingman, S.A. and Rowson, N.A. (1998) Microwave treatment of Minerals-A review of Minerals Engineering, Vol. 11, No.11, pp 1081—1087.
7. Jones, D.A, Lelyveld, T.P, Mavrofidis, S.D, Kingman, S,W, and Miles, N.J, (2002) Microwave Heating Applications in Environmental Engineering—A review, Resources, Conservation and Recycling, Vol. 34, pp 75-90.
8. Bykov, Y.V, Rybakov, K.I, and Semenov, V.E. (2000).High Temperature Microwave processing of materials, Journals of Physics D: Applied physics Vol. 34, pp 55-75.

Desulphurization of Indigenous coal by Oil Agglomeration

U. Tariq[*1], *M.I. Ahmad*[1], *Al. Javaid*[1], *M. Jamil*[1], *S. Khan*[1], *W. Jan*[1], *M.Y. Gul*[1], *M.C. Das*[1]

***Abstract*: The aim of this research work is to reduce sulphur content of local coal in order to use in cement and power industries. Coal used in these industries must have sulphur content up to maximum of 1%. In Pakistan available coal has high sulphur content (above 4%) then required. About 40% of power plants all over the world are coal based so different processes are developed to overcome the problem of high sulphur content. In this research oil agglomeration method was employed on local Dara coal having high sulphur content of 4.44%. The said process formed agglomerates of coal particles as oil come in contact with coal. Experimental work showed 19.32% sulfur reduction for 10% oil dosage and on these conditions reduction of 3.55% of sulphur content was obtained although the result is impressive but still are not enough for EPA standards.**

***Keywords:* Desulphurization, coal, sun flower oil, agglomeration.**

I. INTRODUCTION

Coal is most abundantly used as energy resource all over the world. The main reason for its uses at such level is its availability, cheapness and its high energy content. About 40% of world electricity is generated through coal based power plants [1]. Now the world is trying to shift from coal but in fact there is no such alternative available to take its place. The other resources like fuel and natural gas are already in depletion process. So the coal is still the largest single fossil fuel available on earth [2].

Metallic and nonmetallic impurities are usually present in the coal which causes serious environmental issues. One such impurity is its sulphur content which is consider as a main threat to environment. Ozone layer depletion, acid rain, human health concerns and harmful effects on agricultural corps are some of consequences of coal burning with high sulphur content. Available resources of high grade coal (i.e. low sulphur content) is not enough to meet the demand requirement in long terms. So the interest has been developed to utilize the high sulphur coal resources.

[1]Department of Chemical Engineering, University of Engineering and Technology, Peshawar.
*uzairtariq_67@outlook.com

Pakistan has large deposits of coal. Estimated coal reserves of Pakistan is about 185.5 billion tonnes [3]. Unfortunately the coal deposits of Pakistan are of low grade (i.e. high sulphur content), so it cannot be used directly for power generation. There are different methods used all over the world to make feasible the use of this low grade coal. Chemical demineralization processes, either alone or following physical cleaning processes, have been extensively used for the production of Ultra Clean Coal. Some of these processes include leaching with NaOH [4], NaOH followed by mineral acids [5], KOH-acids [6], Na_2CO_3 , $Ca(OH)_2$ followed by acid washing [7], mineral acids viz. HNO3 [8], HCl [9] , H2SO4 [10], oxidizing agents through H_2O_2, $Fe_2(SO_4)_3$, $K_2Cr_2O_7$ [11], NaOCl [12], HF then HNO_3 [13] and sequential leaching by $NaOH–H_2SO_4$ [14]. Leaching is employed most commonly for coal desulphurization, it includes acid leaching by hydroiodic acid (HI) at 260 ^{0}C and 60 bar pressure [15], and second is alkali leaching with NaOH [16], these both techniques are good but temperature and pressure for these techniques are very high, on other hand extreme care is requird in handling these solutions. Process of dry chlorination results in significant reduction in sulphur content [17] but chlorine is hazardous chemical. Froth flotation [18] is also commonly used method for the said purpose but results in lower combustible recovery. Fine coal cleaning process was investigated. In this process coal with particle size less than 200 micron were subjected to cyclone and thus results in sulphur reduction [19]. This process involve ultrafine coal which again results in higher operating cost involved in crushing the particles to desired size and lower recovery. Oil agglomeration process is a new technique, its processing is very simple and also very economical [20].

II. MATERIAL AND METHODS:

A coal sample from Darra Mines, KPK, Pakistan was taken for this research study. Sun flower oil was used in this work and also a huge amount of water, further Acetone was used for removal of oil adhered to the coal recovered during the process.Rod mill was used to crush the coal into desired particle size, screen

analysis was done by Screen Analyzer. Particle size distribution were shown in Table 1 and figure 1-3.

Table 1: Particle size distribution analysis

SAMPLE 1		
SIZE OF APERTURE (mm)	AMOUNT OF PRODUCT (%)	
0.425	8.93	
0.3	41	
0.25	7.01	
0.125	31.03	
0.106	12.04	
D_n	D_s	D_v
0.1616 mm	0.2339 mm	0.1935mm
SAMPLE 2		
0.425	5.19	
0.3	45.89	
0.25	5.59	
0.125	30.12	
0.106	13.22	
D_n	D_s	D_v
0.159 mm	0.2308 mm	0.1906 mm
SAMPLE 3		
0.425	5.24	
0.3	46.39	
0.25	7.23	
0.125	28.25	
0.106	12.89	
D_n	D_s	D_v
0.1599 mm	0.2337 mm	0.1925 mm

Sieve used for separation was one of the most important parameter because it directly affect the amount of combustible material. As more than 50% coal was in between sizes of -0.5mm to +0.125mm. So sieve of size -0.125 was used for recovery of coal after process.

III. EXPERIMENTAL PROCEDURE:

Flotation cell unit having a container with internal capacity of 3L was used as an agglomerator. Coal samples with different sizes were mixed with water at ratio of 10% to solids. Coal – water mixtures were conditioned at 1000 rpm for five minutes in order to get homogenous mixture of coal and water. Sun flower oil was added in order to form agglomerates of sulphur particles. The mixture was further agitated at 1500 rpm for 10 minutes. The experiments were carried at natural pH of coal – water – oil mixture. After completion of process the separation of combustible/recoverable coal and agglomerates was done by using sieve of -0.125mm aperture size, for this purpose water was used. At the end acetone was used to remove adhered oil from the recovered coal and the sample was dried in Tray Dryer. This experiment was repeated for 15% and 20% oil dosage.

IV. RESULTS AND DISCUSSION:

Size distribution analysis of the sample show that sample 1 having mass of 200 gram contains 88% of particles above +0.125mm mesh, with arithmetic mean diameter (Dn), volume surface mean diameter (Ds) and volume mean diameter (Dv) of 0.162mm, 0.234mm and 0.194 mm respectively. For sample 2, 87% of particles are in fraction of -0.425mm to +0.125mm with Dn = 0.159mm, Ds = 0.231mm and Dv = 0.191mm. Sample 3 also has same mass and about 87% of the particles are in fraction between -0.425mm and +0.125mm with Dn = 0.160mm, Ds = 0.234mm and Dv = 0.192mm. Size distribution analysis are shown in table 1 and figure 1 to 3.

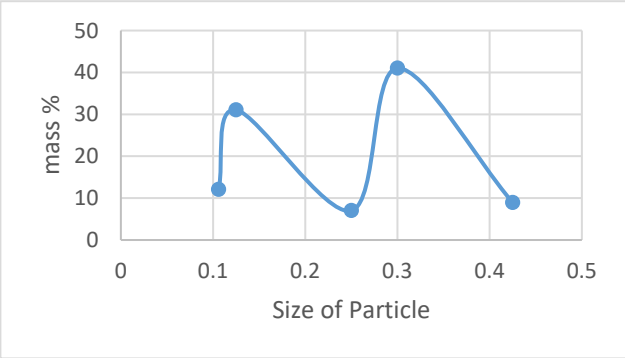

Figure 1:Particle size distribution (Sample 1)

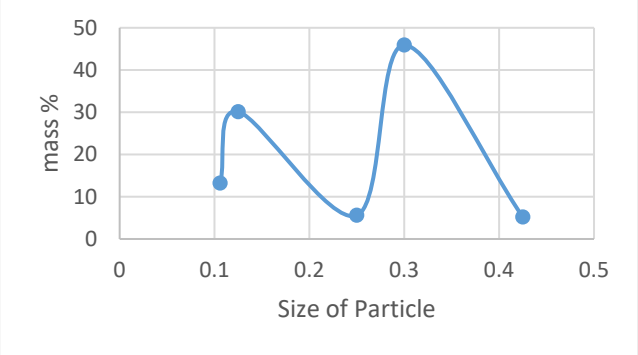

Figure 2: Particle size distribution (Sample 2)

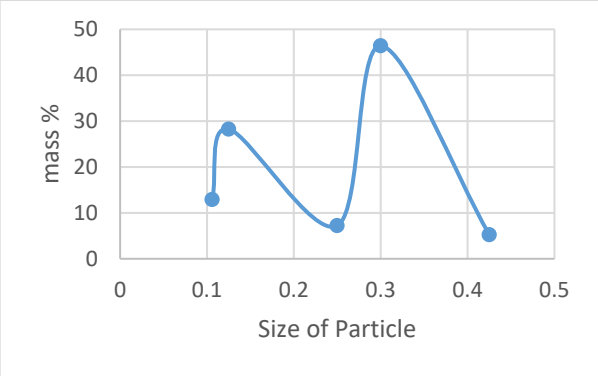

Figure 3:Particle size distribution (Sample 3)

In this experiment a single parameter was studied to check the influence of oil dosage on sulphur reduction of coal. Sample 1 was treated with 10% (solid ratio) sun flower oil and the sulphur content was reduced from 4.40% to 3.55% i-e. 19.32% sulphur reduction. For sample 2, 15% sun flower oil dosage was used and the sulphur content reduced to 3.66% with 16.82% reductionin comparison to raw coal. 20% oil dosage was used for sample 3 and sulphur content reduces to 3.72% with 15.46% sulphur reduction. So with increase in oil dosage sulphur reduction decreases because oil adhering to form agglomerates also causing sulphur to adhered to coal surface. Results are shown in table 2.

Table 2: Experimental Results

Sample	Raw Coal	10% Oil Dossage	15% Oil Dossage	20% Oil Dossage
S %	4.40%	3.55%	3.66%	3.72%

V. CONCLUSION:

Results obtained show maximum sulphur reduction of 19.32% for oil dosage of 10%. For 15% and 20 % oil dosage, sulphur reduction of 16.82% and 15.46% was obtained respectively.

It was observed that with increase in oil dosage sulphur reduction decreased because of sulphur adherence increase as oil dosage increases with coal agglomerates.

The results showed significant decrease in sulphur content but EPA requirements were not met.

REFERENCES:

[1] BP (British Petroleum) statistical review of world energy. London; June 2014.

[2] Singh R, Sinha S.N., Beneficiation of high ash Indian coal-problems and prospects. IndianMinEngJ2003:1–4.

[3] Calkins WH, “The chemical forms of sulfur in coal: a review”, Department of Pakistan coal power generation potential, 2004Chemical Engineering, University of Delaware, Newark, DE 19716, USA.

[4] Balaz P, LaCount RB, Kern DG, Turcaniova L, “Chemical treatment of coal by grinding and aqueous caustic leaching”, Fuel, 2001;80:665–71.

[5] Mukherjee S, “Demineralization and desulfurization of high-sulfur Assam coal with alkali treatment”, Energy Fuels, 2003;17: 59–64.

[6] Kumar M, Shankar RH, “Removal of ash from Indian Assam coking coal using sodium hydroxide and acid solutions”. Energy Sources 2000, 22(2):187–96.

[7] Wang J, Zhang ZG, Kobayashi Y, Tomita A, “ Chemistry of Ca(OH)2 leaching on mineral matter removal from coal”, Energy Fuels, 1996;10:386–91.

[8] Alam HG, Moghaddam AZ, Omid KMR, “The influence of process parameters on desulfurization of Mezino coal by HNO3/HCl leaching”, Fuel Process Technology, 2009;90:1–7.

[9] Mukherjee S, Borthakur PC, “Chemical demineralization/desulfurization of high sulfur coal using sodium hydroxide and acid solutions”, Fuel, 2001;80:2037–40.

[10] Paul M, Seferinoglu M, Ayçik GA, Sandström A, Smith ML, Paul, J. “Acid leaching of ash and coal: time dependence and trace element occurrences”. Int JMiner Process 2006;79:27–41.

[11] Li W, Cho EH. “Coal desulphurization with sodium hypochlorite”. Energy Fuels 2005; 19:499–507.

[12] Steel KM, Besida J, O'Donnell TA,Wood DG. “Production of ultra-clean coal”, Part-III. “Effect ofcoal's carbonaceous matrix on the dissolution of mineral matter using hydrofluoric acid”. Fuel Process Technol 2002; 76:51–9.

[13] Steel KM, Patrick JW. “The production of ultra-clean coal by chemical Demineralization”. Fuel 2001;80:2019–23.

[14] Nabeel A, Khan TA, Sharma DK.”Studies on the production of ultra-clean coal by alkali-acid leaching of low-grade coals.Energy Sources”, Part A: RecovUtil Environ Effects 2009; 31:594–601.

[15] Andres JM, Ferrando AC, Membrado L. “Chemical desulfurization of coal with Hydroiodic acid”. Energy Fuels1996; 10:425–30.

[16] Kara H, Ceylan R. “Removal of sulfur from four central Anatolian lignites by NaOH”. Fuel1988; 67:170–2.

[17] Shen S, He K, Pan M, Zhou Z, Feng C, Liang G, “Effective removal of sulfur from high-sulfur coal prior to use by dry chlorination at low temperature”, Journal of Hazardous Materials 217– 218 (2012) 116– 122

[18] Demirbas A, “Demineralization and desulfurization of coals via column froth flotation and different methods”, Energy Conversion and Management 43 (2002) 885–895.

[19] Rubiera, F., Hall, T.S., Shah, L.C.,”Sulfur removal by fine coal cleaning processes”, Fuel 1997, Vol 76-13, pp. 1187-1194.

[20] Sahinoglu E., Uslu T, “Effect of particle size on cleaning of high-sulphur fine coal by oil agglomeration”, Karadeniz Technical University, Department of Mining Engineering, 61080 Trabzon, Turkey.

Desulfurization of Coal from Cherat by Froth Flotation

M.Y. Gul, M.I. Ahmad, M. Ali, A.U. Khan, S. `Sahibzada, U. Tariq, M.S. Das, A. Khan.

Abstract: **The aim of this research work is to desulfurize indigenous coal by one of the demineralization method to make it feasible for use in power generation and cement industries. Froth flotation method is an efficient method for reduction in sulfur and ash content. The underlying principle of the said process is formation of the froth upon contact of frother with coal particles. Pine oil dosage being the control parameter, the analysis showed that maximum sulfur reduction of 33 % was obtained for 30 minutes flotation time, reducing sulfur content of Cherat coal sample from 3.6 % to 2.4 %. It was found that froth flotation caused significant reduction in sulfur content of Cherat coal, yet the power generation requirements of sulfur content in coal were not met.**

I. INTRODUCTION

Due to the depletion of oil and natural gas, there comes an intense need of an alternate source that can fulfil the requirement of current power generation. Coal being present in an enormous amount worldwide, it can be announced as a suitable energy source replacement due to its high heat content. Coal is used in different sectors like electricity generation, steel and iron industries, power plants, cement industries and in the household in the form of briquettes. As estimated by the world coal association, 70 % of the world's steel production is based on coal and 41 % of the world electricity generation is thorough coal [1]. Coal in its raw form cannot be fully utilized and has been limited due to the presence of significant amount of impurities. Such impurities include, ash, sulfur, silicates, which upon combustion produce toxic gases like Co_2,Co, NOxes, SOxes, and other organic pollutant compounds. Among these, sulfur is the major pollutant and upon combustion produces hydrogen sulphide and sufur dioxide which results in the formation of acid rain. Sulfur and its compounds has a harmful effect on the environment like ozone layer depletion, metal corrosion, agricultural diseases, and respiratory diseases of both the animals and humans.

In coal sulfur exists in two forms.i.e. organic and in organic. A physiochemical process, froth flotation may be used for the reduction of inorganic sulfur which is present in the form of sulfate and sufide compounds. Coal has to be desulfurized prior to combustion by either of the methods. The methods used are physical, chemical and biological in nature. Every process has its own pros and cons.e.g. physical process may be applied for separating the pyritic type of sulfur. Physical process is less economical. Biological method may be applied for removing a specific type of sulfur by using respective microbe but this technique takes too much time. Chemical technique is the most effective one, because with this method in organic as well as some amount of organic sulfur can also be removed.

Demineralization of coal can be achieved by using acidic or basic agents. Basic solutions, such as NaOH, KOH, $Ca(OH)_2$, or acidic solutions such as HF, HCl, H_2SO_4, $HN0_3$, as well as H_2O_2 and combinations of all these chemicals have been attempted to remove the undesired minerals [2]. Besides methods like physical, biological and chemical, other methods include solvent extraction, thermal, nuclear, oxidation, electrochemical, alkali and hydro desulfurization. Reagents may be varied for removing specific type of sulfur and from specific type of coal.

As mentioned earlier coal desulfurization by physical method is cost effective but it can remove only a limited portion of coal. Physical process includes froth flotation, oil agglomeration, jigs, and cyclones, dense medium separation magnetic separation, electrostatic separation, microwave processing.

Froth flotation is a physiochemical method which uses the concept of difference in wettability of coal and sulfur particles. Sulfur being hydrophobic in nature is removed by froth flotation process. Generally this process is used for the coal particle size less than 0.5mm. The carbonaceous mineral constituents of coal being hydrophilic in nature, can be made to preferentially attach to fine bubbles and float to the surface of a dilute slurry, where they can be removed, while in contrast the low carbonaceous inert minerals of the raw coal do not attach to the bubbles [3]. Flotation reagent cost adds up to the processing cost which makes the flotation method more expensive than other physical methods. Yet, to remove inorganic

materials' viz. pyritic sulfur, the most suitable process is flotation to clean coal provided it is liberated in feed [4].

Oil agglomeration like froth flotation uses the principle of hydrophobicity of coal particles for removing sulfur. This method is especially used for ultrafine particles. This method removes mostly the inorganic form of coal and is thus used for coal having less ash and inorganic sulfur percentage. A physical method of cleaning Assam coals from India by agglomeration with xylene and hexane was reported by Baru et al. [5]. The maximum organic matter recovery for xylene has been found to be 92% whereas with hexane the value is about 55% on a dry basis. The highest ash rejection values with xylene and hexane are almost the same (90%).

Magnetic separation is another physical method for desulfurization of coal. This method uses the concept of the difference in the magnetic properties of coal and the associated unwanted materials.

II. Materials, Methods and Analysis

A. Materials

Coal: the coal sample collected from Cherat (25 Km from Nowshera) coal mine in Cherat, Pakistan, Pine oil; Gas oil and copper sulfate ($CUS0_4.5H_20$) were used in flotation of coal. Jaw crusher, Rod-Ball mill, sieve, flotation device, electrical furnace, tray dryer and screen analyser were used in this research. The coal used in this work was obtained from Cherat, KPK of Pakistan. Huge amount of water was used in order to make a pulp (10%). Copper sulfate was used as activator. Activators are specific compounds that make it possible for collectors to adsorb on to surfaces that they couldn't attach to. Pine oil was used as a frother. Frothers are compounds that act to stabilize air bubbles so that they will remain well dispersed in the slurry and will form a stable froth layer. Gas oil was used as collector. Collectors are reagents that are used to selectively adsorb on to the surface of particles. Actually collectors make sulfide particles hydrophobic which aids it in separation from the coal.

B. Methods

Primary crushing of the coal in lump form was done using primary crusher, jaw crusher. Rod Mill was used to grind the coal into desired particle size, screen analysis was done by Screen Analyser in the Mineral Processing Lab of Mining Department. Particle size distribution of the samples is given in Table 1 to 3. Floatation Cell in the Mineral Processing Lab of Mining Department with tank capacity of 3 L and stirrer speed of 1800 rpm was used as a flotation cell.

Froth flotation is a highly versatile method for physically separating particles based on differences in the ability of air bubbles to selectively adhere to specific mineral surfaces in mineral/water slurry. Coal samples were first crushed using primary crushers and are then grinded. For each test Grinded coal with varying particle size were mixed with water and a pulp (10 %) of it is made. Coal water mixtures were conditioned at 1000 rpm for 10 minutes in order to achieve complete wetting of coal particles. Calculated amount of Copper sulfate(20 g/ton coal) was then added and further conditioned for another 10 minutes. Then pine oil (250g/ton coal) and gas oil(100g/ton coal) were added to pulp and is given 10, 20 and 30 minutes flotation time in the flotation unit for three runs respectively. After flotation, the suspensions were transferred to a recovery sieve with an aperture of 0.5 mm to separate the desulfurized coal from water and tailings. Finally, water was removed from the coal in Tray Dryer.

C. Analysis

i. Measuring moisture content

The coal sample was crushed to 200 µm and by using ASTM D-3173 Standard [6], the moisture content of coal was measured to be 0.88%

ii. Measuring ash content

the coal sample was crushed to 200 µm and by using ASTM D-3173 Standard, the moisture content of coal was measured to be 35.4 %.

iii. Measuring volatile matter content

the coal sample was crushed to 200 µm and by using ASTM D-3175 Standard [7], the moisture content of coal was measured to be 18.26 %

Table 1 Particle size distribution analysis of sample 1

Aperture size (mm)	Amount of product (%)
0.0905	12.4
0.1875	27.45
0.1155	60
Ds = 0.1246 mm	

Table 2 Particle size distribution analysis of sample 2

Aperture size (mm)	Amount of product (%)
01155	26
0.1875	34
0.0905	39
Ds = 0.119 mm	

Table 3 Particle size distribution analysis of sample 3

Aperture size (mm)	Amount of product (%)
0.1155	24.6
0.1875	28.3
0.0905	47
Ds = 0.113 mm	

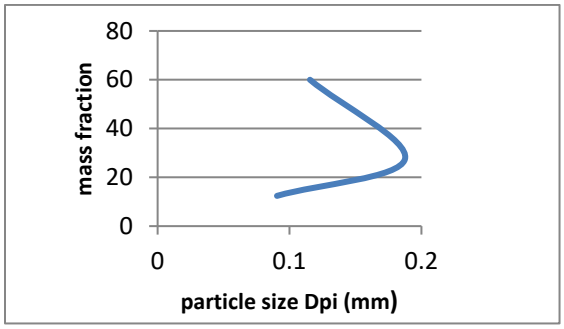

Fig. 1 Particle size distribution of sample 1

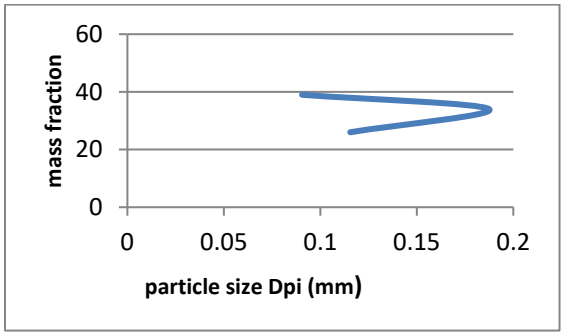

Fig. 2 Particle size distribution of Sample 2

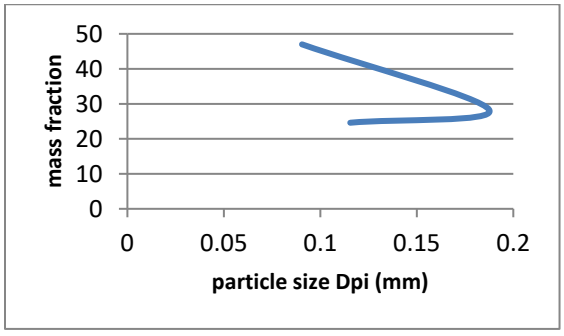

Fig. 3 Particle size distribution of Sample 3

Table 4 Proximate analysis of Cherat coal sample

component	wt %
Moisture content	0.088
Ash content	35.4
Volatile matter	18.26
Fixed carbon	46.252
total	100

III. RESULTS

The coal sample is crushed and grinded and its particle size distribution is done via sieve analysis. Size distribution curves and the mean particle diameter of the samples are given in the figure 1 to 3. The samples were then given flotation time in the flotation unit. It has been found that for a flotation time of 10 minutes, the coal desulfurized from 3.6 % to 3.0 %, to 2.7 % for 20 minutes time and to 2.4 % for a flotation time of 30 minutes. The results have been shown in the table 5

Table 5 Desulfurization vs flotation time data

Sample	Time (min)	Sulfur content
Initial coal		3.6
1	10	3.0
2	20	2.7
3	30	2.4

IV. CONCLUSION

From the results it has been concluded that by keeping all other conditions constant, the flotation time has a direct relationship with the desulfurization of coal. The more the flotation time, an enhanced desulfurization of coal occurs. A lot of work has to be done further by changing the amount and the type of frothers activators and collectors.

REFERENCES:

[1] Singh R, Sinha SN. Beneficiation of high ash Indian coal-problems and prospects. Indian Min Eng J 2003:1-4.
[2] Haidar DD. Beneficiation of non-coking coals: basic concepts and technology routes. In: Singh R, Das A, Banerjee PK, Bhattacharya KK, Goswami NG, editors. Proceedings of the XI International Seminar on Mineral Processing Technology (MPT-2010). Jamshedpur: Allied publishers; 2010. p. 419-27.
[3] Couch GR. Advanced coal cleaning technology, IEA Coal Research. IEA Coal Research Publishers; 1991.
[4] Ozgen S, Tiirksoy VO, Sabah E, Oruc; F. Process development studies on recovery of clean coal from ultra fine hard coal tailings using enhance gravity separator. Can J Chem Eng 2009;87:715-25
[5] Baruah MK, Kotoky P, Baruah J, Bora GC. Cleaning of Indian coals by agglomeration with xylene and hexane. Sep Purif Technol 2000;20:235-41.
[6] American Society for Testing and Materials. ASTM D-3173; 1993. p. 322-3.
[7] American Society for Testing and Materials. ASTM D-3175; 1993. p. 327-9.

Pore Scale Numerical Simulation of Microfiltration of Slotted Pore Filters Via COMSOL Multiphysics - Deformation Behavior of Oil Droplet

Nabeel Ahmad[1] and Muddasar Habib[2]

***Abstract*— Step wise deformation behavior of an individual oil droplet with respect to interfacial tensions between water-oil phases at different in pore filtration velocities (slotted pore dead end microfiltration) is investigated numerically by solving the Navier-Stokes equations in Comsol Multiphysics. Level set method in laminar flow is employed to solve the model where the diameter of individual spherical oil droplet is kept greater (8 µm) as compared to the width (6.68 µm) of understudy slot. We found that during filtration; same droplet is rejected back due to the presence of higher interfacial tension (34 mN/m) forces at specifically low magnitude (< 40 µm/sec) of in pore filtration velocity. It is demonstrated that an early deformation of oil droplet is associated with lower interfacial tensions between liquid phases or higher magnitude of filtration velocity. No droplet entry is noticed without its prior squeeze and subsequent deviation of initial spherical shape of droplet. Influence of drag force due to in pore filtration velocity & static force due to interfacial tension is verified for rejection or passage of oil phase which is in excellent agreement with experimental and numerical works. With increasing interfacial tensions more filtration time is required to deform an oil droplet at sufficiently higher (>40 µm/sec) in pore velocity of permeate. A delay of 20 milli-sec is noted at filtration velocity of 75 µm/sec; between the systems with a values of interfacial tensions set at 9 mN/m & 34 mN/m respectively. Investigation through images/results of numerical simulations shows that spherical shape of an oil droplet within the non-converging slot turns into plate like oblate spheroid. It is indicated that drag force tends to pass a droplet through the slot and it was less effective at lower in pore velocity (<40 µm/sec) and the same is numerically conforming to analytical relation of drag force and change in surface area of deforming oil droplet.**

***Index Terms*—filtration model, level set method of comsol multiphysics, pore scale simulation of oil droplet deformation,**
two phase flow,

[1]Msc Student, Department of Chemical Engineering, UET Peshawar, KPK Pakistan, (qazinabeel@yahoo.com)
[2]Associate professor, Department of Chemical Engineering, UET Peshawar, KPK Pakistan, (muddasarhabib@nwfpuet.edu.pk)

I. INTRODUCTION

Presence of dispersed oil phase in waste water is associated with number of chemical industries such as food processing, pharmaceutical, oil extraction & textile processing units [1]. Bulk quantity of hydrocarbon phase is being emitted from oil and gas producing units which account for many environmental problems. To reduce the impact on aquatic life the concentration of oil phase is maintained upto 30 mg /liter for offshore facilities. [1]. At present, in order to comply with strict environmental regulations and recent development in resource recovery processes have attracted the researchers to improve the current technologies for effective and economical treatment of oil in water emulsions[2]. The conventional processes which involve the application of hydrocyclone, gravity separator and addition of extraneous chemicals have been inadequate with respect to nature and size of oil drops. In last decade; Membrane technology such as microfiltration and ultrafiltration have been investigated and satisfactorily removed the oil concentration from industrial emulsions [1]. Ultrafiltration process can remove the oil drop less 10µm in size, but it can treat only low volume of effluents. The application of Microfiltration has got attention of industrialist to achieve the desired throughput [3]. Cross flow and dead end microfiltration modes of operation are used for separation of oil in water emulsions. A comparative study on critical separation parameters reveals that higher flux is achieved in dead end than cross flow microfiltration [4].

Morphology of membrane is important in filtration. Depth microfiltration is avoided due to the internal complex structure of the pores which resultantly operate at higher transmembrane pressures. Slotted pores true surface filter media provide high area of filtration and operate at substantial low operating cost [5]. Numbers of experimental investigations [2] [6] [1] discloses that deformation of oil drops occurred whenever it passage is observed through the slot having width smaller than diameter of oil drop. A mathematical formulation was made to elaborate the

influence of drag force and static force for the permeation or rejection of drops through membrane respectively [6].

The early work [2] [6] [1] on oil droplet entry or deformation through the pore provide an estimated transmembrane pressure or drag force for the permeation or rejection of oil droplet. These studies aimed only to deliver overall picture of the flow in terms of empirical formulations, and however the entire process of droplet dynamic at microscopic level is still deficient regarding the better understanding of hydrodynamic behavior of an oil drop. With the development of modeling & simulation technique, a shape of an individual droplet in terms of its deformation or passage more precisely be evaluated at any course of time, with respect to different material properties and parameters [7]. To investigate the behavior of an oil droplet pinned at the entrance of microscopic pores, recently numerical studies have been performed for cross flow microfiltration operation only where the effect of shear force and transmembrane pressure were assessed [8].There is a need to explore these effects on dead end microfiltration.

In this paper, we examined the influence of interfacial tensions on droplet deformation, passage or rejection through the slot of membrane with the help of Comsol Model. This model indicates that poor rejection or deformation of an individual droplet is observed due to the low interfacial tension of water oil emulsion system at same in pore velocity. As long as an entry of oil droplet is observed at sufficiently higher in pore velocity(> 40 µm/sec & 40mN/m), it squeeze, pushed towards the membrane, deformed into oblate spheroid and finally permeated through the pore and tries to regain the initial shape. The overall process is demonstrated and found that this numerical work is well agreed with previous analytical models [2] and experimental works [6] [9].

The rest of the paper is organized in different sections as follows. Next section shows model description and detail of numerical simulation. Numerical results based on shape transformation of deforming oil droplet and effects of interfacial tension of the same are described in section. 3. On the basis of visual inspection of numerical simulations the findings are concluded in last section.

II. MODEL DESCRIPTION AND DETAIL OF NUMERICAL SIMULATION

Rejection or permeation of tinny oil droplet into the slot is a complex process which requires the knowledge of fluid dynamics, physics and material properties/ morphology of membrane structures. Pore scale modeling in Comsol Multiphysics is carried out by keeping one of the slots which pretenses the rapid constriction to the flowing fluid like an orifice of short length [5]. For the purpose of understanding of the model conceptual view of oil removal system which is used in whole simulation work is shown in fig.1 [9];

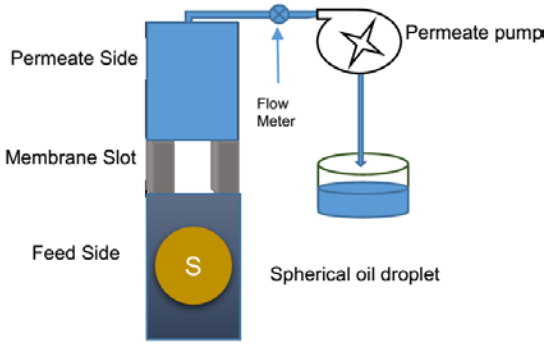

Fig. 1A. Schematic representation of oil water separation system where spherical droplet "S= 8µm" is placed near a slotted pore membrane, A; Macroscopic demonstration

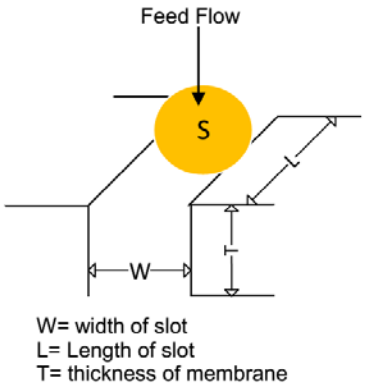

Fig. 1B . Schematic representation of pore scale model used in simulation which shows the cross sectional view of slot. Where values of W; L & T are 6.68 µm, 20.04 µm & 6.66 µm respectively

For the purpose of modeling, a slot is assumed with specific dimensions (see Fig.1) is drawn in Comsol Multiphysics. A spherical oil droplet (D= 8 µm) is kept at a small distance in front of slotted pore membrane makes domain for two phase flow. A snapshot of the same is show in fig. 2;

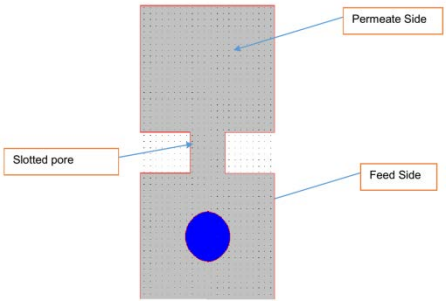

Fig.2. Initial geometry of model with spherical oil droplet (D0= 8 µm) in front of slot (W= 6.68 µm)

Length to width ratio (L/W= 3) and thickness of the membrane (X=

6.68 µm), constricted portion between feed and permeate side shows the slot.

To reduce the simulation resources such that the whole job can be managed on an ordinary PC, the above model is condensed with axial symmetry in Comsol Multiphysics as shown in fig.3;

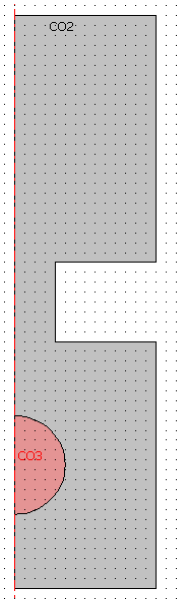

Fig.3. Geometry of model with Axial Symmetry showing the half of the spherical oil droplet with half width of slot (an orifice with finite length)

The width of understudy slot is selected to be greater than the 1.2 times the diameter of spherical oil droplet in order to analyze the actual deformation, behavior in terms of passage or rejection through the slot. Initially, droplet is kept at a distance of 6.25 µm away from the slot and laminar flow is assumed to ensure straight track of droplet towards the slot. Different in pore filtration velocities are set and time dependent simulation continued until the droplet passed through the slot or tries to do the same. The corresponding values and their results are elaborated in next section.
Finite volume & lattice Boltzmann methods previously been used to solve the multiphase flowing problems. Investigations reveal that, these interface capturing techniques are unpredictable where sharp transition of volume does not regain the correct algorithm [10]. In past, efforts were made to correctly evaluate the movement of interfaces during multiphase flow where level set method is used to provide the understating of foaming mechanism and hydrodynamics of droplets/bubbles of viscous liquid [11].
In this study, numerical simulations were carried out by commercial software Comsol Multiphysics V3.4 based on finite element solver technique. Standard level set method in Comsol Multiphysics is employed to track the exact position of moving liquid- liquid interfaces due to the difference of fluids properties such as density, surface tension, viscosity. One additional transport equation is solved along with Navier-Stokes equations and the continuity equation which accounts for conservation of momentum and mass respectively [12]. Two immiscible fluids with different interfacial tensions (9 mN/m, 20mN/m & 34 mN/m): water and oil droplet were filled in respective domains. The phases of these fluids are distinguished by defining colored step function i.e. Level Set Function "ϕ"; which represent the iso-contour of globally defined smooth step function. The value of ϕ is established such that its value is one in a domain and zero in other domain. At interface ϕ= 0.5 and it transiently varies across interface between zero & one [13].
Mathematically level set function is represented as

$$\phi = H_{sm}(\phi_{sd}) = \begin{cases} 0, & \phi_{sd} < -\varepsilon \\ \frac{1}{2} + \frac{\phi_{sd}}{2\varepsilon} + \frac{1}{2\pi}\sin\left(\frac{\pi\phi_{sd}}{\varepsilon}\right), & -\varepsilon \le \phi_{sd} \le \varepsilon \\ 1, & \phi_{sd} > \varepsilon \end{cases}$$

[1]

Where the parameters "ε" is used to find out the thickness of region and value of ϕ varies from zero to one. In our simulation, this parameter is taken same as the element size of mesh. Numerically, the movement of interface is described by the following equation

$$\frac{\partial \phi}{\partial t} + u.\nabla\phi = \gamma\left[\nabla.(\varepsilon\nabla\phi - \phi(1-\phi)\frac{\nabla\phi}{|\nabla\phi|}\right] \quad (2)$$

Where "re-initialization parameter γ (m/s)" accounts for the stabilization in terms of interface movements and same is tuned specifically for each simulation i.e. 10^{-2} to 10^{-3} m/sec which does not disturb the movement or thickness of interface. One momentum equation in each subdomain is solved and "(2)" is coupled with Navier-Stokes equations [14];

$$\nabla.u = 0 \quad (3)$$

$$\rho\left[\frac{\partial u}{\partial t} + u.\nabla u\right] = -\nabla p + \nabla.(\mu(\nabla u + (\nabla u)^T)) + \rho g + \sigma\kappa\delta n + F \quad (4)$$

Where g is the vector gravitational acceleration and three types of forces "gravitational force ρg (N)", "surface tension force σκδ**n** (N)**,** and **"**drag force F (N)", acting on the oil droplet respectively.

In the two phase flow, Surface tension force "F_{st}" is critical parameters and we used alternative formulations for the accuracy of solution [14].

$$Fst = \sigma\kappa\delta n \quad (5)$$

Where σ; surface tension coefficient (N/m) and δ (1/m); Diarc delta function.

Geometric parameters are the "curvature κ (m^{-1}) and unit normal vector (**n**) to the interface which are modeled as;

$$\kappa = -\nabla.\, n|\ \phi = 0.5 \quad (6)$$

$$n = \left|\frac{\nabla\phi}{\nabla\phi}\right|\ \phi = 0.5 \quad (7)$$

For numerical stability "(5)", is replaced with following "(8)",

$$Fst = \nabla.(\sigma(I - (nn^T))\delta) \quad (8)$$

Constant densities of water "$\boldsymbol{\rho_1}$ (Kg/m^3) & oil droplet $\boldsymbol{\rho_2}$ Kg/m^3) and dynamic viscosities of the water $\boldsymbol{\eta_1}$ (Pa-s) & oil phase $\boldsymbol{\eta_2}$ (Pa-s) in terms of level set function are;

$$\rho = \rho 1 + (\rho 2 - \rho 1)\phi \quad (9)$$
$$\eta = \eta 1 + (\eta 2 - \eta 1)\phi \quad (10)$$

The level set function "ϕ <0.5" for water domain and "ϕ>0.5" for oil phase domain. (13)

Appropriate investigation in present study at pore scale is carried out by locating an oil droplet near the surface of slotted pore membrane and laminar flow is assumed where initial size of droplet and slot remain constant throughout simulation. Properties of two phase systems such as oil density, surface tension, and dynamic viscosity, of water and oil phase are held constant for all simulations which have been carried out at different magnitude of in pore filtration velocities. Simulation started with the application of level set function, using the transit initialization analysis with 10^{-3} seconds such that "|ϕ|" varies smoothly from zero to one across the interfaces. This solution is used as initial value for further time dependent transient computational analysis with direct (PARDISO) solver in order to investigate the effect of interfacial tensions during deformation, rejection or passage of oil droplet through slotted pore membrane.

III. Results and Discussions

The effect of drag force "F (N)" as cited in Eq. (4), is an important parameter during the movement of interfaces. Drag force acting on spherical oil droplet moving between two parallel plates is given as;

$$F = 12Kw\pi\eta RspU \quad (11)$$

Where "Kw" is wall correction factor whose value was taken as 1.3 for given system at different in pore filtration velocity in order to keep the convergence of simulations results. The other parameters are dynamic viscosity "$\eta\ (Pa-s)$", in pore filtration velocity "U (μm/s)" of fluid through the slot, and radius of spherical droplet "R_{sp} (um)". We examine the combined effect of drag force and in pore filtration velocity on entry dynamic of oil droplet into a slotted pore for hydrocarbon water system with interfacial tensions (of 9 mN/m, 20 mN/m & 30 mN/m).

It has been investigated that; this relation hold good for different magnitude of in pore velocities (U) at outlet boundary condition. In contrary to this, oil droplet is rejected due to presence of static force acting in opposite direction which is directly related to the value of interfacial tensions between oil/water as long as other parameters such as width of non-converging slot, size of spherical oil droplet remain constant [6].

A. *Shape transformation and droplet entry- A visual analysis*

After thorough examinations and visual inspection of numerical results as illustrated in Fig.4, it is very clear that liquid droplet is being compressed and with the passage of time its apparent size reduces. A significant difference of size cab be analyzed at T=0 & T= 15 millisecond which has been described by color function (volume fraction) of oil phase domain.

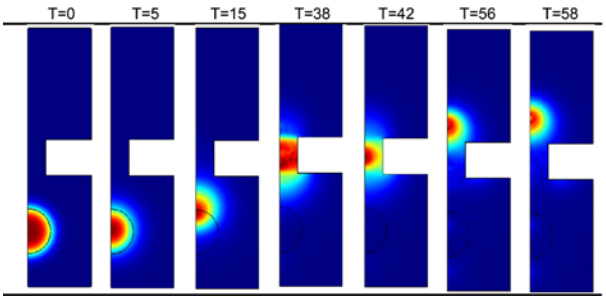

Fig.4. Sequence of snapshots (volume fraction of oil phase) of deforming oil droplet (Rsp =4 μm) near slotted pore of half width=3.34 μm, U= 75 μm/sec interfacial tension= 20 mN/m at different filtration time "T". The basic three steps are squeezing & movement towards slot, significant alteration in the shape during capturing inside of slot, regain of original shape. Filtration Time "T" is expressed in milliseconds.

In these studies the oil droplet is assumed to be compressed equally from both sides due to non-converging behavior of slot such that axial symmetry of the shape is restrained. As regard to conversion of spherical shape, droplet is converted into oblate spheroid while passing through such slot. Visual investigation of oil droplet captured inside of pore reveals that; the diameter along horizontal axis becomes greater than the diameter along vertical axis

such that it flattened just like the shape of earth as shown in Fig.5.

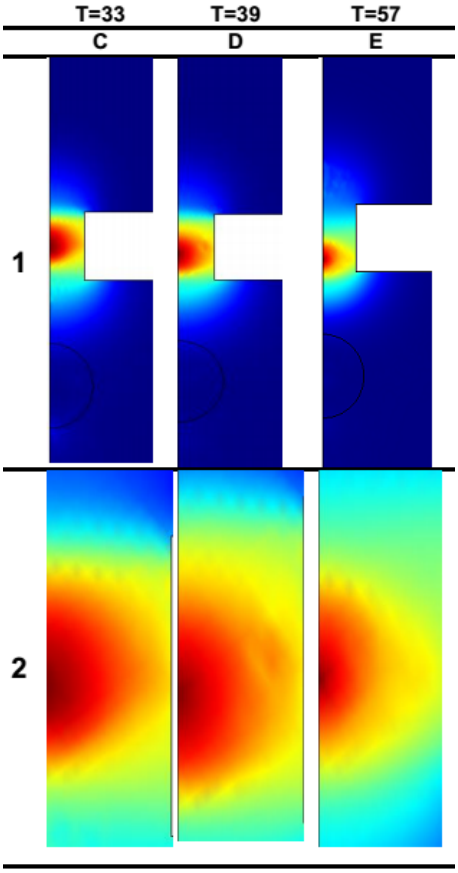

Fig. 5. Sequence of snapshots of deforming droplet (Rsp =4 µm) at in pore filtration velocity (U= 75 µm/sec), near slotted pore (half width=3.34 µm).
The spherical shape of an oil droplet is deformed into oblate spheroid (flatten) The letter denote; (C) low interfacial tension of 9 mN/m, (D)
interfacial tension of 20 mN/m, (D) Interfacial tension of 34 mN/m for water-oil two phase system. The filtartion Time (T) expressed in milliseconds for all domains. Numerical values "1" & "2" shows the complete computational domain and zoomed snap shot of crossponding domain

It seems that oil droplet with low value of interfacial tension is soft and so flexible that can deviate from natural spherical shape in such a way that polar radius becomes smaller than equatorial radius. In sequel to this, individual oil droplet may adopt flattened shape / oblate spheroid until it passed through the narrow slot of membrane. The results are compared with experimental studies carried out by [6] on non-converging slot also shows that the spherical shape of oil droplet transformed into oblate spheroid as the current simulation work well satisfied.

B. Effect of interfacial tension on droplet deformation

To investigate the influence of interfacial tension over the deformation of oil droplet, further simulations at different values of interfacial tension (9 mN/m, 20 mN/m & 34mN/m) were considered. The comparative study for these interfacial tensions at in pore filtration velocities such as 25µm/sec, 50 µm/sec, 75µm/sec were carried out in Comsol Multiphysics. The sequence of snapshots from one of computational model is shown in Fig. 5.

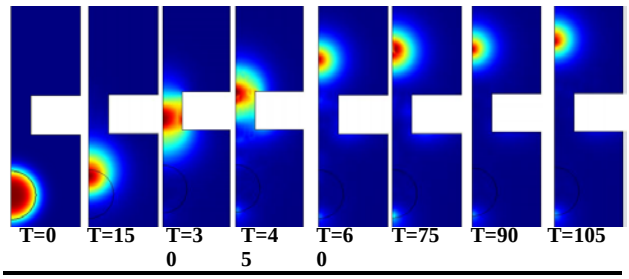

(A)
(B)
(C)

Fig. 6. Sequence of snapshots of deforming droplet (Rsp =4 µm) at in pore filtration velocity (U= 75 µm/sec), near slotted pore (half width=3.34 µm). The letter denote; (**A**) low interfacial tension of 9 mN/m, (**B**) interfacial tension of 20 mN/m, (**C**) Interfacial tension of 34 mN/m for water-oil two phase system. The filtrations Time (T) expressed in milliseconds for all domains.

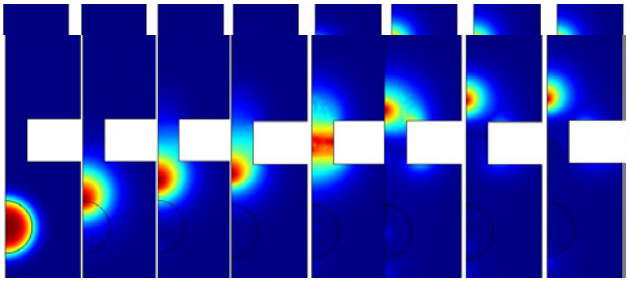

In present research work; an earlier deformation of spherical oil droplet is observed with lower interfacial tension (9 mN/m) as compared to the higher value of interfacial tension (34 mN/m) under the same operating conditions. Visual inspection of Fig. 6 clearly shows that; as the droplet approaches the slot it slows down transiently and remains at the pore entrance. Here, it is to mention that higher residence time & permeation time of droplet is observed with increasing value of interfacial tension. After comparing the computational results, it is apprised that similar observation regarding the entry dynamic of oil droplet were recorded in previous studies of fluent software package for hydrophilic membrane during oil water separation [8] [15]. At filtration time T= 45 m-sec (Fig.6); the droplet of lower interfacial tension (9mN/m) have crossed the slot however, the same droplet could not be passed (at T=45 m-sec) through the slot due to the greater value of interfacial forces

(20 & 34 mN/m). It is concluded that at any time interfacial forces always act in opposite directions and tries to resist the earlier deformation and passage of an oil droplet so that sustainable operation of dead end microfiltration is dependent on the interfacial tension between oil-water phases. In this connection we observed that more simulation time is required when a droplet is captured or passed through the slot which shows transient balance of drag force (F) and static force (F_{st}) as mentioned in modeling equation (Eq.4) i.e. Navier-Stokes Equation. On further investigation, a linear relationship of static force with oil/water interfacial tensions (9mN/m, 20mN/m & 34mN/m) & in pore filtration velocity with drag force hold good agreement with mathematical models and previous experimental studies [6] [2].

C. Increased surface area of deforming droplet and validation of numerical results

Analytical model to find out the change in surface area symbolized as "S_d" (µm^2) of deformed droplet with radius of major axis "Rd" (µm) passing through non converging slot of half width "h" (µm) was reported by [6] and given as;

$$Sd = 2\pi\left[Rd^2 + \frac{h^2}{\sqrt{1-\frac{h^2}{Rd^2}}}tanh^{-1}\sqrt{1-\frac{h^2}{Rd^2}}\right] \quad (12)$$

According to the law of conservation of volume it is stated that volume of drop before deformation (Spherical drop) and after deformation (oblate spheroids) must be equal.

Volume of sphere = volume of oblate spheroid

$$4/3\pi Rsp^3 = 4/3\pi Rd^2 h \quad (13)$$

For the slot with fixed half width "3.4 µm" and radius of spherical oil droplet "Rsp" (4 µm) the radius of major axis of oblate/deformed spheroid (ellipsoid)

R_d = 4.377 µm

The surface area of oblate spheroid from (12) after putting the above values we obtained;

S_d= 203.7 µm^2 (12-A)

In order to compare this analytical model with numerical results the radius of major axis R_d was numerically solved by plotting the mean curvature against filtration time for three sets (9 mN/m, 20mN/m & 34 mN/m) of simulations. One of such graph is shown in fig.7 (13)

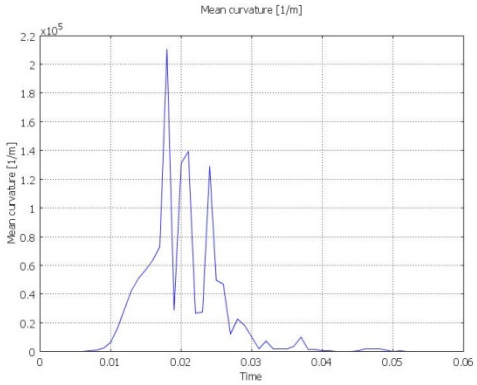

Fig.7. Means curvature (κ, m^{-1}) of oblate spheroid against filtration time (plot parameters results from post processing menu of Comsol multiphysics)

For 2D plane curve the radius of curvature is defined in (14) which is equal to radius of major axis of oblate spheroid obtained by putting maximum value of mean curvature (peak point of fig. 7) (16)

$$Rc = Rd = \frac{1}{k} \quad (14)$$

The resultant value is then employed in (12) and increased surface area of deformed droplet is plotted and shown in fig.8

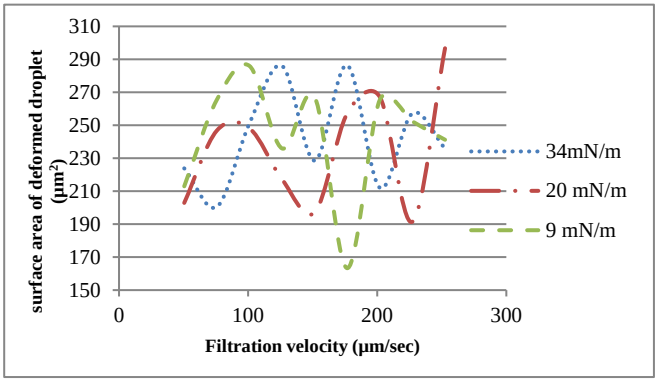

Fig.8. comparison of surface area of deformed droplet "S_d" (µm^2) plotted against filtration velocity "U" (µm/sec) at three different magnitude of interfacial tension.

It has been concluded from above fig.8; the increased in surface area of deformed droplet partially depends upon the interfacial tension in contrary to (12). After thorough investigation it has been revealed that the approximate error in numerical results is 18.9% when compared with (12-A). The difference in both the solution may exist due to the constraints associated with modeling and simulation such as size of mesh element, mesh refinement and time bound converging of numerical solution.

IV. CONCLUSIONS AND RECOMMENDATIONS

The current simulation work is carried out on dead end slotted pore microfiltration process for the separation of oil phase from produced water with the application of Comsol Multiphysics. Based on the numerical results; it has been concluded that earlier or delayed deformation of oil droplet is dependent upon the interfacial forces which exist between two liquid phases. At lower filtration velocity 25µm/sec; better rejection of oil particles is observed with 34 mN/m of interfacial tension. On the other side, increase in the magnitude of drag force acting on oil droplet has been found related with increasing in pore filtration velocity. The balancing of static forces (interfacial tensions) & drag force detected for instant of time (slower motion) when droplet captured inside of membrane. This model can be further used to find out the deformation, rejection, or passage of spherical shaped oil phase droplets in emulsions other than produced water. The flexibility of Comsol Multiphysics also allows use the wide range of interfacial tensions to investigate the other relevant real world problems.

REFERENCES

[1] Holdich, Muhammmad Abbas Ahmad Zaini Iain W. Cumming & Richard, "Rejection of Oil Emulsion using Tubular Surface Filters," *Sains Malaysiana*, Vol. II, pp. 159–166., 2003

[2] Muhammad abbas ahmad Zaini, RichaRd G. holdich & ian W. cumming. Malaysia "Cross-flow microfiltration of oil in water emulsion via tubular filters: evaluation by mathematical models on droplet deformation and filtration," *Jurnal Teknologi*,*Vol. 53*, pp. 19-28, Sep 2010.

[3] Ullah, R.G. Holdich M. Naeem V.M. Starov , "Shear enhanced microfiltration and rejection of crude oil drops through a slotted pore membrane including migration velocities," *Journal of Membrane Science*, Vols. 421-422, pp. 67-74, 2012.

[4] Ahmed Faiq, Al-Alawy and Samah Mohsin Al – Musawi "*Microfiltration Membranes for Separating Oil / Water Emulsion*," Iraqi Journal of Chemical and Petroleum Engineering, Vol. 14, pp. 53-7, April 2013.

[5] Richard Holdich, Serguei Kosvintsev, Iain Cumming, Sergey Zhdanov "Pore Design and Engineering for filters and membrane," *philosophical transactions of the royal society*, vol. 364, pp. 161-174, December 2005.

[6] Ullah S.W. Khan, A. Shakoor d, V.M. Starov, "Passage and deformation of oil drops through non-converging and converging micro-sized slotted pore membranes" *Separation and Purification Technology*, Vol. 119, pp. 7-13, 2013.

[7] Chemmalasseri, E.A. "Numerical Modelling of droplet formation in Mesh Nebulizers," Msc dissertation, mechanical engineering, Delft University of Technology, Laboratory for Aero & Hydrodynamics, September 2012.

[8] Tohid Darvishzadeh, Nikolai Priezjev, "Oil droplet behavior at a pore entrance in the presence of crossflow- Implications for microfiltration of oil-water dispersions," *journal of membrane science, vol*.447, pp. 442-451 November 2013,

[9] Ullah, R.G. Holdich, M. Naeem, S.W. Khand, V.M. Starov "Prediction of size distribution of crude oil drops in the permeate using a slotted pore membrane," *chemical engineering research and design*, vol.92, issue 3, pp.2775-278, February 2014

[10] Kreiss, Elin Olsson Gunilla. "A conservative level set method for two phase flow." *Journal of Computational Physics*, vol. 210 , pp. 225–246, 2005.

[11] Monno, B.Chinè and M. Paris "A Model of Gas Bubble Growth by Comsol Multiphysics," presented at comsol conference Paris 2010,

[12] Schlegel, Fabrice. COMSOL Blog. [Online] 2015. [Cited: jan 17, 2016.] http://www.comsol.com/blogs/which-multiphase-flow-interface-should-i-use/.

[13] AB, COMSOL. "Comsol Multiphysics Chemical Engineering Module User's Guide. Burlington," *COMSOL AB*, 2007, pp. 165-169, October 2007.

[14] Tohid Darvishzadeh, Nikolai V. Priezjev, "Effects of cross-flow velocity and transmembrane pressure on microfiltration of oil-in-water emulsions," *journal of membrane science*, vol. 423-424 pp. 468-476, September 2012.

[15] Siavash Darvishmanesh, Johan Vanneste, Jan Degrève, Bart Van der Bruggen, "Computational fluid dynamic simulation of the membrane filtration module" presented at 20th European Symposium on Computer Aided Process Engineering – ESCAPE20, Vol. 28, pp. 13-21, 2010,.

[16] Goldman, Ron. Houston, "Curvature formulas for implicit curves and surfaces," Elsevier, TX 77005-1892, USA Vol. 22, pp. 632-658, July 2005.

Prediction of Size Distribution of Crude Oil Drops Through a Non- Converging Slotted Pore Membrane

Saad Ullah Khan[1], Asmat Ullah[1*]

***Abstract*— the study focuses to develop a model that predicts the size distribution of crude oil drops through a non-converging membrane slot. The force through which drops pass through the membrane is referred as the drag force while the force opposes the drag force and prevent the drops from the permeation through the membrane is named as the static force. When the drag force is balanced by the static force the point is called 100% cut-off through the membrane. Linear fit approach was used to predict the size distribution below 100% cut-off point. Two different types of crude oil drops sample analyzed experimentally. These experimental results were compared with the predicted model. The predicted model was an reasonable agreement with the experimental data point. The developed model can be used to predict overall oil concentration in order to investigate, the limitation of oil concentration according to international standards.**

***Index Terms*—Permeate size distribution prediction, 100% rejected drops, linear line approach**

I. INTRODUCTION

Produced water is the waste in the form of liquid generated in large amount during oil and gas exploration [1]. Volume of 3.3 million m3 produced water has estimated in 2007 in the onshore production at the United States [2]. The amount of produced water generated annually from oil and gas industry are in an array of 15-20 billion barrels, which is comparable to a volume of 1.7 to 2.3 billion gallons generated daily [3].

Produced water is hazardous to the environment. It cannot be disposed directly and special measure should be imposed before disposal. According to the international standards, the oil concentration in produced water should be limited to 10-30 ppm [4].

Produced water treatment technologies improve the quality of the waste stream by removing impurities. Conventional technologies have been studied for oil/water removal but it did not meet the requirement. Like hydrocyclone, it cannot remove oil drops of size less than 10 µm [5]. Membrane separation makes more beneficial as compare to the other conventional separation process are [6]: It gives reliable finished water quality regardless of raw water quality (without chemical optimization), it is a physical process and it is energy efficient.

Various shapes of membrane pore structure have been studied to overcome the membrane fouling further [7] - [8]. The slotted pore membrane was proofed more efficient than a circular pore membrane. The area provided to the dispersed drops and suspended particles is more open by the slotted pore structure as compared to circular pore type structure membrane [9].

Drag force has produced by surrounding fluid flow and helps the drops in permeation through membrane slot. Static force opposes the drag force and prevents the oil drops from permeation. When the influence of drag force on the drops is greater than static force, then drops will pass through membrane. When the static force on drops becomes equal to or greater than drag force, then the drops will be rejecting through membrane slot [10].

The purpose of this study is to predict a model that is used to predict the permeate strength (concentration) of crude oil drops through the membrane in order to investigate the limit of oil drops in water.

1Department of Chemical Engineering, University of Engineering & Technology Peshawar, KPK Pakistan

Corresponding E-mail address: a.ullah@uetpeshawar.edu.pk

II. MATERIAL AND METHODS

Static force has calculated from the equation (1) presented as [10]:

$$F_{cx} = 2\pi\sigma\left[\frac{3R_{sp}^2}{h} + \frac{h^2}{1-\frac{h^3}{R_{sp}^3}}\frac{1}{R_{sp}}\right]\frac{3}{2} - \tanh^{-1}\sqrt{1-\frac{h^3}{R_{sp}^3}}\frac{3h^3}{R_{sp}^3 2\sqrt{1-\frac{h^3}{R_{sp}^3}}}\Bigg] - 4R_{sp}\Bigg]$$

Drag force has calculated from the equation (2) presented as [11]:

$$F_d = k_w 12\pi\mu R_{sp} U \quad (2)$$

Where, k_w, is a wall correction factor, μ is the viscosity of the feed and U is the feed velocity.

100% rejection points have calculated from the equilibrium of equation (1) and (2) [8]. Rejected drops below than 100% rejection points have calculated from the extension of 100% rejection points to the origin of rejection graphs [8]. It is further extended and fraction of permeated drops has multiplied to the feed dimension division of oil drops and permeated drops has predicted.

The two different types of (22 and 27 0API) crude oil drops have studied in the present work. The materials used and experimental method has provided in [12].

III. RESULTS AND DISCUSSION

100% rejection points have calculated from the equilibrium of static and drag force. Drag force increases with increasing flux rate and it is balanced by static force at higher drops size and higher 100% cut-off points obtained by increasing flux rate. Similarly, static force increases with interfacial tension of oil drops and higher cut-off points has achieved at higher interfacial tension. Rejected drops below than 100% cut-off points have calculated from the extension of 100% cut-off points to the origin of rejection graphs. The ratio of rejected drops increases with increasing the 100% cut-off points. Fig.2 and 3 represent the predicted permeated drops through the membrane slot. It shows that dimension distribution of crude oil drops increases with increasing flux rate. It also shows that the dimension distribution of crude oil drops increases with increasing API values of oil drops. Fig.1 represents the size distribution of crude oil drops in feed, reported from [12].

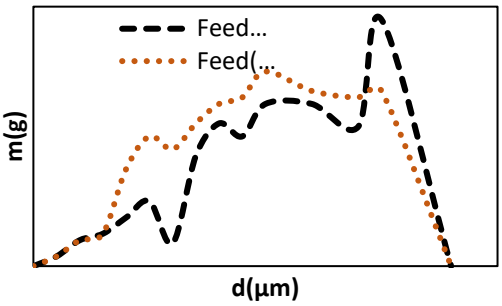

Fig.1- Dimension distribution of 22 and 27 API crude oil drops in feed having concentration of 400 ppm

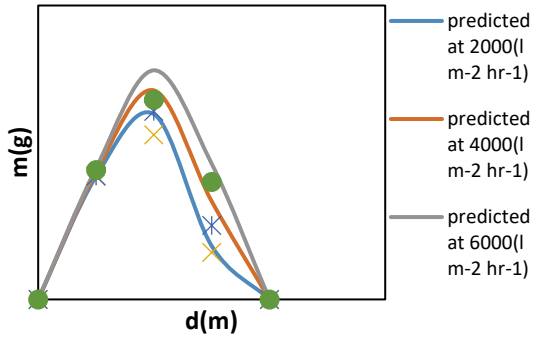

Fig. 2 Predicted dimension distribution and experimental dimension distribution of permeate of 22 API crude oil drops, decreasing 400 PPM feed concentration to permeate concentration of 10, 12 and 14 at flux rate of 2000, 4000 and 6000 l m-2 hr-1 respectively

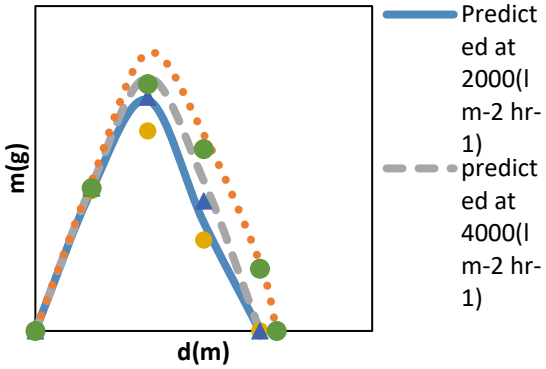

Fig. 3 Predicted dimension distribution and experimental dimension distribution of crude oil drops, decreasing 400 ppm oil feed concentration to 15, 17 and 22 ppm at flux rate of 2000, 4000 and 6000 l m-2 h-1

IV. CONCLUSION

A model has developed that predict the permeated drops through non-converging membrane slots. 100% rejection points has calculated from the equilibrium of static and drag force and these 100% rejection points has extended to the origin of rejection graph and permeated drops has calculated. It is concluded from the study that the predicted model has function of feed dimension distribution drops, flux rate, API value of oil drops and size of membrane slot.

REFERENCES

[1] R.D. Vidic, "Sustainable Water Management for Marcellus Shale Development", Marcellus Shale Natural Gas Stewardship: Understanding the Environmental Impact, Marcellus Shale Summit, Temple University, Philadelphia, PA, 2010.

[2] C.E. Clark, and J.A. Veil, "Produced water volumes and management practices in the United States" (No. ANL/EVS/R-09-1), Argonne National Laboratory (ANL), 2009

[3] J. Veil, and C. Clark, "Produced water volume estimates and management practices', SPE Production & Operations, 26(03), pp.234-239, 2011.

[4] A. Bevis, "The treatment of oily water by coalescing", Filtr, 295-301. Sep, 29, 1992.

[5] J. Mueller, Y. Cen, R.H. Davis, " Cross-flow microfiltration of oil water", J. Membr. Sci.129, 221-235, 1997

[6] C.T. Cleveland, "Big advantages in membrane filtration", American Water Works Association Journal, 91(6), p.10, 1999.

[7] S.Kuiper, C.J.M.V. Rijin, W. Nijdam, G.J.M. Krijnen, M.C. Elwenspoek, "Development and applications of very high flux microfiltration membranes", J. Membr. Sci. 150, 1-8, 1998.

8] A.J. Bromley, R.G. Holdich, and I.W. Cumming, "Particulate fouling of surface microfilters with slotted and circular pore geometry", Journal of membrane science, 196(1), pp.27-37, 2002.

[9] M. Chandler, and A. Zydney, "Effects of membrane pore geometry on fouling behavior during yeast cell microfiltration", Journal of membrane science, 285(1), pp.334-342, 2006.

[10] A. Ullah, S.W. Khan, A. Shakoor, and V.M. Starov, "Passage and deformation of oil drops through non-converging and converging micro-sized slotted pore membranes", Separation and Purification Technology, 119, pp.7-13. 2013.

[11] S.R. Kosvintsev, P.D. Sutrisna, I.W. Cumming, R.G. Holdich, G. Mason, "The passage of deforming oil drops through a slotted microfilter", Trans. I.Chem. E 85, 530-536, 2007.

[12] A. Ullah, R.G. Holdich, M. Naeem, S.W. Khan, , and V.M. Starov, "Prediction of size distribution of crude oil drops in the permeate using a slotted pore membrane", Chemical Engineering Research and Design, 92, pp. 2775-2781, 2014.

Sensitivity Analysis of key Parameters of an Amine Sweetening Unit

Muhammad Sher Khan[1,*], Muhammad Imran Ahmad[2], Jamil Ahmed[3], Amir Muhammad[4]

***Abstract*— The present study focus on sensitivity analysis of key parameters of amine sweetening unit which utilizes MDEA (20% by weight concentration), at Haseeb Gas Field, Sindh. High amine concentration results in lower circulation rate which in turn reduces reboiler duty. The amine sweetening process is simulated in Aspen HYSYS 2006.5. Along with the base case, MDEA blends with different DEA compositions used as a solvent were simulated in HYSYS. Sensitivity analysis of key parameters like amine circulation rate, reboiler duty, rich amine loading and amine vaporization losses was performed for each solution. Among all the solutions 45% MDEA concentration gives the better results in terms of lower reboiler duty and circulation rate, comparatively less rich amine loading and vaporization losses.**

***Index Terms*— Amine sweetening, simulation, sensitivity analysis.**

I. INTRODUCTION

Energy generation by the use of natural gas has become the prime need for the industrial and domestic purpose. To deliver the natural gas for the consumption there are different processes from wellhead to the consumer. These processes are very necessary for the removal of contaminants that carries with natural gas and these contaminants can cause problems like corrosion, erosion, freezing, health problems plugging and safety hazard [1]. Natural gas has very miniature importance until it brought to the customers, which may be of thousands of kilometer from wellhead. The traditional way to move the gas from source to customer is through pipelines, However when the distance increases transportation through pipeline become uneconomical [2]. Acid gases i.e. CO_2 and H_2S are among the major contaminants of natural gas. There are different processes for gas purification in which popular methods are absorption into liquid, adsorption on a solid bed, permeation through membrane, chemical conversion to another compound and condensation. The impurities of natural gas like acid gases e.g. carbon dioxide CO_2 and hydrogen sulfide H_2S are necessary to remove. H_2S content of natural gas if exceeds from 5.7 mg m−3 then the natural gas is considered to be sour. Gas sweetening process is a method to remove H_2S and CO_2 from natural gas [3]. Presence of water and acid gases in the natural gas are very corrosive in nature. Because of the privation of heating value of CO_2 and the toxic nature of H_2S, sales gas agreement demands to sweeten the natural gas to 4 parts per million H_2S, 1-3 mole% of CO_2 and have a heating value of no less than 920 to 980 Btu/SCF, depends upon the agreement [4]. Utilizing the different alkanoamines, in the chemical solvent process, is the most broadly employed natural gas treating process [1].

Haseeb gas field amine sweetening unit is used to remove acid gases i.e. H_2S and CO_2 from sour gas. This plant is located in Sindh (Shikarpur). The plant is designed by SPEC Pvt. Ltd. and is operated by Energy Processing Services Pvt. Ltd. The plant is designed for processing 30 MMSCFD sour natural gas but currently only 10.5 MMSCFD gas is processing due to the only one well being drilled. This plant was commissioned in 2011 for sweetening and dehydration of sour gas. Haseeb Well gas which is processed at SPEC Gas Processing Facility contains about 3 to 4 mole % Carbon dioxide and 400 ppm H2S. Sales gas agreement dictates that CO_2 content not to exceed 2 %, H_2S 0.2 grain per 100 SCF and total sulphur not more than 3.0 grain per 100 SCF. This excess CO_2 and H_2S in the gas stream is reduced by treating with Methyl diethanol amine in which CO_2 and H_2S is selectively absorbed.

Manuscript received May 13, 2017. This work was supported by Department of Chemical Engineering, University of Engineering and Technology, Peshawar, Khyber Pakhtunkhwa, Pakistan.

All the authors are affiliated with Department of Chemical Engineering, University of Engineering and Technology, Peshawar, Khyber Pakhtunkhwa, Pakistan
M. S. K. (e-mail: sherkhan_59@yahoo.com)
M. I. A. (e-mail: Imran.ahmad@nwfpuet.edu.pk)
J. A (e-mail: engrjamilahmad@gmail.com)
A. M (e-mail: engr_amir14@yahoo.com)

A. Haseeb gas field amine sweetening unit

In order to eliminate entrained water and liquid hydrocarbons, the gas is fed into a scrubber. Then it enters though the bottom of absorber (trayed or packed column). After acid gases removal gas exits from the top of absorber. In amine absorber, the lean amine which is regenerated in stripper, fed at the top of the contactor tower from where it come down and gas moves upward and where these two have counter current contact. In this column acid gases i.e. H_2S and CO_2 with the chemical reaction absorbed into the amine solution. The amine solution when reaches at the bottom of column, loaded with acid gases called rich amine. Rich amine then after filtration and flashing operations enters at the top of regenerator/Stripper to recover amine. The acid gases exits from the accumulator, which is connected with stripper. Steam strips the acid gases from rich amine and reflux water coming from the accumulator helps stripping. After regenerating, amine is fed back again to the absorber column.

B. General considerations for selecting amines

Among the several available solvents for the elimination of CO_2 from sour natural gas stream the alkanoamines are generally the most accepted and widely utilized [3]. The readiness at low cost and their reactivity especially MDEA (Methyldiethanolamine) and DEA (Diethanolamine), have made these solvents attained a principle place in the gas processing facilities [5]. The criteria usually applied for the selection of amine for the gas sweetening have changed over the years. The first amine considered for any sweetening application was MEA (Monoethanlamine), until the 1970's. Then in 1970's, switching from MEA to DEA (Diethanolamine) generated favorable results [6]. MDEA (Monoethynolamine), DGA (Diglycolamine) and the mixed amines have steadily gained the popularity in the past ten years [7]. The mixture of amines utilized in the 80s, by adding different amount of reactive amines to Metyldiethanolamine (MDEA). An enhancement in absorption rate, absorption capacity and also saving in requirements of solvent regeneration can possible by using blended amines [8].

C. Process key parameters sensitivity analysis

The initaial investment of between 50-70 % for an amine sweetening unit is straightaway linked with the amount of circulation rate of solvent and the initial investment of about 10-20 % rest on the requirement of regeneration energy. The reason for this effect is because the size of the equipments like stripper, absorber and pipeing depends upon the circulation rate up to some extent [9].

About 70 percent of amine sweetening unit operating cost, eliminating labor costs, is due to the regeneration energy requirement for the solvent. The proper choice of the amine can significantly diminish the energy requirement for solvent regeneration and solution circulation rate [8].

Subsequently the proper amine and suitable concentration can greatly reduce both the regeneration energy requirement and solution circulation rate, choice of the amine or combination of amines best suited to the conditions can have a dramatic impact on the overall costs associated with a sweetening unit [7]

Amine strength/concentration used in Haseeb gas field amine sweetening unit is 20% by weight. In order to determine whether MDEA increased concentration as compare to present MDEA concentration i.e. 20% by weight gives the better results or MDEA blends with DEA gives a bit improvement in operating cost due to reduction in circulation rate and hence the reboiler duty. So for this purpose sensitivity analysis of key parameters for amine concentrations (MDEA and MDEA blends with DEA) is carried out. For base case i.e. 20% MDEA concentration and other three proposed solvents concentration, four operating parameters are analyzed for each solvent i.e. amine circulation rate, reboiler duty, vaporization losses and rich amine.

These solvents are analyzed on the base of lower circulation rate, lower reboiler duty, lesser vaporization losses and comparatively lower rich amine lading. So the better choice of suitable amine solvent is mainly selected on the basis of lower reboiler duty or lower circulation rate, because lower circulation rate results lower reboiler duty and high circulation rate gives high reboiler duty and hence more operating cost [10].

II. METHODOLOGY AND SIMULATION CASES

Aspen HYSYS 2006.5 simulation software is used for the sensitivity analysis of Haseeb gas field (H.G.F) amine sweetening unit. Steady state simulation is used to simulate all the cases. HYSYS have distinct fluid package i.e. "Amine Package", design for modeling of amines sweetening unit. Reaction kinetics and experimental solubility data over wide range of conditions are built-in in this special package. [11]. Kent-Eisenberg thermodynamic model and non-ideal vapor phase model are selected for all simulations. The following simulations cases are performed:

Experiment -1: Using 20% MDEA concentration
Experiment -2: Using 45% MDEA concentration
Experiment -3: Using 30% MDEA and 10% DEA
Experiment -4: Using 40% MDEA and 5% DEA

Amine sweetening unit sensitivity analysis of key parameters i.e. lean amine circulation rate, lean amine

temperature, reboiler duty, rich amine loading and solvent losses are performed for each of the above solution.

After successfully simulation of Haseeb Gas Feld amine sweetening unit the snapshot of simulated plant is shown in the fig1.

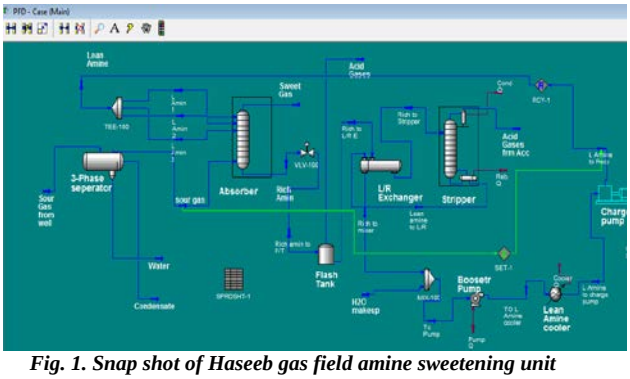

Fig. 1. Snap shot of Haseeb gas field amine sweetening unit

MDEA and its blends effects are observed by first simulating the plant having MDEA as solvent then entering the HYSYS basis environment and adding other amine in the component list and then changing amine composition in the Lean amine stream in the HYSYS simulation.

III. RESULTS AND DISCUSSION

After successful simulation of all cases the first parameter that was studied for all cases is amine circulation rate.

A. Amine circulation rate

Higher MDEA concentration as compare to existing plant amine concentration i.e.20% and MDEA blends with DEA circulation rate effect studied on gas sweetening. Lean amine temperature, reboiler duty, amine concentration and condenser temperature etc. are fixed. Sweet gas pipeline specifications are not fixed with the amine circulation rate in order to find out the maximum and minimum amine flow rate at which the sweet gas does not go off-spec. The results shows that by increasing circulation rate CO_2 concentration decreases and then becomes constant after a specific low rate while H_2S concentration first decreases and then goes beyond the pipeline specification. This is due to the fact that as the reboiler duty is fixed, when we increase the flow rate there is more steam require to strip the acid gases from rich amine in stripper, so the reboiler cannot perform its normal task and as a result H_2S concentration increases in the sweet gas because H_2S concentration is far less than CO_2 concentration in sour gas, as a result CO_2 concentration not effected as much. Among the four experiments 45%MDEA concentration gives the better result as compare to its blends because it slip a more CO_2 in sweet gas and also gives pipeline specification i.e. 4PPM H_2S and 2 mole% CO_2 at lower flow rate. The minimum and the maximum flow at which sweet gas goes not go off-spec can be seen (Fig. 2 and 3)

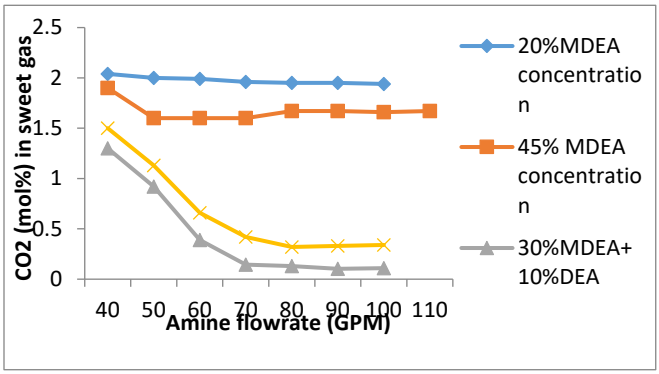

Fig. 2. Amine flow rates vs CO_2 concentration in the sweet gas

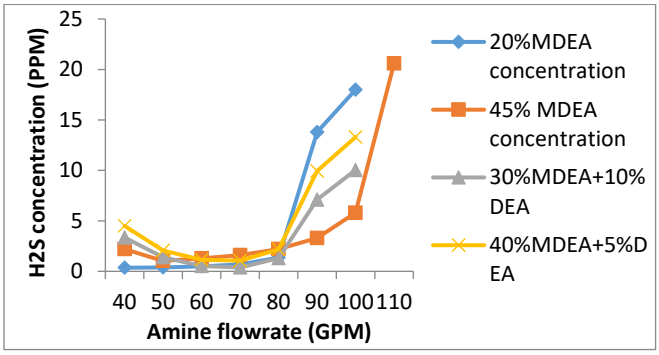

Fig. 3. Amine flow rates vs H_2S concentration in sweet gas

B. Reboiler duty

Increasing amine concentration reduces circulation rate which results reduction in reboiler duty. For this purpose, reboiler duty vs acid gas concentration in sweet gas is plotted to see that which solution have lower rebolier duty and also give on-spec gas. These results are obtained by setting 110 GPM foe 20% amine concentration and 50GPM for other cases. So, the results shows that as we reduce reboiler duty CO_2 concentration in sweet gas is very minutely effected, while for H_2S the gas goes beyond specs after a specific reboiler duty.20%MDEA have the

highest reboiler duty to achieve gas pipeline specifications while 45%MDEA have the lowest reboiler duty to achieve on-spec gas, as shown in the fig 4 and 5.

After observing overall performance for each solution, it is concluded that the 45% MDEA concentration will be best suit for the process.

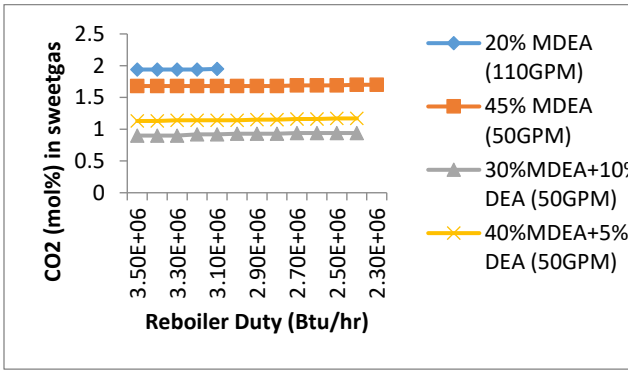

Fig. 4. Reboiler duties vs CO_2 in sweet gas

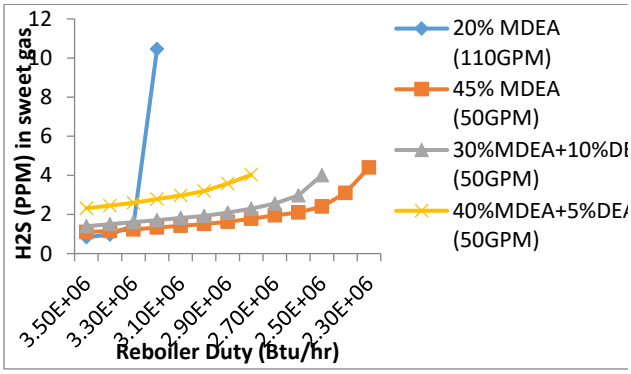

Fig. 5. Reboiler duties vs H_2S in sweet gas

C. Lean amine temperature effect on vaporization losses

As a rule of thumb, lean amine temperature should be 5-10 ^{0}C above the inlet sour gas in absorber in order to avoid hydrocarbon condensation which results foaming. Main effect of lean amine temperature is on the solvent losses. Amine vaporization losses occur from absorber, flash tank and accumulator. Amine losses increase with increase in temperature for all cases. We can see that by increasing MDEA concentration from 20 to 45 weight%, so losses increases (Fig. 6). Most of the amine losses occur from the amine absorber while losses from flash tank and accumulator are minor. The simulation result shows that 40% MDEA+5% DEA have most and 20% MDEA have least amine losses.

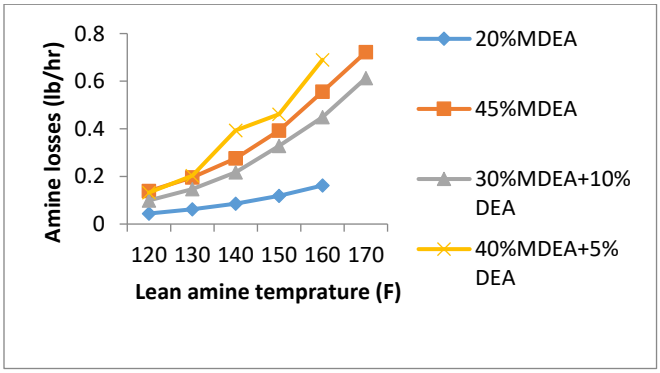

Fig. 4. Lean amine temperature effects on solvent losses

D. Rich Amine loading

Another operating parameter that was studied is rich amine loading which is defined as "the number of moles of acid gas removed from the natural gas to the number of the moles of the material, which is used for the purpose of absorption". When the acid gas loading is high then the corrosion rate will be high and vice versa. We can observe that by increasing circulation rate rich loading decreases little bit (Fig. 7). Among 4 simulations, 45% MDEA have lowest while 30% MDEA+10% DEA have high rich loading. So in case of rich amine loading 45% MDEA gives the best results.

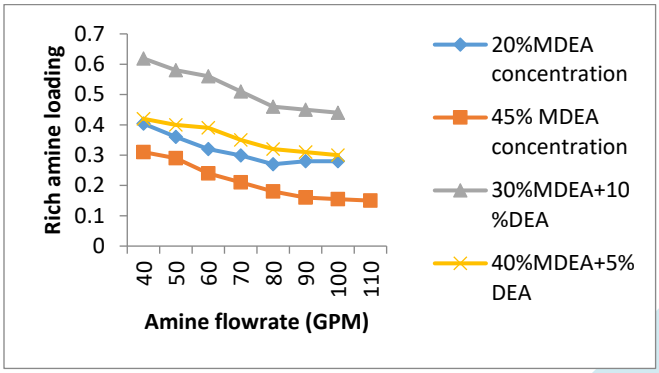

Fig. 7. Solvent circulation rates vs rich amine loading

IV. CONCLUSIONS

Existing plant having 20% MDEA solution is simulated by using Aspen HYSYS and sensitivity analysis of key parameters for MDEA and MDEA blends with DEA performed. Higher MDEA concentration up to 45% and MDEA blends with DEA was different candidate solution for verifying which one has better performance. Haseeb gas field sour gas have lower H_2S concentration as compare to CO_2, so therefor it shows different trend for 20% MDEA concentration as compare to higher MDEA concentration and mixture of amines. For the selection of suitable amine, besides the operational and capital cost there are other aspect like corrosion rate, efficiency and availability of amine which should be consider. So it is concluded that due to lower reboiler duty requirement, lower rich amine loading and slipping a comparatively greater portion of CO_2 in sweet gas, 45% MDEA is best suited for the process among the other contestant amine solutions.

REFERENCES

1. Mitra, S., "A Technical Report on Gas Sweetening by Amines," *Petrofac Engineering India Ltd*, Vol.(1), 2015.
2. Chang, H., B. Lee, and B. Gu, "A Raise Plan of competitiveness of Internal Company in the overseas Plant market," *Construction & Economy Research Institute of Korea*, Vol. 2-30, 2007.
3. Kohl, A.L. and R. Nielsen, "Gas purification". 1997: *Gulf Professional Publishing*.
4. Sharif Dashti, S., A. Shariati, and M.R. Khosravi Nikou, "Sensitivity analysis for selection of an optimum amine gas sweetening process with minimum cost requirement," *Asia-Pacific Journal of Chemical Engineering*, Vol. (5), pp. 709-715, 2015.
5. Polasek, J. and J. Bullin, "Selecting amines for sweetening units," *ENERGY PROGRESS.*, Vol. (3), pp. 146-149, 1984.
6. Beck, J. *Diethanolamine an energy conserver*. in *Gas Conditioning Conference, Norman Oklahoma*. 1975.
7. Bullin, J.A., J.C. Polasek, and J.W. Holmes. Optimization of new and existing amine gas sweetening plants using computer simulation. in Proceedings of the sixtieth GPA annual convention. 1981. *Gas Processors Association Tulsa*.
8. Abedinzadegan, H.K.A.Z.M. and H. Ghadirian, "revamping of gas refineries using amine blends," *IUST International Journal of Engineering Science*, Vol. (3), pp. 27-32, 2008.
9. Chan, C.W. and P. Tontiwachwuthikul, "A decision support system for solvent selection of CO 2 separation processes," *Energy conversion and management*, Vol. (6), pp. 941-946, 1996.
10. Mokhatab, S. and W.A. Poe, *Handbook of natural gas transmission and processing*. 2012: Gulf Professional Publishing.
11. HYSYS, A., *Aspen HYSYS Help Section*. Aspen Technology, Inc, ed. A.P. Azapagic. 2004, Burlington, MA, USA. .

Design, Mathematical Model, and Parametric Analysis of a Solar Desalination System with Humidification and Dehumidification

Rasikh Tariq

***Abstract*— In this research paper, a solar assisted desalination unit is numerically simulated. Saline water is heated using flat-plate solar collector. Heated saline/brackish water is used to humidify the atmospheric air in a humidification chamber. Condensate/fresh water is collected from the humid air in dehumidification chamber. In this research paper, a mathematical model of the components of the system (solar collector, brackish water storage, humidifier, and dehumidifier) is developed. The governing equations are numerically simulated on Matlab. The simulation results are validated by a comparison with previously published experimental results. A parametric study is conducted by varying environmental temperature, humidity, and mass flow rate of saline water. It is concluded that the fresh water productivity is increased by increasing environmental temperature, decreasing humidity and increasing saline water flow rate.**

***Index Terms*— Dehumidification, Desalination, Humidification, Mathematical Model, Parametric Study**

I. Introduction

The high consumption of water in a hot climatic region have tended to use a solar desalination system. A solar-assisted desalination unit with humidification and dehumidification is the most economically viable option among other desalination systems. Qiblawey [1] provided a comparative study on different solar-assisted desalination technologies including flash desalination, vapor compression, reverse osmosis (RO), electrodialysis and humidification and dehumidification. They reported that a humidification and dehumidification desalination unit is potentially very cost competitive as it can operate on a very low-grade heat like solar energy. Chandrashekara [2] recommended that a solar assisted humidification and dehumidification unit is most viable near beaches and sea because it basically works on the moisture content in the atmospheric air.

The process of solar assisted humidification and dehumidification mimic the natural water cycle. Several researchers conducted experimental work [3]–[7], numerical simulations [8]–[10] and both [11]–[15] on solar-assisted humidification and dehumidification desalination process.

Dai et al. [4] conducted an experimental study on solar-assisted humidification and dehumidification unit. They observed system performance parameters by changing mass flow rate of feedwater, air and their temperature. Al-Enezi et al. [16] conducted an experimental study and focused more on different operating parameters of humidification and dehumidification unit.

Nawayseh et al. [9] only conducted a numerical simulation of this system. They solved the governing non-linear equations using numerical methods. Their numerical model is in good agreement with the experimental setup of desalination unit constructed in Malaysia and Jordon.

Farhad et al. [17] theoretical model which predicts the experimental performance of a humidification and dehumidification unit. They analyzed the system based on energy and exergy analysis and found out that a solar-assisted humidification and dehumidification unit have high exergetic efficiency. M. H. Hamed et al. [15] studied a desalination unit with humidification and humidification using theoretical knowledge and experimental setup. Their theoretical fresh water production matches with experimental freshwater production. They average productivity of their system is 22 liters/day. According to the literature review conducted and by the author's best knowledge, there is still a need to analyze a solar-assisted desalination unit working on humidification and dehumanization process by varying different parameters including feed water flow rate, air flow rate, brackish water flow rate, temperature and humidity of the air.

In this research paper, a mathematical model of a solar-assisted desalination unit is developed by applying governing equations on each component. The governing equations are numerically simulated and are programmed on Matlab. A parametric study is conducted by varying the parameters including feed water flow rate, air flow rate, air temperature, air humidity and brackish water flow rate.

II. System Description

The presented solar-assisted desalination unit with humidification and dehumidification unit consist of a flat-plate solar collector, brackish water storage, humidification and a dehumidification unit. The system is shown in fig. 1. Saline water is stored in brackish water storage. A flat-plate solar collector is used to the elevate the temperature of saline water. The saline water is supplied to a humidification section using pump 2. In the humidification section, the saline water and the air are in direct contact with each other, and as a result, the moisture content of the air increases and salt go back to the brackish water storage. The humid air enters the dehumidification section or condenser. Feed water is provided in the dehumidification section through an indirect

Manuscript received May 29, 2017.
Rasikh Tariq is with the Heat Transfer and Air Conditioning Lab, Department of Mechanical Engineering, HITEC University, Taxila, 44000 Pakistan (e-mail: rasikhtariq@gmail.com, rasikh.tariq@hitecuni.edu.pk).

contact with air using a shell and tube heat exchanger. Fresh water is collected as a condensate in a storage tank, and air leaves the system.

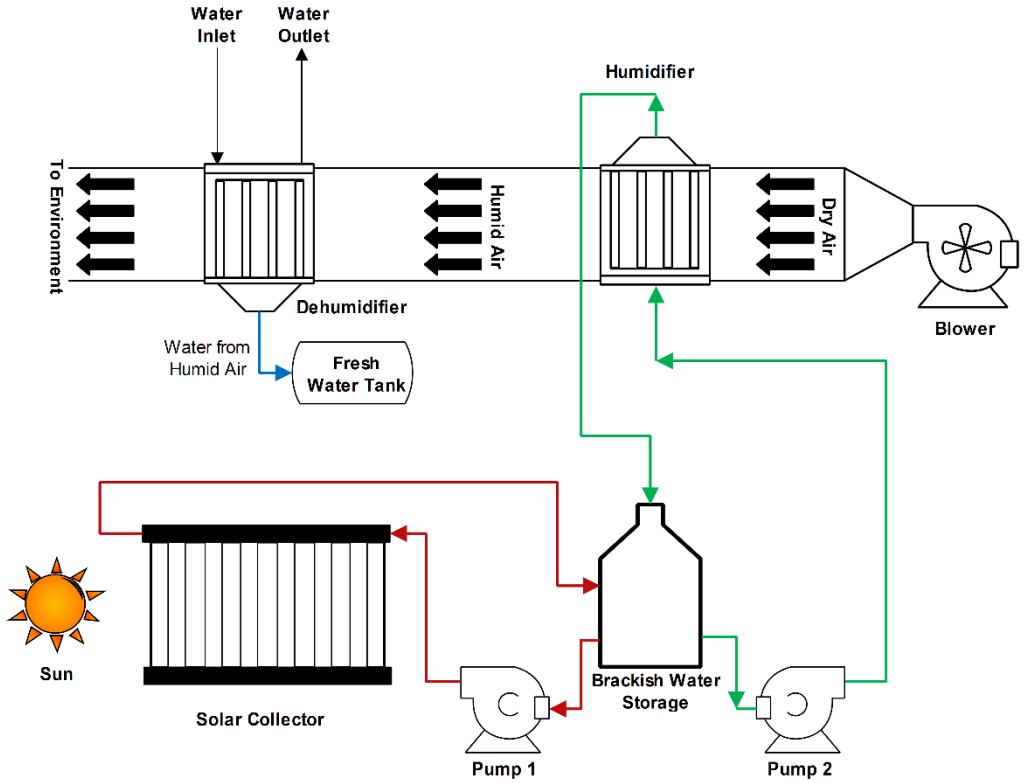

Fig. 1. Solar Assisted Humidification and Dehumidification Desalination Unit

III. MATHEMATICAL MODEL

A flat-plate solar collector is designed for the system as it is the most appropriate choice for applications involving up to 100ºC temperature [18]. Following assumptions are made:

1. The solar collector and humidification section is undergoing through the steady-state process.
2. Header only cover a small area of the collector which is negligible and provide uniform flow rates to all the tubes of the solar collector.
3. Heat flow through back insulation is negligible.
4. Heat flow through the glass cover is one dimensional.
5. There is no shading of the absorber plate.
6. There is no heat loss from the humidifier.
7. Kinetic and potential energy terms are neglected.
8. The falling film is laminar and there is no wavy motion at the water-air interface.

The total useful energy provided by the solar collector is calculated using [18]:

$$Q_u = A_c \left[S - U_L \left(T_{pm} - T_a\right)\right] \quad (1)$$

The absorbed solar radiation (S) is calculated using a beam, diffused and reflected components of solar radiation. Since solar radiation is a transient process, therefore, the solar angles are calculated for the day of March 21st from 11:30 AM to 12:30 PM as in I.

The diffused radiation is calculated by means of the hourly clearance index ($k_T = \frac{I}{I_o}$) in its appropriate range by using Erbst Correlation [19] and the extraterrestrial radiation is calculated using:

$$I_o = \frac{12x3600}{\pi}$$

$$G_{sc}\left(1+0.033\cos\frac{360n}{365}\right)\left[\begin{array}{l}\cos\phi\cos\delta\left(\sin\omega_2-\sin\omega_1\right)+\\ \frac{\pi\left(\omega_2-\omega_1\right)}{180}\sin\phi\sin\delta\end{array}\right] \quad (10)$$

The parallel and perpendicular component of reflectance, transmittance, and absorbance are calculated using:

$$\tau_{II/\perp} = \tau_a \frac{1-r_{II/\perp}}{1+r_{II/\perp}}\left(\frac{1-r_{II/\perp}^2}{1-\left(r_{II/\perp}\tau_a\right)}\right) \quad (1)$$

$$\rho_{II/\perp} = r_{II/\perp}\left(1+\tau_a\tau_{II/\perp}\right) \quad (2)$$

$$\alpha_{II/\perp} = 1-\rho_{II/\perp}-\tau_{II/\perp} \quad (3)$$

The parallel and perpendicular components of Fresenal's expression [18] is calculated using:

$$r_\perp = \frac{\sin^2\left(\theta_2-\theta_1\right)}{\sin^2\left(\theta_2+\theta_1\right)}; r_{II} = \frac{\tan^2\left(\theta_2-\theta_1\right)}{\tan^2\left(\theta_2+\theta_1\right)} \quad (4)$$

The angle of incidence for the beam radiation is same as developed in (3). The angle of incidence of diffused radiation is calculated using [18], and Snell's law is used to find transmittance angle [18].

The heat loss from the absorber plate is also calculated by using a thermal resistance diagram and developing following equation.

$$R_L = \frac{1}{\frac{1}{h_{c,g-a}} + \frac{1}{h_{r,g-a}}} + \frac{1}{\frac{1}{h_{c,p-g}} + \frac{1}{h_{r,p-g}}} \quad (5)$$

The Nusselt number between the absorber plate and glass cover is calculated using appropriate correlation.

Mass, momentum, and energy equations are developed for the humidification section which are:

$$\frac{\partial v}{\partial y} = 0 \quad (6)$$

$$v\frac{\partial v}{\partial y} = -\frac{1}{\rho_a}\frac{\partial P}{\partial y} + \gamma_a \frac{\partial^2 u}{\partial y^2} \quad (7)$$

$$u\frac{\partial T}{\partial x} + v\frac{\partial T}{\partial y} = \alpha_a \frac{\partial^2 T}{\partial y^2} + \frac{\gamma_a}{c_p}\left(\frac{\partial u}{\partial y}\right)^2 \quad (8)$$

The water evaporation rate in the humidification section is predicted by using relationship developed by Eams [20].

The dehumidification section is modeled as a parallel flow shell and tube heat exchanger. A mass and an energy balance on the condenser yields the following equations:

$$M_w = \dot{m}_a(\omega_{cin} - \omega_{cout}) \quad (9)$$

$$Q_{con} = (\dot{m}c)_{min}\,\varepsilon_c\left(T_{c,out} - T_{c,in}\right) \quad (10)$$

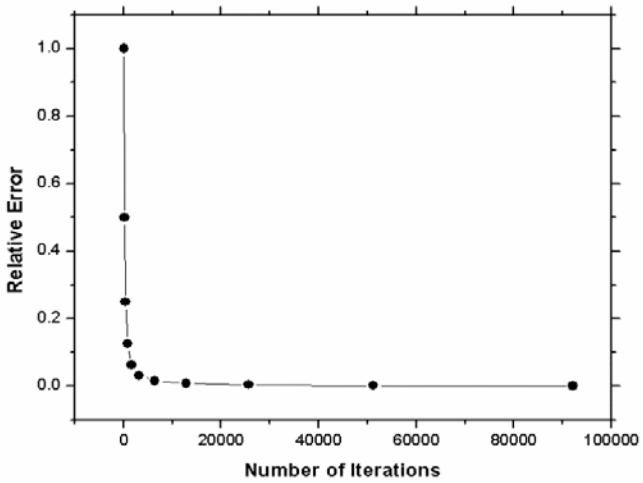

Fig. 2. Convergence Study

TABLE III: CALCULATION OF SOLAR PARAMETERS

Sr. No.	Solar Parameters	Equation	Eq. No.
1	Earth Titling Angle [18]	$\delta = 23.45\sin\left[360\left(\frac{284+n}{365}\right)\right]$	(2)
2	Solar Altitude Angle [18]	$\alpha_s = \sin^{-1}(\cos\phi.\cos\omega.\cos\delta + \sin\phi.\sin\delta)$	(3)
3	Sunrise/Sunset Hour Angle [18]	$\omega_s = \cos^{-1}(-\tan\phi.\tan\delta)$	(4)
4	Solar Azimuth Angle [18]	$\gamma = \cos^{-1}\left[\frac{\cos\phi.\sin\delta - \cos\delta.\cos\omega.\sin\phi}{\cos\alpha_s}\right]$	(5)
5	Day Length [18]	$N = \frac{\omega_s}{15}$	(6)
6	Zenith Angle [18]	$\theta_z = \frac{\pi}{2} - \alpha_s$	(7)
7	Tilt Factor [18]	$R_b = \frac{\cos\theta}{\cos\theta_z}$	(8)
8	Angle of Incidence [18]	$\theta_z = \cos^{-1}[\cos\phi.\cos\delta.\cos\omega + \sin\phi.\sin\delta]$	(9)

IV. METHODOLOGY

The governing equations established in the mathematical model are numerically solved and programmed using Matlab. Equation (2) to (14) are solved using successive substitution method, and (1) is solved using iteration until convergence criteria on the temperature of absorber plate is achieved. Equation (16) to (18) are numerically simulated by re-writing them in first order finite difference formulation and iterating in space step. Equation (19) and (20) are solved simultaneously. Operating parameters used for simulation are shown in II.

It makes sure that the results are independent of numerical disturbances, therefore, a convergence study is conducted on the outlet temperature of the feed water tank. Fig. 2 shows the grid independence test for numerical study. The iterations are performed until a relative error of 0.0001 is achieved in the outlet temperature of feed water tank.

V. VALIDATION OF RESULTS

The numerical results are compared with the previously published experimental results of Y. J. Dai et al [21]. They conducted a mathematical and experimental study of solar desalination unit with humidification and dehumidification.

In their experimental setup, they replaced the solar collector with a boiler to acquire lab results more rapidly. The experimental conditions of Y. J. Dai et al [21] are carefully replicated in the Matlab simulation code and results are obtained. Fig. 3 shows the variation of the temperature of saline water and water productivity at an air mass flow rate of 615.6 kg/hour. The maximum discrepancy; calculated using $\text{Error}(\%) = \left|\frac{\text{Exp} - \text{Num}}{\text{Exp}}\right| \times 100$, is 8.5% at a saline water temperature of 85°C.

TABLE IV: OPERATING PARAMETERS

Sr. No.	Quantity	Unit	Value
1	Mass Flow Rate of Air	kg/sec	0.027
2	Mass Flow Rate of Cooling Water	kg/sec	0.05
3	Mass Flow Rate of Saline Water	kg/sec	0.028
4	Temperature of Cooling Water Inlet	°C	20
5	Inlet Temperature of Air	°C	45
6	Inlet Humidity of Air	RH	30
7	Ambient Temperature	°C	45
8	Latitude	°	33.74
9	Month of the Year	-	21 March 2017

VI. PARAMETRIC STUDY

In this section, a parametric study is conducted by changing various parameters (mass flow rate of saline water, mass flow rate of air, the temperature of the air, and mass flow of cooling water) to observe their effect on freshwater productivity.

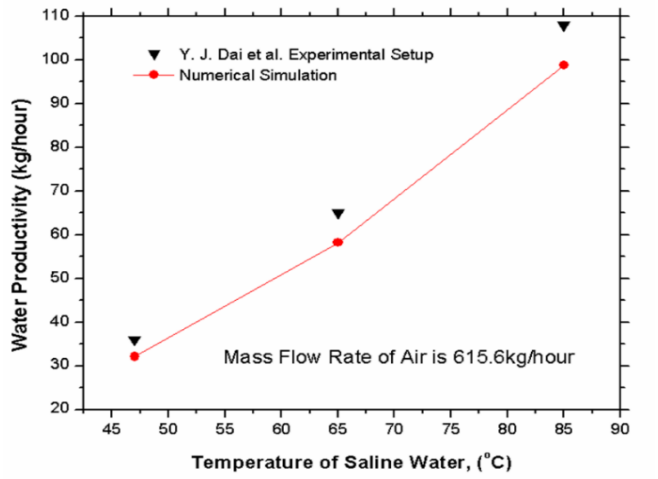

Fig. 3. Validation of Results

A. Influence of Mass Flow Rate of Saline Water

The mass flow rate of saline water is varied from 200kg/hour to 1800kg/hour and its influence on freshwater productivity is observed. The

simulation is carried for four different film water temperatures.

It is observed from fig. 4 that the fresh water productivity is increased by increasing the mass flow rate of saline water. This is due to the fact that increasing the mass flow rate of saline water influences the Reynolds number which increases the heat transfer coefficient, hence, the mass flow rate of fresh water is increased. Furthermore, it is recommended to use a mass flow rate of saline water ranging between 800kg/hour to 1200kg/hour, as slop of graph is near consistent in this region.

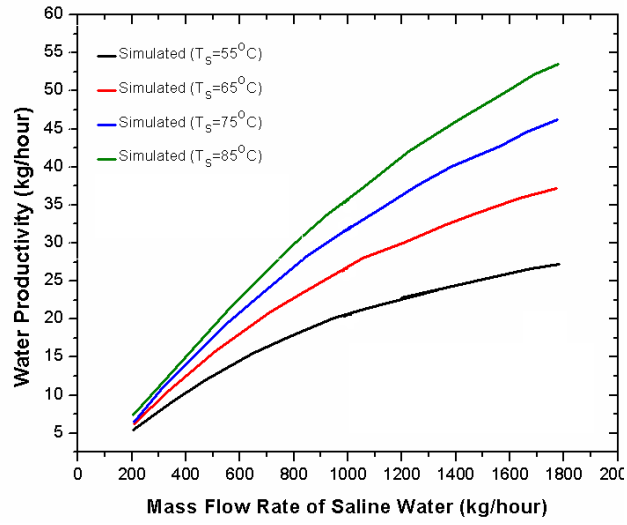

Fig. 4. Influence of Mass Flow Rate of Saline Water on Fresh Water Productivity

B. Influence of Mass Flow Rate of Air

The mass flow rate of air directly concerns the blowing power of the fan. Therefore, this parametric study plays an important role. In this parametric study, the mass flow rate of air is varied from 200kg/hour to 1800kg/hour for different falling water temperatures.

It is observed that increasing the mass flow rate of air increases the freshwater productivity. This is due to the fact that mass flow rate of air directly influences heat transfer characteristics inside the humidification chamber, therefore, it increases the freshwater productivity. This result is presented in fig. 5.

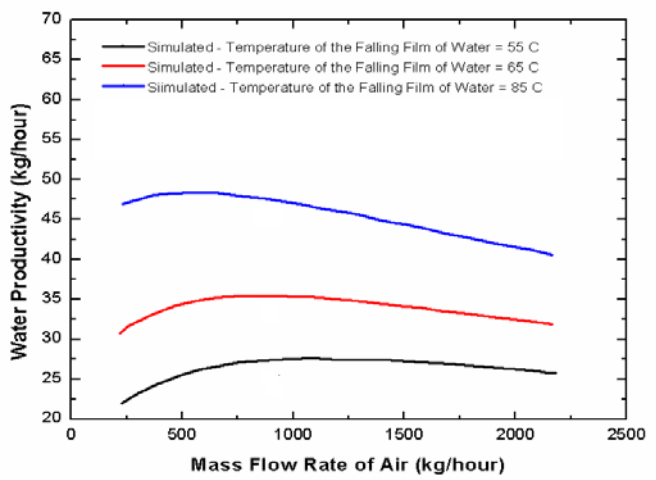

Fig. 5. Influence of Mass Flow Rate of Air on Fresh Water Productivity

C. Influence of Temperature of Air

In this section, the fresh water productivity is reported against the temperature of air for different humidity conditions. This parametric study determines the applicability of desalination unit in different climatic zones.

It is observed from fig. 6 that the fresh water productivity is increased with the increase in the temperature of the outside air. Similarly, the fresh water productivity is higher for lower values of relative humidity. This is due to the fact that a higher value of outside temperature and lower value of humidity have more affinity to cause water evaporation, thus, it enhances the freshwater productivity.

It is concluded that humidification-dehumidification based solar desalination unit are more applicable for hot and dry climatic zones.

D. Influence of Mass Flow Rate of Cooling Water

The mass flow rate of cooling water requires the pumping power of the pump, and therefore, it is an important parameter to identify the performance of the desalination unit. In this section, the mass flow rate of cooling water is varied from 1300kg/hour to 4000kg/hour and its effect on freshwater productivity is reported in fig. 7. Since a shell and tube heat exchanger is used as a condenser, therefore, the NTU values of the heat exchanger are also varied.

It is observed that increasing the mass flow rate of cooling water increases the freshwater productivity. This is due to the fact that mass flow rate directly

influences heat transfer properties. It is also observed that water productivity is higher for higher values of NTU of the heat exchanger.

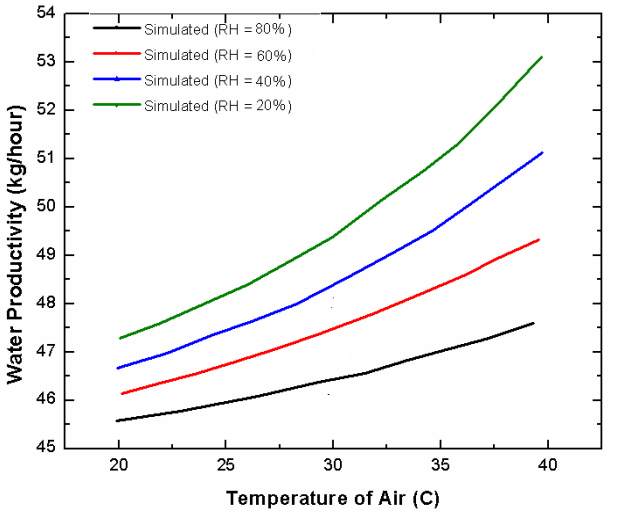

Fig. 6. Influence of Temperature of Environmental Air on Fresh Water Productivity

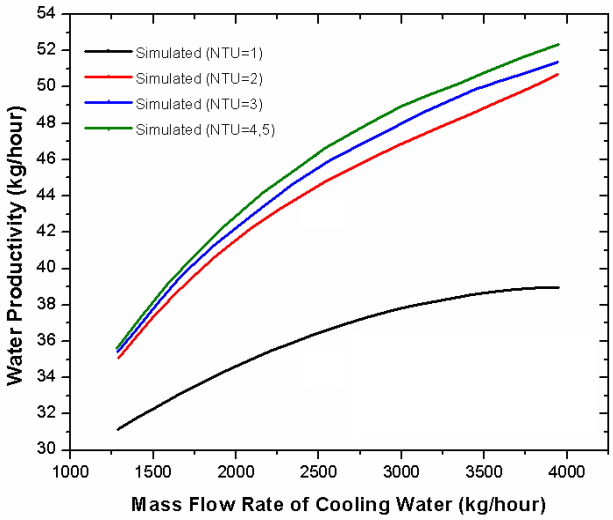

Fig. 7. Influence of Mass Flow Rate of Cooling Water on Fresh Water Productivity

VII. CONCLUSION

In this research paper, a solar-assisted desalination unit with humidification and dehumidification section is analyzed. In this system, brackish water is heated using flat-plate solar collector. The water is supplied to the humidification section where it comes in direct contact with the environmental air. The air becomes humid at the exit of humidification section. The condensate from the humid air is collected using a dehumidification/condenser unit. The fresh water from the condenser is stored.

In this research paper, a mathematical model is established for the desalination unit. The mathematical model also incorporates the design of flat-plate solar collector. Mass, momentum, and energy balance equations are established for humidification section. The dehumidification section is modeled using a parallel-flow shell and tube heat exchanger with one shell and one pass. All the governing equations are numerically simulated on Matlab. Convergence study is conducted to remove numerical discrepancies from the results. Validation is conducted for the developed model by a comparison with previously published experimental results.

At the end, a parametric study is conducted by varying numerous parameters of the desalination unit. It is reported that an increase in the mass flow rate of saline water, mass flow rate of air, temperature of air, and mass flow rate of cooling water increases the freshwater productivity. It is recommended to use 800kg/hour to 1200kg/hour of mass flow rate of saline water. The desalination unit is more effective for hot and dry climatic zones.

In the future work, it is proposed to use a parabolic trough type solar collector as they can provide much higher values of freshwater productivity.

VIII. NOMENCLATURE

No.	Quantity	Symbol	Units
1	Absorber Plate Energy	Q_u	W
2	Collector Area	A_c	m^2
3	Absorbed Solar Radiation	S	W/m^2
4	Overall Heat Loss Coefficient	U_L	$W/m^2.K$
5	Absorber Plate Temperature	T_{pm}	K
6	Ambient Air Temperature	T_a	K
7	Sky Clearance Index	k_T	-
8	Hourly Incident Radiation	I_o	W/m^2
9	Solar Constant	G_{sc}	W/m^2
10	Number of Day of the Year	n	-
11	Hour Angle	ω	degree
12		ϕ	degree
13	Earth's Declination Angle	δ	degree
14	Transmittance	τ	-
15	Reflectivity	ρ	-
16	Angle of Reflectance	θ_2	degree
17	Angle of Incidence	θ_1	degree
18	Overall Thermal Resistance	R_L	$m^2.K/W$
19	Convective Heat Transfer Coefficient between glass and absorber plate	$h_{c,g-a}$	$W/m^2.K$
20	Radiative Heat Transfer	$h_{r,g-a}$	$W/m^2.K$

	Coefficient between glass and absorber plate		
	Convective Heat Transfer		
21	Coefficient between ambient air and glass	$h_{c,p-g}$	W/m^2.K
	Radiative Heat Transfer		
22	Coefficient between ambient air and glass	$h_{r,p-g}$	W/m^2.K
23	Velocity	v	m/sec
24	Density of Air	ρ_a	kg/m^3
25	Pressure	P	Pa
26	Kinematic Viscosity	γ_a	m^2/sec
27	Temperature	T	K
28	Thermal Diffusivity	α_a	m^2/sec
29	Specific Heat	c_p	J/kg.K
30	Mass Flow Rate of Fresh Water	M_w	kg/hour
31	Mass Flow Rate of Air	$\dot{m}_a$	kg/sec
32	Absolute Humidity of Air	ω	g_{H20}/kg_{air}
33	Heat Transfer in Condenser	Q_{con}	W
34	Effectiveness of Condenser	ε_c	-

REFERENCES

[1] H. M. Qiblawey and F. Banat, "Solar thermal desalination technologies," *Desalination*, vol. 220, no. 1–3, pp. 633–644, 2008.

[2] C. M. and A. Yadav, "Water desalination system using solar heat: A review," *Renew. Sustain. Energy Rev.*, vol. 67, pp. 1308–1330, 2017.

[3] K. Zhani and H. Ben Bacha, "Experimental investigation of a new solar desalination prototype using the humidification-dehumidification principle," *Renew. Energy*, vol. 35, no. 11, pp. 2610–2617, 2010.

[4] Y. J. Dai and H. F. Zhang, "Experimental investigation of a solar desalination unit with humidification and dehumidification," *Desalination*, vol. 130, no. 2, pp. 169–175, 2000.

[5] A. S. Nafey, H. E. S. Fath, S. O. El-Helaby, and A. Soliman, "Solar desalination using humidification-dehumidification processes. Part II. An experimental investigation," *Energy Convers. Manag.*, vol. 45, no. 7–8, pp. 1263–1277, 2004.

[6] G. Yuan, Z. Wang, H. Li, and X. Li, "Experimental study of a solar desalination system based on humidification-dehumidification process," *Desalination*, vol. 277, no. 1–3, pp. 92–98, 2011.

[7] J. hong Wang, N. yun Gao, Y. Deng, and Y. li Li, "Solar power-driven humidification-dehumidification (HDH) process for desalination of brackish water," *Desalination*, vol. 305, pp. 17–23, 2012.

[8] H. Ettouney, "Design and analysis of humidification dehumidification desalination process," *Desalination*, vol. 183, no. 1–3, pp. 341–352, 2005.

[9] N. K. Nawayseh, M. M. Farid, A. A. Omar, and A. Sabirin, "Solar desalination based on humidification process—II. Computer simulation," *Energy Convers. Manag.*, vol. 40, no. 13, pp. 1441–1461, 1999.

[10] S. S. Sablani, M. F. A. Goosen, C. Paton, W. H. Shayya, and H. Al-Hinai, "Simulation of fresh water production using a humidification-dehumidification seawater greenhouse," *Desalination*, vol. 159, no. 3, pp. 283–288, 2003.

[11] E. Chafik, "A new seawater desalination process using solar energy," *Desalination*, vol. 153, no. 1–3, pp. 25–37, 2003.

[12] C. Yamali and I. Solmus, "A solar desalination system using humidification-dehumidification process: experimental study and comparison with the theoretical results," *Desalination*, vol. 220, no. 1–3, pp. 538–551, 2008.

[13] N. K. Nawayseh, M. M. Farid, A. A. Omar, S. M. Al-Hallaj, and A. R. Tamimi, "A simulation study to improve the performance of a solar humidification-dehumidification desalination unit constructed in Jordan," *Desalination*, vol. 109, no. 3, pp. 277–284, 1997.

[14] M. S. Mahmoud, T. E. Farrag, and W. A. Mohamed, "Experimental and Theoretical Model for Water Desalination by Humidification - dehumidification (HDH)," *Procedia Environ. Sci.*, vol. 17, pp. 503–512, 2013.

[15] M. H. Hamed, A. E. Kabeel, Z. M. Omara, and S. W. Sharshir, "Mathematical and experimental investigation of a solar humidification-dehumidification desalination unit," *Desalination*, vol. 358, pp. 9–17, 2015.

[16] G. Al-Enezi, H. Ettouney, and N. Fawzy, "Low temperature humidification dehumidification desalination process," *Energy Convers. Manag.*, vol. 47, no. 4, pp. 470–484, 2006.

[17] F. Nematollahi, A. Rahimi, and T. T. Gheinani, "Experimental and theoretical energy and exergy analysis for a solar desalination system," *Desalination*, vol. 317, pp. 23–31, 2013.

[18] W. A. Duffie, John A; Beckman, *Solar Engineering of Thermal Processes*, 4th Editio. New York: John Wiley & Sons.

[19] D. G. Erbs, S. A. Klein, and J. A. Duffie, "Estimation of the diffuse radiation fraction for hourly, daily and monthly-average global radiation," *Sol. Energy*, vol. 28, no. 4, pp. 293–302, 1982.

[20] I. W. Eames, N. J. Marr, and H. Sabir, "The evaporation coefficient of water: a review," *Int. J. Heat Mass Transf.*, vol. 40, no. 12, pp. 2963–2973, 1997.

[21] Y. J. Dai, R. Z. Wang, and H. F. Zhang, "Parametric analysis to improve the performance of a solar desalination unit with humidification and dehumidification," *Desalination*, vol. 142, no. 2, pp. 107–118, 2002.

INDEX

INTERNATIONAL CONFERENCE ON
ENERGY SYSTEMS FOR SUSTAINABLE DEVELOPMENT

Department of Chemical Engineering
COMSATS Institute of Information Technology Lahore
http://essd.ciitlahore.edu.pk/